ATMOSPHERIC ELECTRICITY INVESTIGATIONS:

THE MEASUREMENT OF ATMOSPHERIC CONDUCTIVITY

JAMES R. ARATHOON

VOLUME 1

This thesis is submitted in partial fulfilment of the requirements for the B.Sc. degree in Geophysical Sciences at the University of Lancaster.

January 1991.

ABSTRACT

Continuous measurement of Gerdien condenser air conductivity currents, requires a low drift electrometer. Most recent invesigators have used a vibrating reed electrometer, for this reason. However these instruments are extremely expensive, bulky and currently difficult to obtain. For this dissertation project a drift compensated DC amplifier electrometer, was developed. A true drift compensated signal level was calculated by finding the difference in the electrometer output voltage, when an input signal was and was not applied. The use of sampling also allowed the 'simultaneous' measurement of both polar conductivities with a single instrument.

Atmospheric conductivity was measured for about a week in the summer of 1990 and fair weather conditions prevailed. It was found that there were differences in the character of the variations between day and night, and effects due to sunrise and sunset were also seen. For most of the time both polar conductivities varied in unison, however positive conductivities were normally greater than negative. A major disturbance found on one trace, believed to be due to nearby evaporating volatiles, led to idea that changes in space charge density might produce displacement currents within the condenser. This idea was investigated theoretically and was found to be possible if the space charge densities varied quickly enough. The effects of aliasing on the measurement record were also investigated.

Notation

A	-	amplifier gain	
	-	area	m^2
a	-	radius of inner electrode	m
b	-	radius of outer electrode	m
C_e	-	exposed capacity	F
C_i	-	op-amp input capacity	F
E	-	electric field strength	$V\ m^{-1}$
E_Z	-	component of electric field normal to the surface.	$V\ m^{-1}$
e	-	electronic charge	C
i_s	-	current flowing to a small area dS	A
i_{in}	-	input signal current to op-amp	A
i_b	-	op-amp input bias current	A
i_n	-	op-amp input noise current	A
i_P	-	positive ion current	A
i_N	-	negative ion current	A
L	-	length of polarized outer cylinder	m
Q, q	-	charge	C
R_E	-	radius of the earth	m
R_F	-	feedback resistance	Ω
R_S	-	shunt resistance	Ω
V_1	-	voltage to op-amp inverting input	V

V_2	-	voltage to op-amp non-inverting input	V
V_{out}	-	op-amp output voltage	V
V_p	-	polarization voltage	V
V_{PP}	-	electrometer output voltage with positive polarization	V
V_{NP}	-	electrometer output voltage with negative polarization	V
V_{ZP}	-	electrometer output voltage with zero polarization	V
V_{REF}	-	A/D converter reference voltage	V
w	-	mobility	$m\ s^{-1}\ C^{-1}$
λ_P	-	positive ion conductivity	$\Omega^{-1}\ m^{-1}$
λ_N	-	negative ion conductivity	$\Omega^{-1}\ m^{-1}$
σ	-	surface charge density	$C\ m^{-2}$

Contents

VOLUME 1

1. Introduction.....1

1.1. What is atmospheric electricity ?.....1

1.2. The earth's surface charge.....3

1.3. Conductivity of the air.....4

1.4. Theory of ions.....5

1.5. Ion mobility and air conductivity.....6

1.6. The production and destruction of ions in the atmosphere.....7

1.7. The maintenance of the earth's charge.....7

2. Measurement techniques and theory.....8

2.1. The Gerdien condenser.....8

2.2. Measuring small currents.....11

2.3. Electrometers.....11

2.4. DC Amplifier electrometers.....13

2.5. Drift and noise in DC Amplifiers.....17

3. Instrument design, construction and testing.....19

3.1. The design of the old Gerdien condenser...19

3.2. The design of the new instrument.....20

3.3. Construction of the picoammeter.....28

3.4. Testing and Development.....29
3.5. Computer measurement and logging of the results.....31

4. Using and calibrating the instrument.....34

4.1. Calibrating the Gerdien condenser.....34
4.2. Measurement drift and noise.....41
4.3. Maintaining adequate insulation.....47

VOLUME 2

5. Results and data analysis.....49

5.1. Descripton of the results obtained.....49
5.2. Interpretation of the results.....52
5.3. Aliasing and Spectral analysis.....63

6. Summary and conclusions.....66

6.1. Summary of the dissertation.....66
6.2. Conclusions.....67

7. Suggestions for further work.....69

References

Appendices

Acknowledgements

1. Introduction

1.1 What is atmospheric electricity ?

Although the subject of atmospheric electricity is commonly associated with the study of the lower atmosphere alone, the phenomena covered by the title in its broadest sense, ranges from the electrical nature of the lower atmosphere to the magnetosphere and beyond. In practice there is, as in all atmospheric studies, a demarcation between those who study the upper atmosphere and space environments and those who study the lower atmosphere, as I will be. For a long time the atmospheric electrical nature of the lower atmosphere has been seen as a fairly self-contained subject, since there did not appear to be any obvious links with the earths other well known electrical phenomena, such as its magnetic field and associated variations, earth currents and the host of upper atmospheric electrical phenomena that take place. Although Webb(1980) has recently called for a more unified approach with regard to the study of the electrical phenomena of the upper and lower atmosphere, there does not seem to have been much progress made in this direction as yet.

There are two main types of electrical activity constantly taking place in the lower atmosphere, one is the intense local electrification accompanying storms and the other is the much weaker fair-weather electrical activity which is of global extent (Chalmers,1967).

Many of the problems central to atmospheric electricity have still not been satisfactorily solved, such as the nature of charge separation, both in non-storm and storm clouds, for example there is still no generally accepted theory of thunderstorm electrification (Saunders,1988). Also the general relationships between meteorology and atmospheric electricity are still far from understood (Israël,1971,1973).

There have been historically two basic, often competing notions as to the relationship between meteorology and atmospheric electricity. Theories invoking electrical forces have often in the past been used to provide an explanation for various meteorological phenomena, such as the rising of water vapour and the various electrical theories of rain that have been put forward (Knowles Middleton,1965). Virtually all the theories of this type have never gained significant support, the exception being perhaps electrical tornado theories put forward by, amongst others, Vonnegut(1960).

Much more wide spread and sustained support has been given to the idea that the observed atmospheric electrical phenomena are solely secondary effects to what might be vaguely called 'the workings of the atmospheric engine'. This is believed to be true since 'heat' energy transfers in the atmosphere are many orders of magnitude greater than the observed 'electrical' energy transfers that take place.

The major works covering the electrical phenomena of the lower atmosphere are Chalmers(1967), Israël(1971), Israël(1973) and Schonland(1953).

1.2 The earth's surface charge

The atmospheric "fair-weather" field when measured on flat ground has a strength of the order of 100 V/m and acts downwards; that is the earth appears to be negatively charged with respect to the atmosphere. (see Fig. 1.2.1)

Let us assume that the earth is spherical with radius R_E and is a good conductor so that any charge it holds is uniformly distributed over its surface.

Using Gauss's Law the total charge on the earth's surface can be related to the electric flux passing through an arbitrary Gaussian surface surrounding the earth.

Gauss's Law states

$$\int \underline{E} \cdot d\underline{A} = \frac{1}{\varepsilon_o} \sum_{i=1}^{N} q_i \qquad (1.2.1.)$$

$$= Q / \varepsilon_o$$

where in this case Q is the total charge on the earths surface.

If we consider for simplicity a spherical gaussian surface with a radius just a little larger than that of the earth we find that

$$Q = E.4\pi R_E^2$$

and defining surface charge density, σ, as

$$\sigma = Q/4\pi R_E^2$$

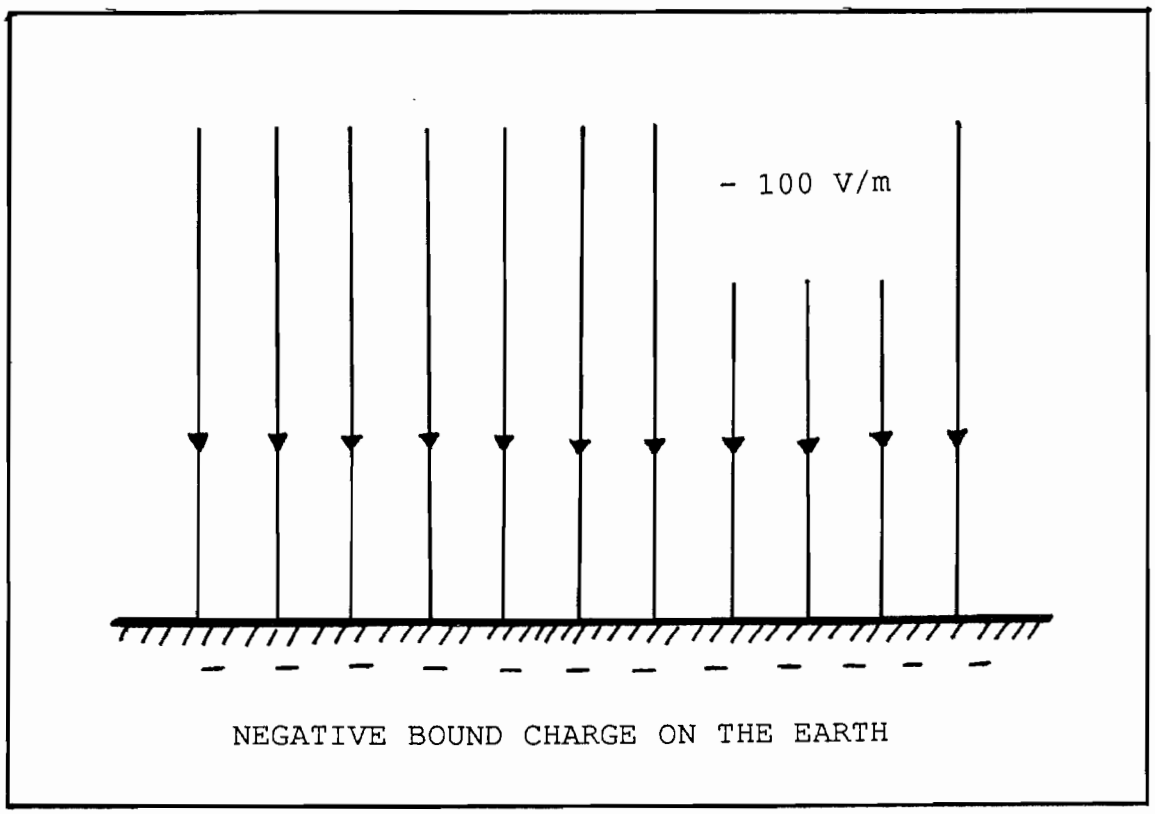

Fig. 1.2.1. Diagram to show the direction of the fair weather electric field at the earths surface.

we arrive at the relation

$$\sigma = \varepsilon_0 E \qquad (1.2.2.)$$

Therefore the charge density on the earth's surface for a fair weather field of -100 V/m is

$$\sigma = -100 \times 8.85 \times 10^{-12}$$

$$= -8.85 \times 10^{-10} \text{ coulombs/m}^2$$

Taking the radius of the earth, R_E to be 6400 km the total bound charge on the earths surface, for a global fair weather field of -100 V/m is

$$Q = -460{,}000 \text{ coulombs}$$

It is generally assumed that there is an equal and opposite charge somehow distributed in the atmosphere above, however the distribution of charge in the atmosphere cannot be investigated with the use of land based measurements, but requires airborne measuring apparatus as first pointed out by Lord Kelvin (Chalmers,1967). Incidentally this surface charge exerts a negligible outward pressure and cannot be used to account for the earths magnetic field (see Appendix A1).

1.3 Conductivity of the air

That the air is not a perfect insulator was first discovered by Coulomb(1785) and is perhaps best demonstrated using a gold leaf electroscope with a removable charging plate, see Fig. 1.3.1.

If the electroscope is charged, and left to stand as above, it will remain charged for no more than a few hours. If a fan is used to blow air around the top plate

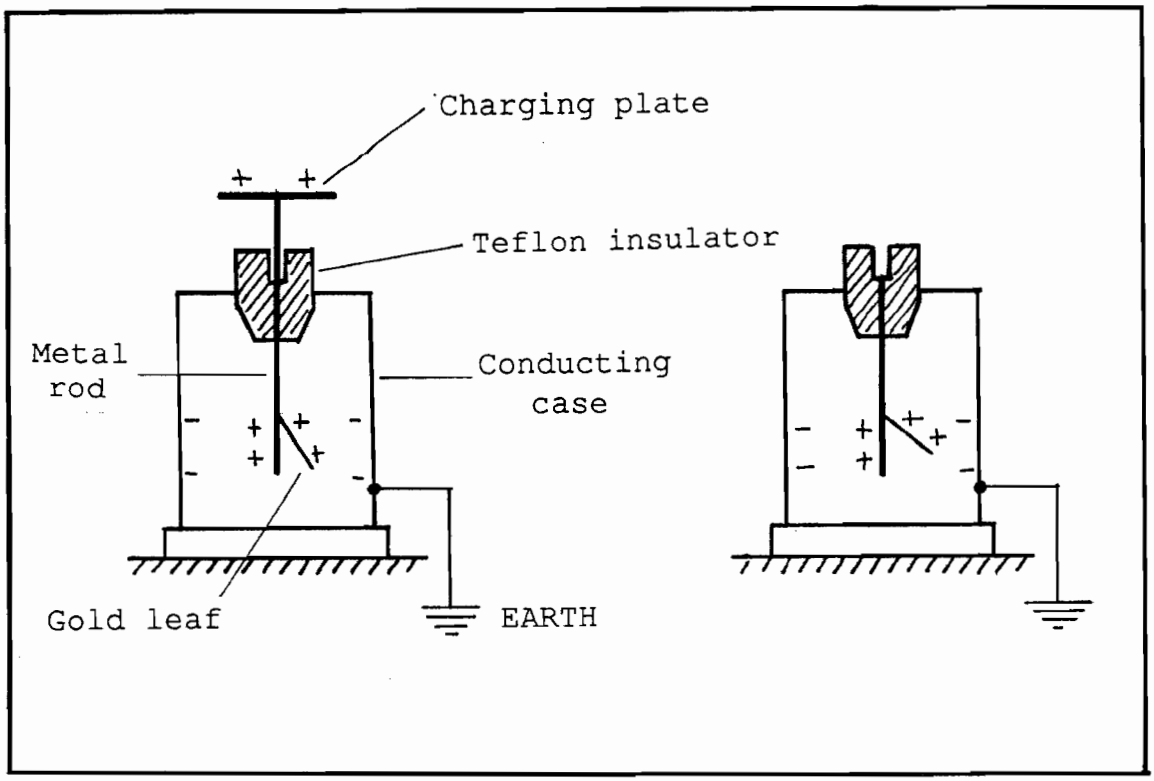

Fig. 1.3.1. Two charged gold leaf electroscopes, one with the charging plate in position, the other without. Both are slowly discharging in air.

the electroscope will be found to discharge more quickly than before.

If next, after charging the electroscope, the top plate is removed the deflection on the gold leaf may take several days to fall to zero.

These qualitative experiments, which can be readily repeated, show that there is some charge lost from a charged conductor in the 'open' air, which cannot be accounted for by the leakage of charge across, in this case, a PTFE(Teflon) insulator.

The details of why this took place and especially why the 'conductivity' of the air should reduce so significantly when charged conductors were sealed in small air filled containers only began to become clear with the work of J.J.Thomson(1898) and others in England and Elster and Geitel(1899,1900) in Germany.

1.4 Theory of ions

The discovery of X-rays by Rontgen in 1895 was quickly followed by the curious observation that charged bodies rapidly lost their charge when X-ray apparatus was used close by. The loss of charge was found to take place through the air, which was temporarily rendered more conductive by the passage of X-rays through it.

It was shown that the increased conductivity was due to the creation of positive and negative charged particles, which by analogy with the charge carriers in electrolytic conduction were termed gaseous ions. These ions were, according to the electron theory, molecules of

a gas which had either lost or gained one or more electrons. These ideas formed the basis of the theory of ions put forward by Thomson(1898).

The objective reality of ions was placed beyond all reasonable doubt by the experiments of C.T.R. Wilson(1897,1899), who showed that they could serve as nuclei for the condensation of water drops in a supersaturated cloud chamber.

1.5 Ion mobility and air conductivity.

When in an electric field ions in a gas are initially accelerated, however they soon reach a 'terminal' velocity, the size of which depends on various properties of the ion, including its size and charge. The ions are said to **migrate** in the field. The ions are continually being struck by the randomly moving gas molecules which prevents them from being accelerated. The velocity acquired by an ion in a unit electric field (1 V/m) is termed the **mobility** of the ion; the velocity of the ion in an electric field of X V/m is wX m/sec where w is the mobility.

The **conductivity** of the air depends on the number and mobility of the ions in the air. If ions of only one mobility are present in the air the positive and negative conductivities are respectively:

$$\lambda_P = n_P \, e \, W_P, \quad \lambda_N = n_N \, e \, W_N$$

assuming ions have a single electronic charge, and where n_P and n_N are the number of ions in the volume under

consideration. If there are several types of ions of different mobility then the above expressions obviously become more complex. It is usual to distinguish 3 types of ion by name **small ions** (high mobility), **intermediate ions** (medium mobility) and **large ions** (low mobility). (see Chalmers(1967), Twomey(1977) or Israël(1971)).

1.6 The production and destruction of ions in the atmosphere.

Ions are produced in the atmosphere by cosmic rays, the disintegration of radioactive material in the air and on the ground, by corona discharge under thunderstorm conditions and by charge separation in thunderstorms.

Ions are removed from the atmosphere by recombination with ions of opposite sign and also by conduction to earth (Israël,1971; Twomey,1977).

1.7 Maintenance of the earth's charge.

That positive ions are continually conducted to earth posed a serious problem to scientists for a long time because although the earth's field, and thus its charge, had been present at least since measurements began, some 200 years ago, order of magnitude calculations suggested that the earth should become fully discharged within an hour or so. It is now generally believed that lightning discharges bring enough negative charge to earth to maintain its surface charge (Chalmers,1967).

2. Measurement techniques and theory

2.1. The Gerdien condenser

2.1.1. Description of the Gerdien condenser

The Gerdien condenser (Fig. 2.1.1.) has become the standard instrument with which to measure atmospheric conductivity. A major component of the instrument, as its name suggests, is a capacitor which consists of a hollow outer cylinder as one plate, with a smaller coaxial bar or wire placed inside it, as the other. A potential of up to $\pm$100 volts is applied to the outer cylinder and the inner electrode is connected through a very sensitive current meter to earth. The voltage applied to the outer cylinder is usually called the **polarization voltage;** changing the sign of the polarization voltage changes the direction of the electric field in the region between cylinder and electrode. A fan at the far end of the condenser draws air through the apparatus and ions present in the air migrate, depending on their sign, to either the inner electrode or the outer cylinder. Since only the current from the inner electrode can be measured, the instrument can either be set up to measure the positive or the negative conductivity of the air, but not both simultaneously.

2.1.2. Coulomb's Law of charge dissipation

Consider a small surface element dS of a positively charged conductor. If the element dS has an average

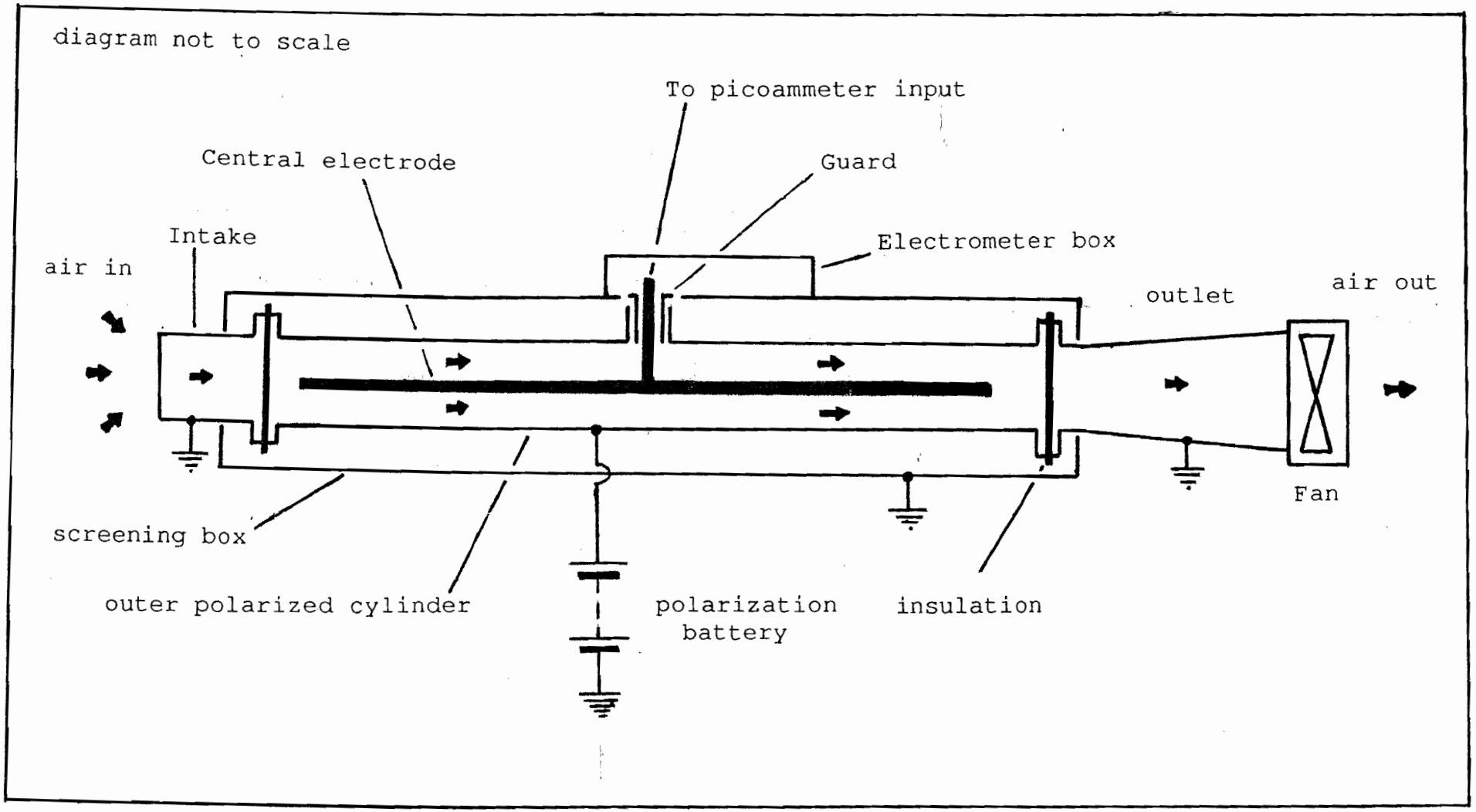

Fig. 2.2.1. Sketch of the Gerdien condenser used for this dissertation.

charge density σ then the total charge on it is σ dS. If the curvature of the elemental area is small the field for some distance above it will be uniform.

Thus $E_z = \sigma / \varepsilon_o$

If i_S is the current flowing to the area dS and ohms law holds then,

$$E_z = i_S / \lambda_N \qquad (2.1.1.)$$

where λ_N is the negative ion conductivity.

Thus equating these two expressions gives,

$$i_S = \lambda_N \sigma / \varepsilon_o$$

Now by assuming λ_N constant and integrating over the whole surface of the conductor,

$$i = \int i_S \, dS$$
$$= \lambda_N q / \varepsilon_o \qquad (2.1.2.)$$

where q is the total charge on the conductor.

The conservation of charge requires that, $i = - \frac{dq}{dt}$

where dq/dt is the rate of change of charge on the conductor.

Thus $$\frac{dq}{dt} = - \lambda_N q / \varepsilon_o \qquad (2.1.3.)$$

which is coulomb's law of charge dissipation for a positively charged body. A similar expression for a negatively charged body would incorporate the positive ion conductivity, λ_p.

2.1.3. Theory of the Gerdien Condenser

When an exposed charged body is used to measure the electrical conductivity of the air by the gradual dissipation of its charge, the chief source of error in the measurements is due to the depletion of ions in the immediate vicinity of the body (Hess,1928). This is known as the **electrode effect**. The electrode effect is most apparent when the air in the neighbourhood of the charged body is either still or slowly moving and is also found to take place at the earth's surface. In order to avoid this happening Gerdien(1905) developed the apparatus which is now named after him and which is described above.

The charge held on the section of the central electrode open to the air flow is given by

$$q = C_e V_p \qquad (2.1.4.)$$

where V_p is the polarization voltage and C_e is the capacity of that part of the electrode system which is exposed to the air flow (Swann,1914). This I will call the **exposed capacity**. However Israel(1971) calls it the 'effective capacity' and Gunn(1965) calls it the 'critical capacity'. (see section 4.1.1 for details on the determination of C_e).

Thus combining equation (2.1.4.) with equation (2.1.2.) we arrive at a simple expression for the current flowing either to or from the central electrode

$$i = \lambda_N C_e V_p / \varepsilon_o \qquad (2.1.5.)$$

This formula holds true as long as only a small fraction of the ions present in the air migrate to either electrode, as the air passes through the instrument. The

above current is very small, typically less than a picoamp (10^{-12} amps).

The Gerdien condenser can be used to measure ion mobility and ion concentration, that is the number of ions per unit volume, as well as atmospheric conductivity (Chalmers,1967).

2.2. Measuring small currents

The Ampere is the SI unit of current and is one of the basic units of the SI system. Current balances are employed in standardizing laboratories such as the National Physical Laboratory in this country to make absolute measurements of current. However the magnetic field produced by very small currents is insufficient to allow them to be measured using galvanometric type apparatus. **Electrometers** are required to measure currents below the range of these instruments and ultimately need to be calibrated with reference to standard resistors or capacitors.

2.3. Electrometers

The term electrometer is usually applied today to a direct current coupled instrument capable of carrying out any or all the following functions.

(a) High impedance voltage measurement normally below 100 volts, with an input impedance that is typically above 10^{14} ohms.

(b) Measurement of small currents. Electrometers have been made which can measure currents down to 10^{-17} amps or 160 electrons per second. However the typical resolution is 10^{-15} amps. An electrometer dedicated to the measurement of small currents is called a **picoammeter** (Keithley et al, 1984).

(c) Measurement of charge.

General purpose solid-state electrometers such as those made by Keithley Instruments Ltd. can be used to measure voltage, current, resistance and charge over a considerable range of values, as they have the necessary standard components built in and the meter is calibrated to give a direct reading of the quantity required. Regular recalibration is important for the smallest current ranges on these instruments, mainly because the large resistors required, drift in value with age.

Historically there have been five main technological steps in the development of electrometers. (see Fig. 2.3.1.). However I will only describe the operation of the DC Amplifier electrometer in any detail. The most recent review of electrometry I have found is Barker(1979) and a good source of general information is Keithley et al.(1984). Manufacturers data sheets and instrument manuals are another helpful source of information.

FOR AN ELECTROMETER COMPARISON CHART

The dynamic capacitor electrometer (Palevsky et al., 1947), usually a vibrating reed type, has been used by

ELECTROMETER TYPE	INPUT IMPEDANCE	INPUT CURRENT	INPUT CURRENT TEMP. Co.	INPUT OFFSET VOLTAGE TEMP Co.	SENSITIVITY LIMITED BY	LONG TERM DRIFT RATING / DEPENDS ON	SOURCE OF INFORMATION
REPULSION/ ATTRACTION PASSIVE ELECTROMETER	$>10^{16}\ \Omega$	—	—	—	GROUND * VIBRATION, BROWNIAN MOTION	GOOD/ * CONTACT POTENTIALS NON-ELASTIC STRAIN IN SUSPENSION	* PALEVSKY ET AL (1947)
DYNAMIC CAPACITOR/ VIBRATING REED	$>10^{16}\ \Omega$ †	$\ll 1$ fA †	—	30 μV/°C †	THERMAL * AGITATION NOISE	GOOD/ * CONTACT POTENTIALS	† BARKER (1979) * PALEVSKY ET AL (1947)
VARACTOR BRIDGE (VOLTAGE VARIABLE CAPACITANCE)	$10^{11}-10^{14}\ \Omega$	~10 fA	x2/10°C	30 μV/°C		MEDIUM/ TEMPERATURE, SUPPLY VOLTAGE	BURR-BROWN DATA SHEET 3430/3431
VALVE	$>10^{3}\ \Omega$ $	2-100 fA $			THERMAL * AGITATION AND SHOT NOISE	MEDIUM TO POOR/ * SUPPLY VOLTAGE, CONTACT POTENTIALS	$ ISRAEL (1971) * PALEVSKY ET AL (1947)
MOSFET	$10^{14}\ \Omega$	1-10 fA	0.1-1 fA/°C	50-150 μV/°C	VARIOUS VOLTAGE AND CURRENT NOISE SOURCES	POOR / TEMPERATURE, SUPPLY VOLTAGE, AGING, LOADING	BARKER (1979)
JFET DC AMPLIFIER	$10^{14}\ \Omega$	10-300 fA	x2.3/10°C	20-50 μV/°C	VARIOUS VOLTAGE AND CURRENT NOISE SOURCES	POOR / TEMPERATURE, SUPPLY VOLTAGE, AGING, LOADING	DATA SHEETS FOR AD549 AD515A

FIG. 2.3.1. ELECTROMETER COMPARISON CHART.

most recent investigators of atmospheric conductivity, for example Sharpless et al.(1971) and Gunn(1964,1965). This is mainly because the instrument has a very small zero drift with time. However dynamic capacitor electrometers are difficult to manufacture and thus extremely expensive. The best modern alternative to the dynamic capacitor electrometer is to use a dc amplifier electrometer. These are relatively cheap to build, but unfortunately have greater zero drift with time. However by using sampled measurements it is possible compensate for amplifier drift, as will be seen later.

2.4. DC Amplifier Electrometers

DC or operational amplifiers are direct current coupled amplifiers available in the form of inexpensive integrated circuits. They are characterized by very high gains and are invariably used with negative feedback, in order to give highly predictable performance. A good introduction to operational amplifiers and their many uses is Clayton(1979).

A DC amplifier in its simplest form has just 5 connections as shown in Fig. 2.4.1. The positive supply ($+V_S$), negative supply ($-V_S$) and output connections are obvious. The amplifier has two inputs, denoted by + and - and they are known respectively as the **non inverting** and **inverting** inputs. The amplifier amplifies the voltage between these two inputs. Thus if the amplifier has a gain A, then the output voltage is related to the input voltages by the formula,

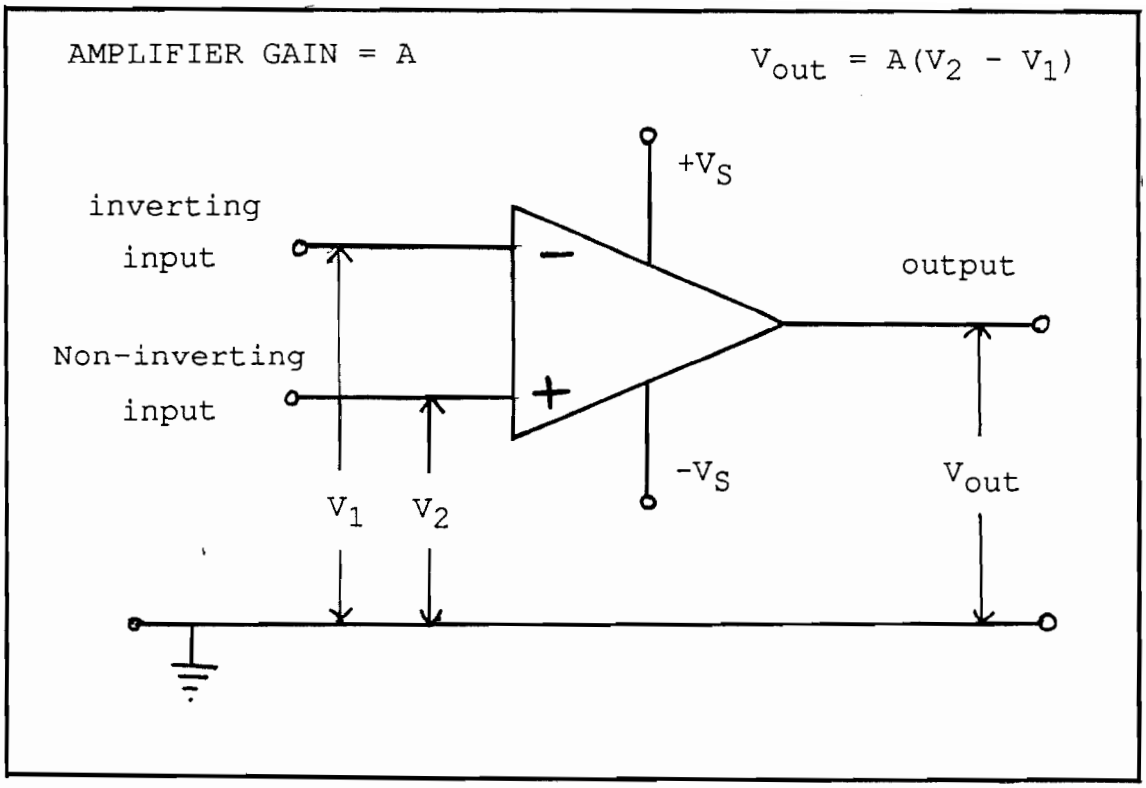

Fig. 2.4.1. A DC amplifier in its simplest form.

$$V_{out} = A(V_2 - V_1) \qquad (2.4.1.)$$

where V_1 is the voltage between the inverting (-) input and earth and V_2 is the voltage between the non inverting (+) input and earth.

To illustrate this further, let us assume that the - input is connected to 0V and an input signal is applied to the + input, as shown in Fig. 2.4.2. It will be found that the output varies in phase with the input. If we reverse the input connection, and connect the signal to the -input, and the + input to 0V, as shown in Fig. 2.4.3., the input and output will be found to be in anti-phase. Thus the terms inverting and non inverting refer to the phase relationship between input and output when a signal is applied to a particular terminal.

DC amplifier electrometer chips have high input impedanaces, low input bias currents and a small input offset voltage as well as high gain. (See Appendix A2.1. for an introduction and reference guide to DC amplifier terminology). The chips can be constructed using either MOSFET or JFET technology. JFET chips are usually used today because of their lower voltage noise and their less stringent overload protection requirements. For a detailed list of pro's and con's consult Keithley et al.(1984). Fig. 2.4.4. gives selected manufacturers data for a range of DC amplifier electrometer chips currently available.

There are two basic ways of using DC amplifiers to measure currents. One is in a non-inverting amplifier circuit (Fig. 2.4.5), which when used for small currents

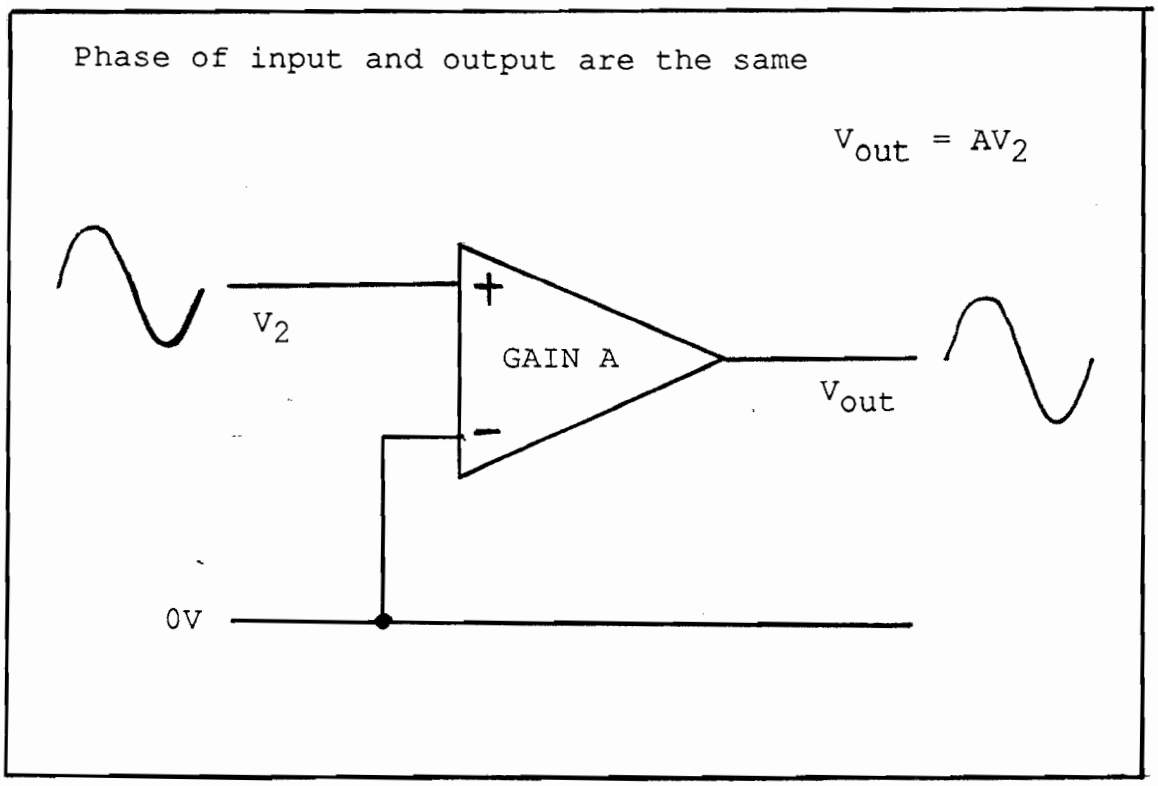

Fig. 2.4.2. DC amplifier with signal applied to the + input and the - input connected to 0 V.

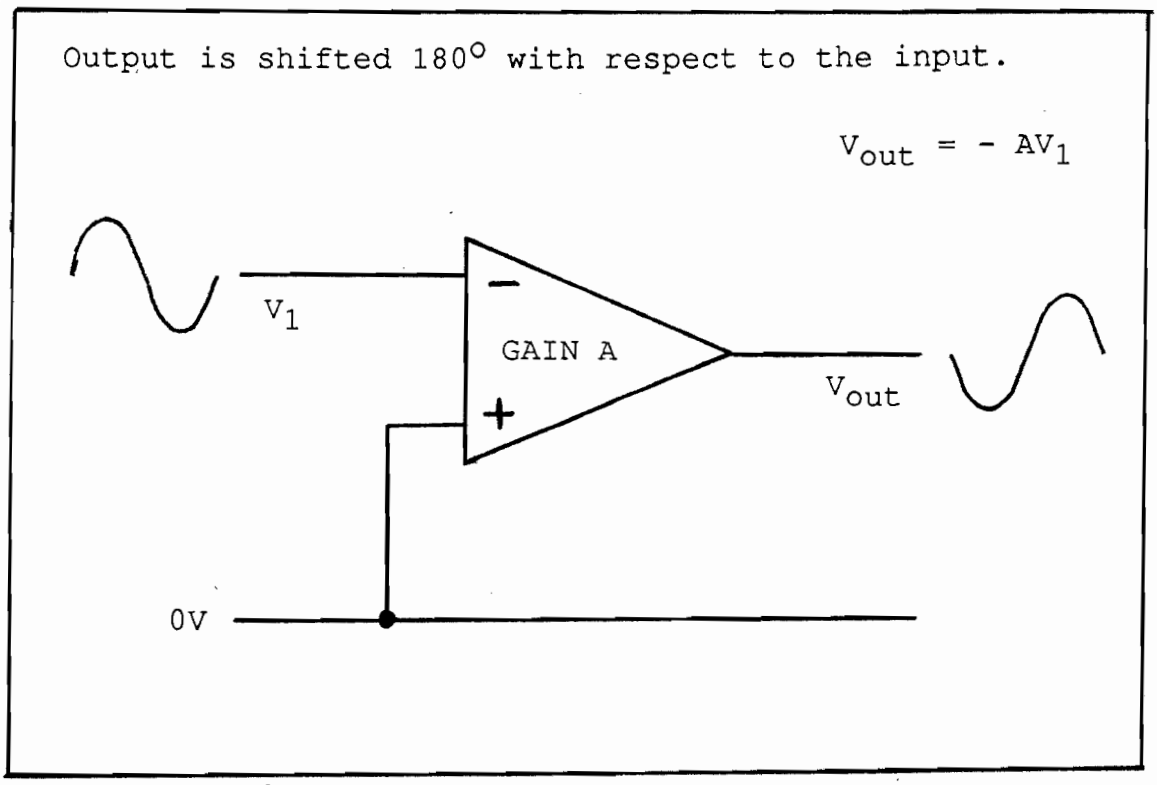

Fig. 2.4.3. DC amplifier with a signal applied to the - input and the + input connected to 0 V.

ELECTROMETER OP-AMP DEVICE COMPARISON CHART	OPA128 (JM)	AD515A (JH)	AD549 (JH)	OP-80G
INPUT IMPEDANCE				
RESISTANCE/Ω DIFFERENTIAL/COMMON MODE	10^{13} / 10^{15}	10^{13} / 10^{15}	10^{13} / 10^{15}	10^{13} / 10^{16}
CAPACITANCE / pF DIFFERENTIAL/COMMON MODE	1 / 2	1.6 / 0.8	10 / 0.8	
BIAS CURRENT / fA	±300 MAX	300 MAX	250 MAX	2000 MAX
OFFSET CURRENT / fA	65		50	100
OFFSET VOLTAGE / mV	± 1 MAX	3 MAX	1 MAX	2.5 MAX
OFFSET VOLTAGE TEMP CO. * / μV/°C	± 20 MAX	50 MAX	20 MAX	
CURRENT NOISE f=0.1Hz to 10Hz / fA p-p	4.2	3.0	0.7	
VOLTAGE NOISE f=0.1Hz to 10Hz / μV p-p	4.0	4.0	4.0	
OPEN LOOP GAIN (R_L = 10kΩ) / V/mV	50 MIN (R_L=2kΩ)	40 MIN	300 MIN	75 MIN
MAX DIFFERENTIAL INPUT VOLTAGE / V		± V_S	± 20	
COMMON MODE REJECTION RATIO / dB	80-118	66-94	80-90	50-90
SUPPLY VOLTAGE / V	±5 to ±18	±5 to ±18	±5 to ±18	±5 to ±8
SUPPLY CURRENT / mA	1.5 MAX	1.5 MAX	0.7 MAX	0.325 MAX
SUPPLY REJECTION RATIO / dB	80-120			60-80

* OFFSET VOLTAGE ALSO CHANGES IF THE SUPPLY VOLTAGE VARIES.

Fig. 2.4.4. Selected manufacturers data for a range of DC amplifier electrometer chips currently available.

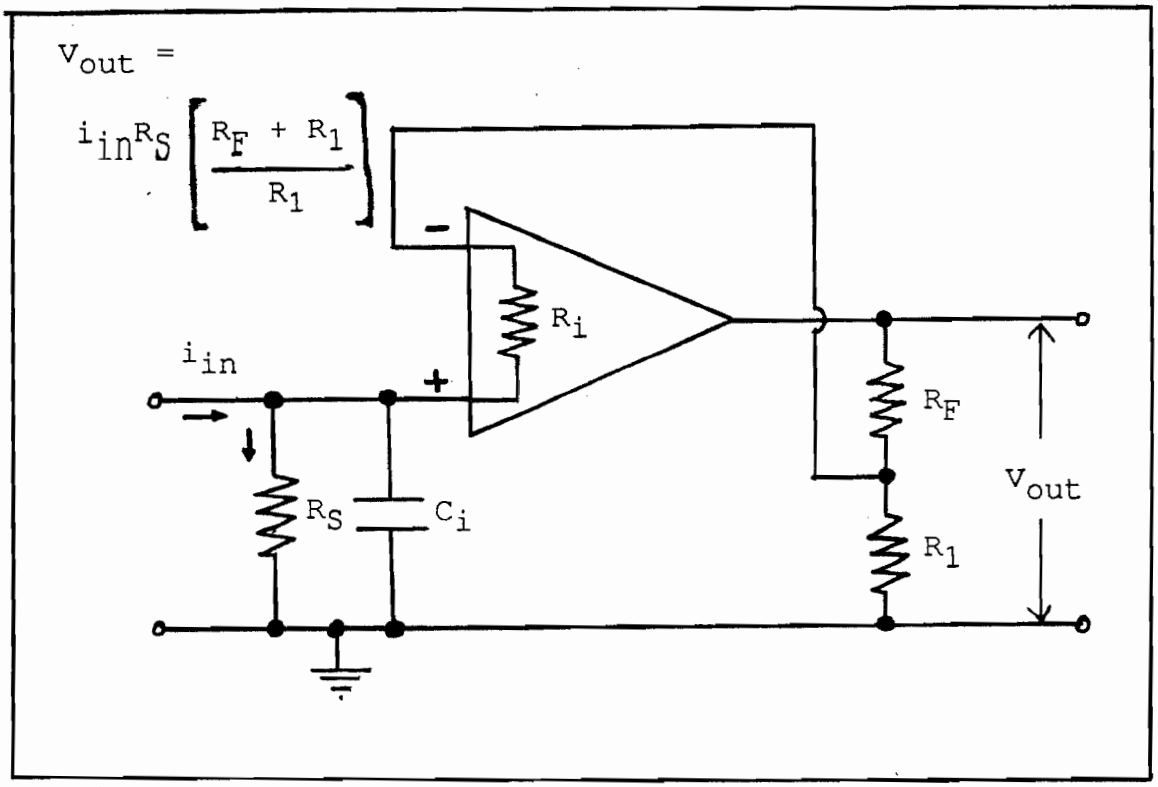

Fig. 2.4.5. Non inverting current amplifier - a shunt picoammeter.

is referred to as a **shunt picoammeter** and the other is in an inverting amplifier circuit (Fig. 2.4.6.), which when used to measure small currents is called a **feedback picoammeter** (Keithley et al.,1984).

(a) The Shunt Picoammeter

As the input resistance of the amplifier, Fig. 2.4.5. is large compared with the shunt resistance R_S all the current at the input flows through R_S, giving an input voltage V_2 of

$$V_2 = i_{in}R_S$$

since the input impedance of the amplifier is high R_F and R_1 form an unloaded potential divider. Therefore V_1 in terms of V_{out} is

$$V_1 = \left(\frac{R_1}{R_F + R_1}\right) V_{out}$$

substituting for V_1 in equation (2.4.1.) it is found that

$$V_{out} = V_2 \left(\frac{R_F + R_1}{R_1}\right)$$

$$= i_{in}R_S \left(\frac{R_F + R_1}{R_1}\right) \qquad (2.4.2.)$$

Notice the amplifier input capacitance C_i in Fig. 2.4.5. and any stray shunt capacity, is in parallel with the shunt resistance, severely limiting the frequency response of the amplifier. If $R_S = 10^{11}$ ohms and the total shunt capacity was just 50 pF, then the above amplifier would act as a first order low pass filter with a time constant C_SR_S = 5 seconds. Thus the circuit would take over 15 seconds to fully respond to a current step input (see Appendix A2.2.).

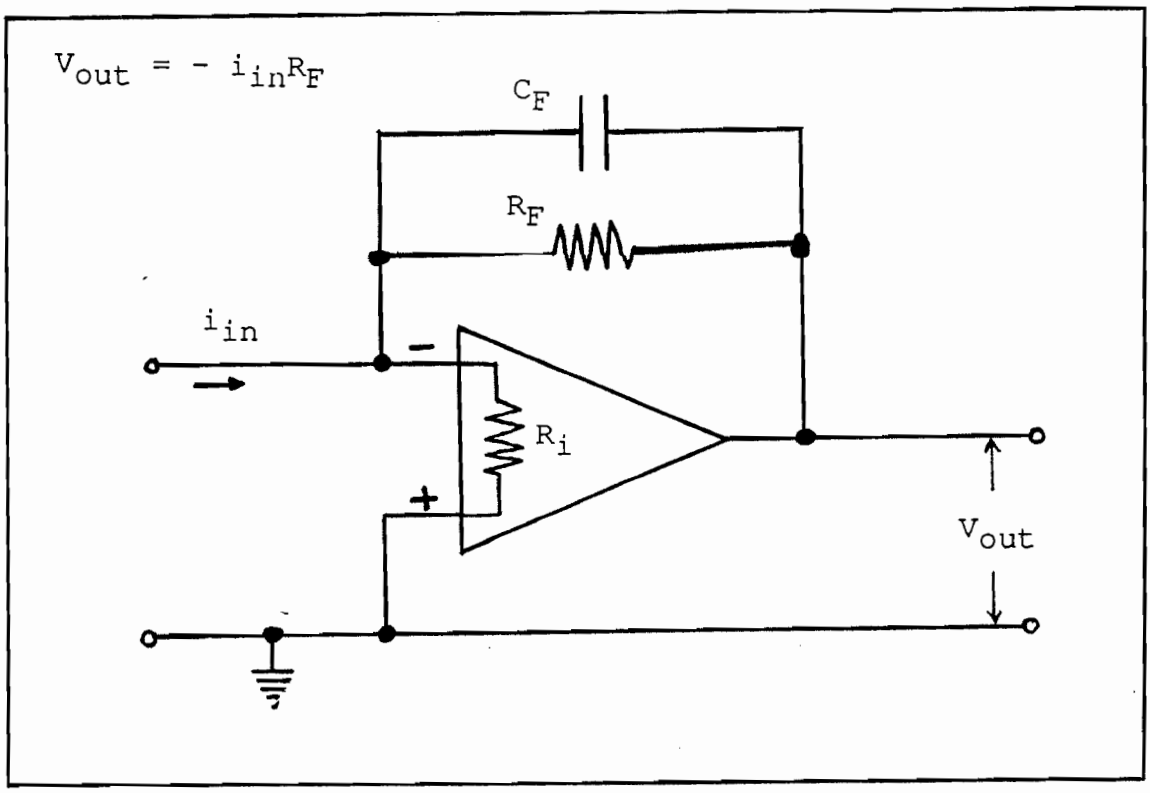

Fig. 2.4.6. Inverting current amplifier - Feedback picoammeter.

(b) The Feedback Picoammeter

In the circuit in Fig. 2.4.6. the input current i_{in} flows through the feedback resistor R_F. Assuming the amplifier is ideal, the voltage across R_F is $i_{in}R_F$ and simple analysis using ohm's law shows that

$$V_{out} = V_1 - i_{in}R_F \qquad (2.4.3.)$$

Since $V_2 = 0$ it follows that $V_{out} = -A\ V_1$ from equation (2.4.1.) and so rearranging gives

$$V_1 = - V_{out} / A. \qquad (2.4.4.)$$

Substituting this back into equation (2.4.3.) gives

$$V_{out} = -(V_{out} / A) - i_{in}R_F$$

and so

$$V_{out}\ (1 + 1/A) = - i_{in}R_F$$

and since $A >> 1$,

$$V_{out} = - i_{in}R_F \qquad (2.4.5.)$$

Thus equation (2.4.5.) shows that the output voltage is directly proportional to the input current, which is why the circuit is often called a **current to voltage converter.** The sensitivity of the circuit is determined by the feedback resistor R_F.

If the op amp gain A is made very large, then as can be seen from equation (2.4.4.) V_1 becomes very small and in fact almost equal to 0V. This is why the inverting input in this circuit is often referred to as a **virtual earth.** Having a only a negligible voltage across the input terminals reduces the effect of the input shunt capacity on the frequency response of the circuit. The

rise time of the amplifier is now limited by the $C_F R_F$ feedback network. However the stray feedback capacity, C_F is usually much smaller than C_S giving a significant improvement in frequency response over the shunt picoammeter.

2.5. Drift and Noise in DC Amplifier circuits

2.5.1. Drift

Amplifier drift is an important problem with direct coupled measurements. AC signals can be amplified without worrying about changes in the zero level of the circuit, but this is not true for the measurement of slowly varying signals where changes in the zero level of the circuit can not be distinguished from changes in the input signal.

When measuring small currents using a dc amplifier electrometer output drift will arise from changes in the input offset voltage (V_{io}) and the input bias current (i_b), due to changes in temperature, supply voltage and component aging.

2.5.2. Noise

Noise in the output of any circuit has many origins. For example mains hum pick up, resistor Johnson noise, and various internal DC amplifier noise sources. The noise may be split up into current noise (i_n) and voltage noise (V_n) (Barker,1979).

Thus the full equation relating current in to voltage out for a non-ideal feedback picoammeter (Fig. 2.5.1.) is

$$V_{out} = - i_{in}R_F - i_bR_F - i_nR_F + V_{io} + V_n \qquad (2.5.1.)$$

This includes the output offsets, due to the bias current (i_b) and input offset voltage (V_{io}) and noise made up of current (i_n) and voltage noise (V_n). If the total noise (V_{tn}) of the circuit is defined by

$$V_{tn} = V_n - i_nR_F$$

and the total output voltage offset (V_{vo}) is defined by

$$V_{vo} = V_{io} - i_bR_F$$

then equation (2.5.1.) reduces to

$$V_{out} = - i_{in}R_F + V_{vo} + V_{tn} \qquad (2.5.2.)$$

2.5.3. Compensating for drift

If the input current is removed, the output voltage changes and simply equals the output voltage offset plus noise. If this voltage is subtracted from V_{out} in equation (2.5.2.) a voltage V_C is obtained which directly proportional to i_{in} and independent of V_{vo}.

Thus $V_C = - i_{in}R_F$

Notice that this will only work if the circuit noise levels are low. This only compensates for drift in the output voltage offset; the circuit will still drift slightly because R_F will change with temperature.

$$V_{out} = - i_{in}R_F - i_bR_F - i_nR_F + V_{io} + V_n$$

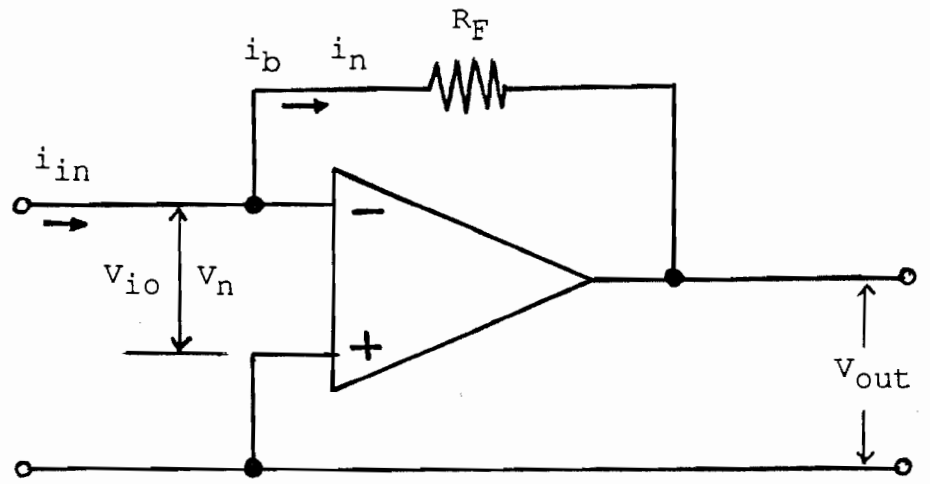

Fig. 2.5.1. Non ideal feedback picoammeter.

3. Instrument design, construction and testing.

3.1 The design of the old Gerdien condenser

The Gerdien condenser that I adapted was originally built for an atmospheric science course that was discontinued several years ago. The electrometer amplifier used was a varactor bridge type (manufactured by Burr-Brown) intended for use as a non-inverting amplifier. The circuit was a very simple one and is shown in Fig. 3.1.1.

The electrometer had a zero control which consisted of a multiturn potentiometer connected to the offset null terminals of the amplifier. The large feedback resistor was found to be very nearly 10^{11} ohms when I measured it with a Keithley electrometer (model 602) using the external voltage method. (I used this resistor later in my own electrometer design). The amplifier had a gain of 100, so that a current of 10^{-13} amps would give an output of 1 volt.

There was a reed switch connected across the input from the central electrode to earth. A magnet manually placed on the outside of the electrometer housing could be used to short the electrometer to earth. Once this had been done the polarization voltage could be switched without damaging the sensitive amplifier.

There had been a lot of difficulties with using the varactor bridge electrometer. Although these devices normally have good drift stability, they do drift excessively after being overloaded (Barker,1979). I did

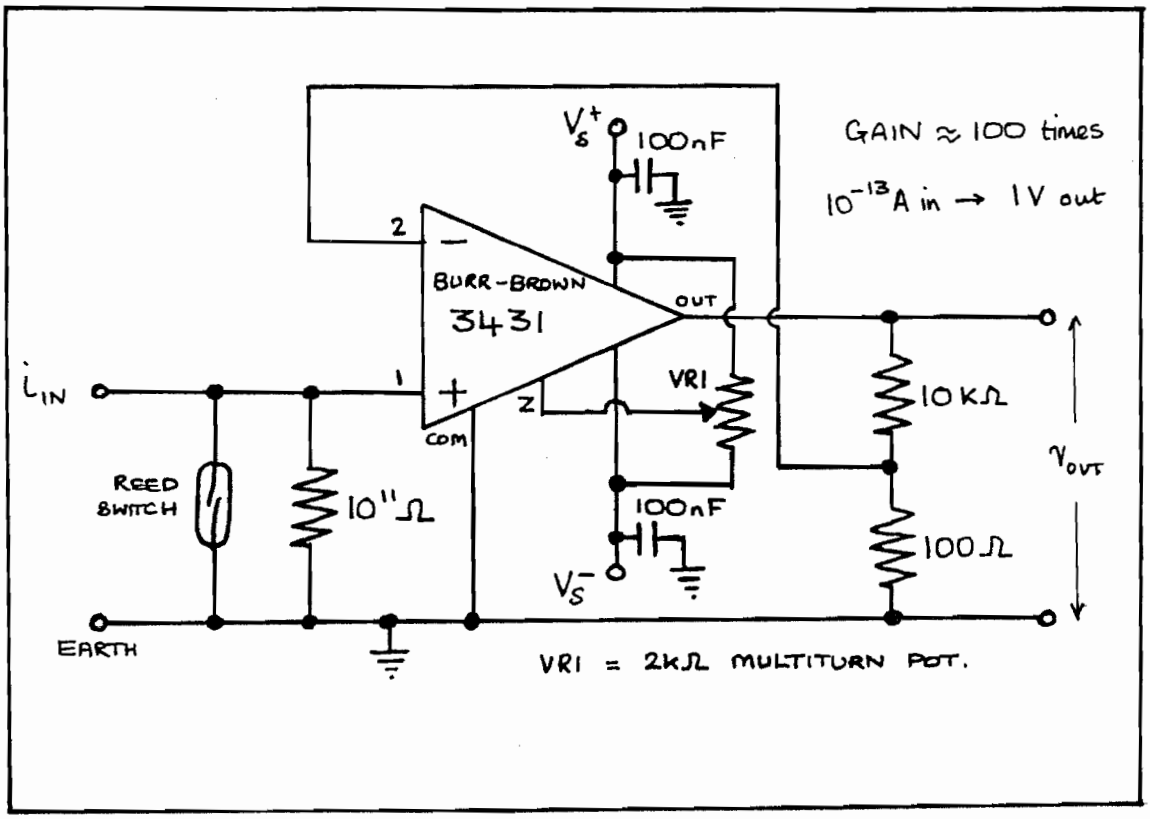

Fig. 3.1.1. Circuit diagram of the electrometer amplifier previously used with the condenser.

not attempt to use it and decided to design and build a new electrometer for the Gerdien condenser.

The Gerdien condenser had been constructed without a guard being placed between the central electrode and the outer polarized cylinder. The metallic guard is used to separate the insulating material in contact with the central electrode, from that in contact with the outer cylinder. It is maintained at a potential close to that of the central electrode, but at much lower impedance. The guard is used to help reduce the error currents that might otherwise flow across the insulator. For example if the polarization voltage was 20 V and say the measured conductivity currents where of the order 10^{-13} A, then an insulator resistance of 2×10^{15} ohms would lead to an error current just 10 times less than this, that is 10^{-14} A.

3.2 Design of the new Instrument

As we have seen the size of the conductivity currents measured depends on a number of factors: the volume density of ions, their mobilities, the polarization voltage and also the exposed capacity of the apparatus. Thus the size of the currents measured depends to some extent on the design of the apparatus itself.

3.2.1 Initial Measurements

Initially I used a Keithley electrometer (model 602) to measure the conductivity currents from the Gerdien condenser. At this stage, I had two objectives in mind,

the first was simply to get some idea of the size of the currents obtained and the second was to see over what range, the conductivity current was proportional to the polarization voltage. A guard had already been fitted to the Gerdien condenser by this time. A low impedance battery source was used for the polarization voltage; this was in order to minimise noise pick-up by the central electrode via the outer polarized cylinder. The currents had to be measured via a short length of high quality screened cable. The cable had to be kept still while the measurements were made since spurious noise currents were generated when it moved. This is due to the piezo-electric effect (Keithley et al., 1984). The set up was in fact very similar to that used by Moore and Vonnegut (1988).

Measurements of conductivity current were made using polarization voltages up to 50 volts. These results are plotted in Fig. 3.2.1. As can be seen the conductivity current is very nearly proportional to the polarization voltage up to at least 40 volts or so.

An estimate for the air conductivity in the physics lab was made. From equation (2.2.5.)

$$\lambda = i \varepsilon_o / C_e V_p$$

Using the formula for a cylindrical capacitor (see section 4.1.1.) C_e was found to be 22×10^{-12} F. As the current for a polarization voltage of 20 volts was 4.4×10^{-13} amps the conductivity was equal to

$$\lambda = 8.9 \times 10^{-15} \text{ ohm}^{-1} \text{ m}^{-1}$$

Fig. 3.2.1. Graph of conductivity current against voltage

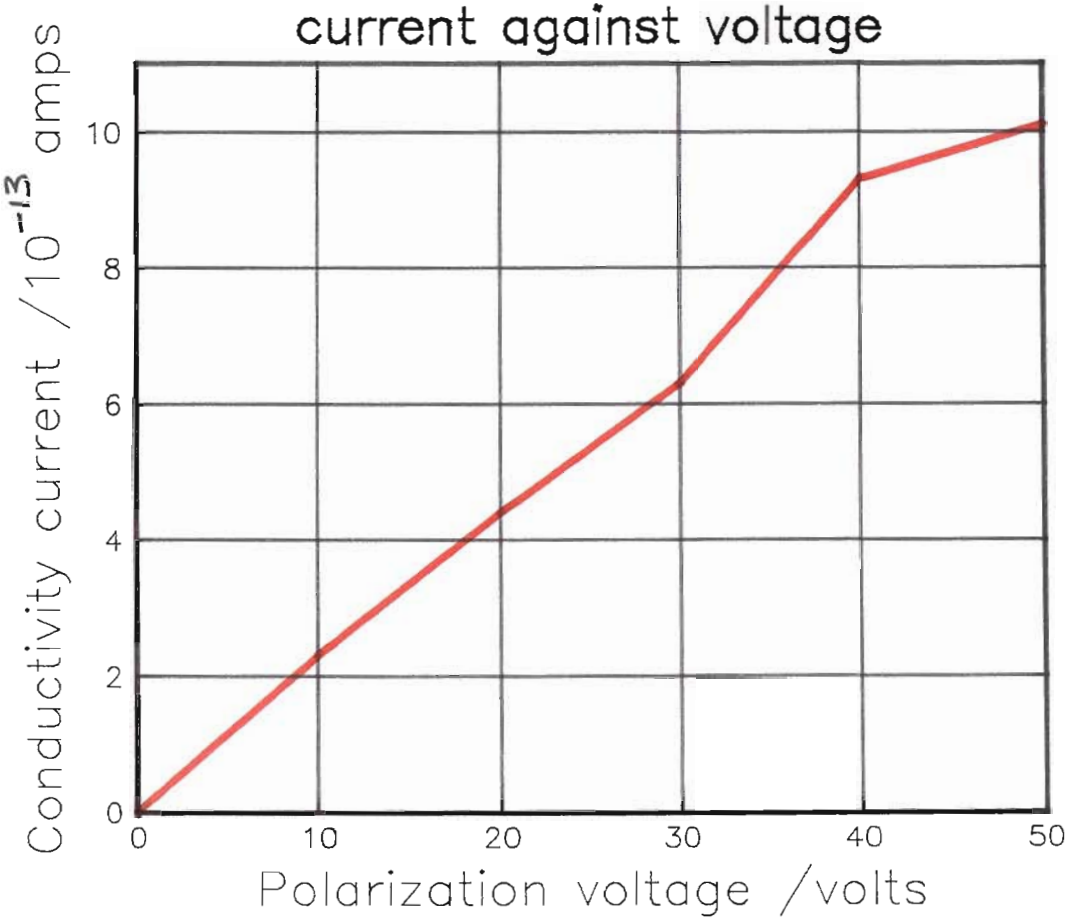

3.2.2. Computer Controlled Conductivity Measurements

In order to use a single Gerdien condenser unit to measure both positive and negative conductivities over time it is necessary both to switch the sign of the polarization voltage and to short the electrometer while this is done, to protect it from the large current surge as the bound charge on the capacitor is either released or stored. Also to compensate for drift the picoammeter output voltage offset needs to be measured. In the case of the Gerdien condenser, the output voltage from the picoammeter needs to be measured with positive polarization, negative polarization and zero polarization. I have labelled these respective output voltages V_{PP}, V_{NP} and V_{ZP}. With positive polarization, the positive ion current is measured, with negative polarization, the negative ion current is measured and with zero polarization the output voltage offset is measured. Therefore the respective currents can be calculated, with compensation for output offset drift, using the following formulae

$$V_{PP} - V_{ZP} = - i_P R_F \qquad (3.2.1.)$$

$$V_{NP} - V_{ZP} = - i_N R_F \qquad (3.2.2.)$$

The electrometer can shorted, while the polarization voltage is changed, by placing a switch across the feedback resistance, R_F. The minimum number of steps required to measure both the positive conductivity current (i_P) and the negative conductivity current (i_N) are:

1) Short R_F

2) Switch polarization off

3) Open short

4) **Measure V_{ZP}**

5) Short R_F

6) Switch to negative polarization

7) Open short

8) **Measure V_{NP}**

9) Short R_F

10) Switch to positive polarization

11) Open short

12) **Measure V_{PP}**

and then back to 1 if the cycle of measurements is to be repeated.

There is therefore a minimum of 12 steps required to complete one cycle of measurements. This series of operations would be very tedious to do manually, but if the apparatus is computer controlled it becomes very easy. As well as controlling the apparatus the computer can be used to log both the results and the time of the measurement.

From the outset I had decided to use a BBC micro (model B) as the control / datalogger computer, with a disc drive unit connected for data storage. The BBC micro amongst other things is equipped with a user port and an analogue to digital converter, both of which can easily be put under software control. (Coll, 1982; Bray et al., 1983)

(a) The BBC user port

The user port is an 8-bit bidirectional port that can be used either to accept control information (read mode) or to control devices under software command (write mode).

By using the command *FX151,98,255 all eight lines can be put into the write mode. Then the command *FX151,96,N (where N is an integer between 0 and 255) can be used to latch any combination of the lines to either logic 1 (4.8V) or logic 0 (0.4V). Thus writing *FX151,96,0 would cause all 8 lines to be latched at logic 0 and by writing *FX151,96,255 all lines would be latched at logic 1.

The outputs from the user port cannot be directly used to control devices such as relays, since the outputs can only supply about 1mA and even low current relays need about 30mA or so to operate them.

(b) The Analogue to Digital Converter (A/D converter)

The BBC micro has 4 A/D converter channels. The circuit diagram of the A/D converter is shown in Fig.3.2.2. The important point to note is that the voltage reference (V_{ref}) for the A/D chip is provided by three IN4148 signal diodes which give a combined voltage drop of 3 x 0.6 = 1.8V. These three diodes were replaced by a more stable 1.2V bandgap reference diode. On installing the bandgap reference V_{ref} was measured using a digital voltmeter and was found to be 1.237 V. The A/D converter will only measure voltages in the range 0 to V_{ref} (in fact to just a little below V_{ref}) and since I

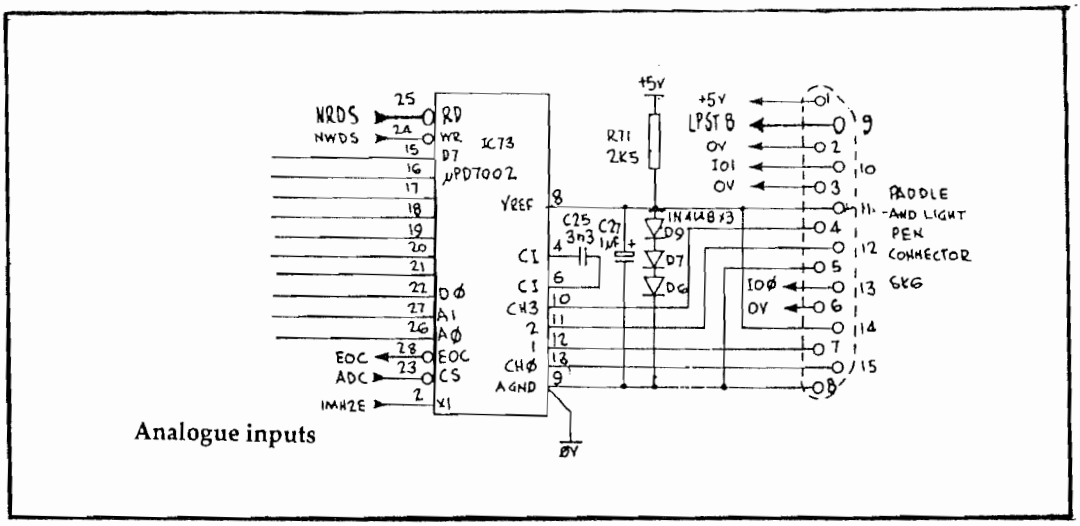

Fig 3.2.2. The A/D converter circuit diagram. From Coll(1982).

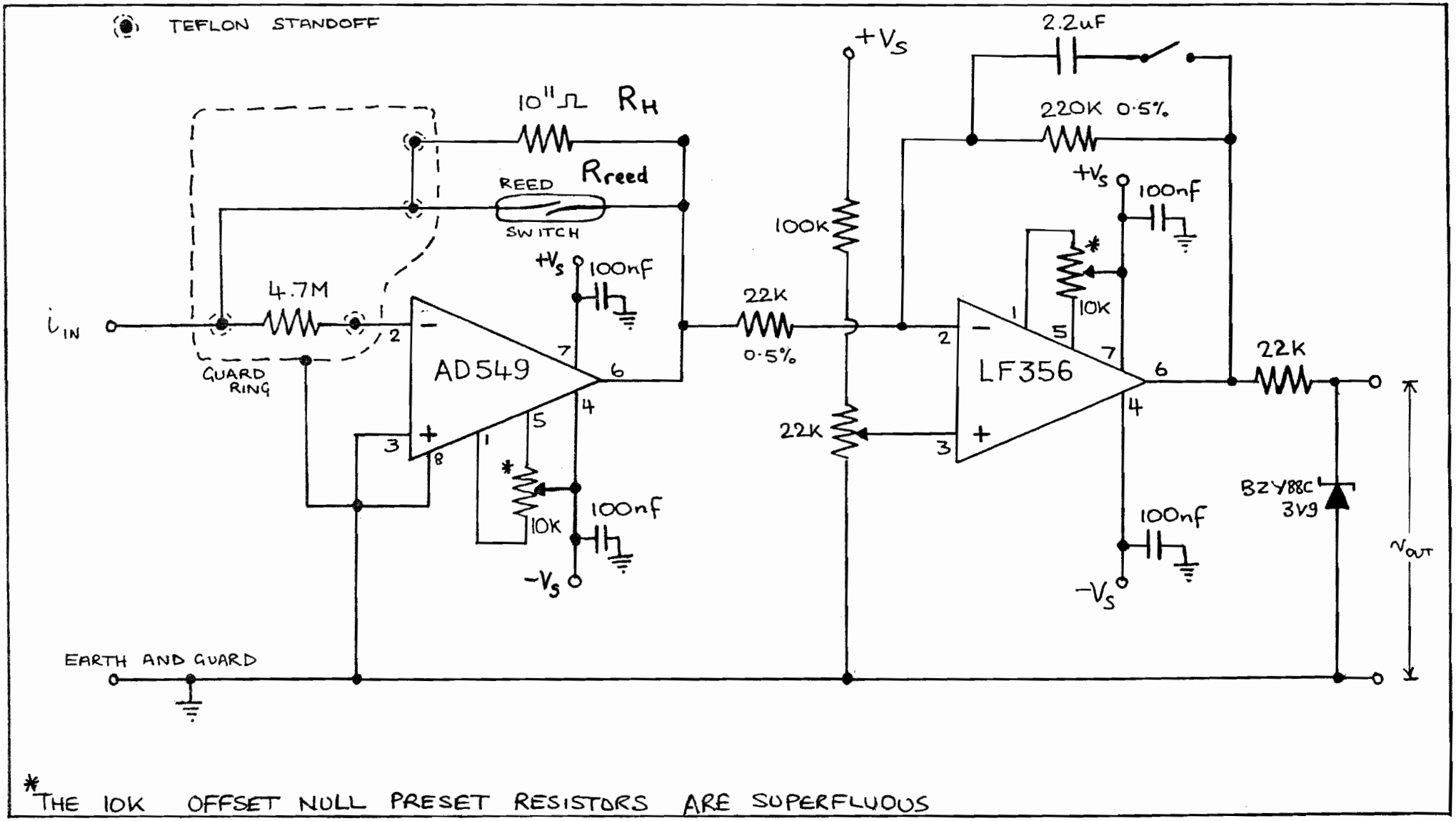

Fig. 3.2.3. Circuit diagram of the picoammeter designed for use with the condenser.

(a) The Reed Relay

The reed relay was needed to short the high value resistor R_H so that the polarization voltage could be reversed without disturbing the amplifier. Reed switches are high impedance switches the contacts of which can be closed by bringing a magnet near to the glass case. The reed chosen was a readily available type bought from RS components. The reed was specified to have a resistance (R_{reed}) of greater than 10^{11} ohms. However after cleaning I found it to have a resistance of greater than 10^{12} ohms (see section 4.1.2.). The total feedback resistance is a parallel combination of R_H and R_{reed}. A specially designed reed operating coil was also initially used.

(b) Input protection

Although some devices have internal input protection, most electrometer IC's need some sort input protection arrangement. For example the monolithic FET operational amplifier (AD549J) that I used must be protected against the destructive currents that can flow if the signal voltage moves outside the limits set by the power supply rails. Protection is easily achieved by placing a large resistor inside the feedback loop of the electrometer amplifier (Fig. 3.2.3). This has virtually no effect on the operation of the circuit apart from the addition of resistor Johnson noise to the amplifier input noise. For the AD549J, a continuous overload current must remain below 100uA and a transient overload (less than 1

second) must remain below 1mA (see data sheet). Thus the 4.7 mega-ohm resistor used in the circuit gives an over-voltage protection of up to 470 volts and a transient over voltage protection of well over 4000 volts, assuming the resistor does not breakdown. The resistor will protect the electrometer against damage if the polarization voltage should become shorted to the central electrode and against static charges should the central electrode be touched.

(c) Output conditioning circuitary

A second inverting amplifier was added with a voltage gain of 10 and a DC offset of roughly 0.6V, midway along the A/D converter measurement range. Thus positive currents at the electrometer input lead to a voltage greater than 0.6 V and negative currents lead to a voltage smaller than 0.6 V. A capacitor can be switched in across this second op amp so that it becomes a half a second time constant, low pass amplifier. There is a 3.9V zener diode across the output to limit the maximum circuit output voltages to -0.6V and +4.0V.

3.2.4. Instrument control circuitary

The design and of the control circuitary was fairly straight forward and is shown in Fig. 3.2.4. The relays used for changing the polarization voltage were operated using a 12 V supply and a current amplifying transistor switch, controlled by the computer via the user port. The relays required about 30mA to operate them. The reed

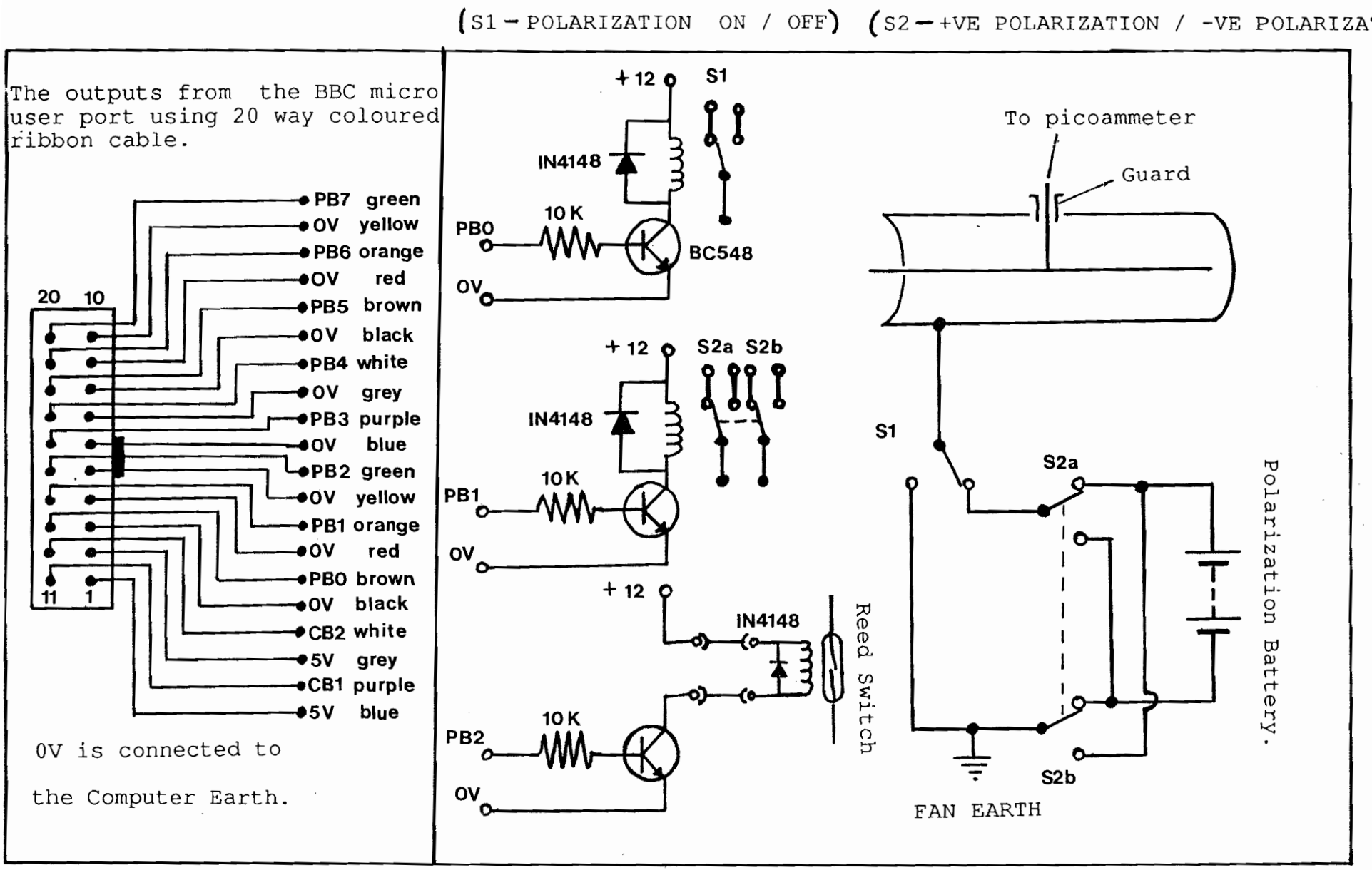

Fig. 3.2.4. Diagram to show the instrument control circuitary.

switch coil was also operated using a computer controlled transistor switch with the same twelve volt supply. The twelve volt supply used was completely independent from the picoammeter power supply in order to minimise picoammeter circuit disturbance when the reed and relays were used.

The Gerdien Condenser and picoammeter were earthed through the fan mains lead. The computer earth was kept separate by isolating the reed and relay control circuitary from the other measurement circuitary and by connecting the zero volt line of the A/D converter to the fan earth, instead of the computer earth.

3.3. Construction of the picoammeter

The picoammeter circuit was constructed on a double sided printed circuit board. Only the bottom side of the board was etched , the component side was used as an earth plane to help with screening. See Fig. 3.3.1. for the printed circuit board design. Teflon standoffs were used for the high impedance connections, but otherwise all the components were soldered in the normal way.

The circuit board was mounted in a diecast box with a square hole made in the base through which the central electrode and guard could protrude, when the unit was mounted on the condenser. Two five pin DIN sockets were used to make external connections. One was used for the double rail power supply and the other was used for the reed switch control line. Two toggle switches were mounted externally, one being the electrometer on/off

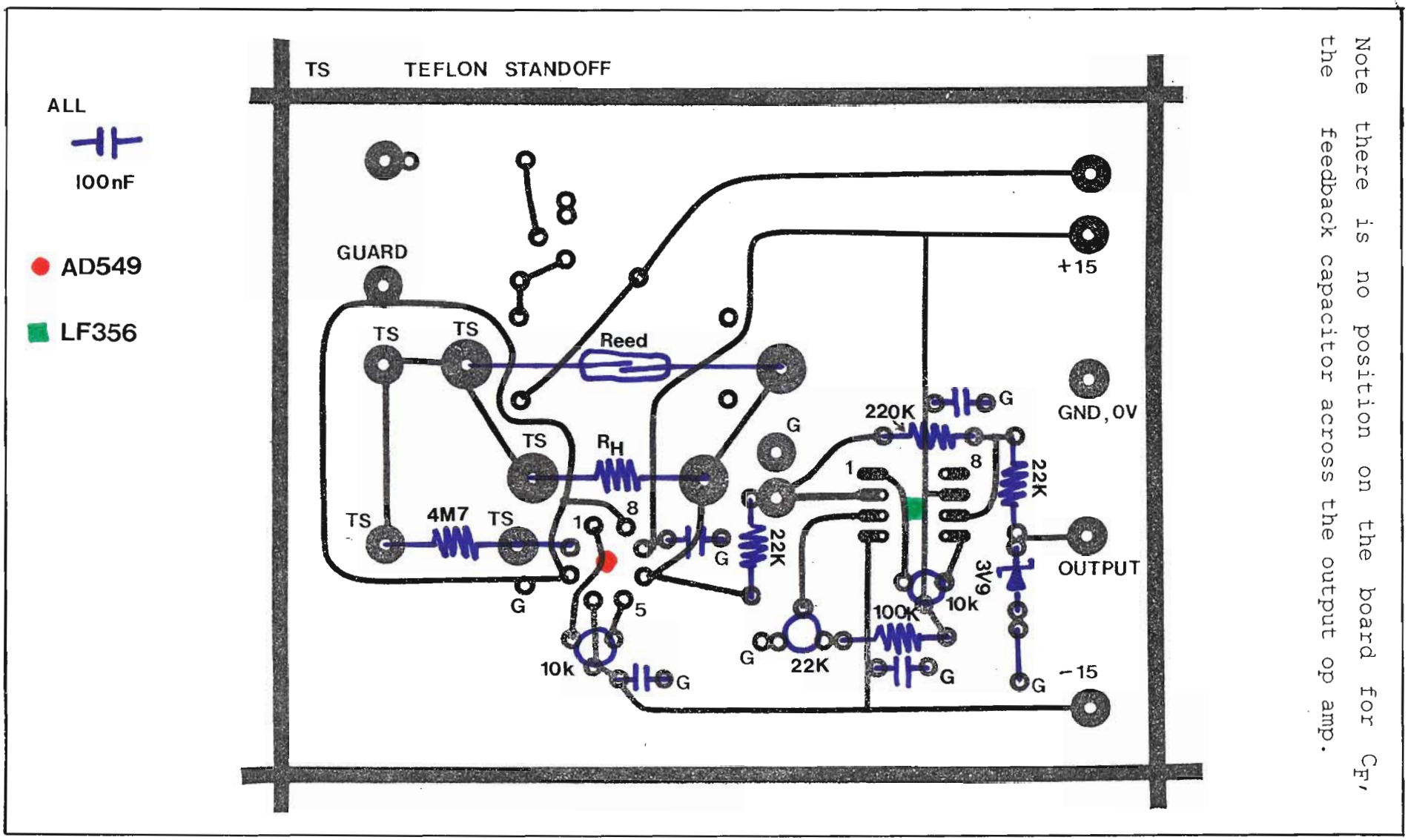

Note there is no position on the board for C_F, the feedback capacitor across the output op amp.

Fig. 3.3.1. Printed circuit board design as would be seen from above with component layout. Enlarged from original size of 110mm x 85mm.

switch, the other being the low pass filter on/off switch.

3.4. Testing and Development

I initially used the reed switch within its specially designed coil. The coil was operated using a 12 volt supply switched on and off under computer control.

However it soon became clear that there was a major problem with this circuit; when the reed switch was opened in order to make a reading a large current spike was produced at the electrometer input. This large transient took several seconds to die away. The problem was soon traced to the reed control voltage; although nominally at 12 volts, if this voltage was varied while the reed was open, the electrometer output voltage would change, showing that a current was being generated in its input stage. Thus the reed control voltage was capacitively coupled to the electrometer input. If the stray capacitance C_S was of the order of 1pF and the reed control voltage varied at a rate of 1 volt/second then the current generated at the electrometer input would be given by,

$$i = C_S \frac{dV}{dt}$$

and is equal to 1 picoamp using the values given above. This was of the order of magnitude of the currents being measured.

Now consider the circuit in Fig. 3.4.1. When the reed switch is closed the stray capacity C_S stores a

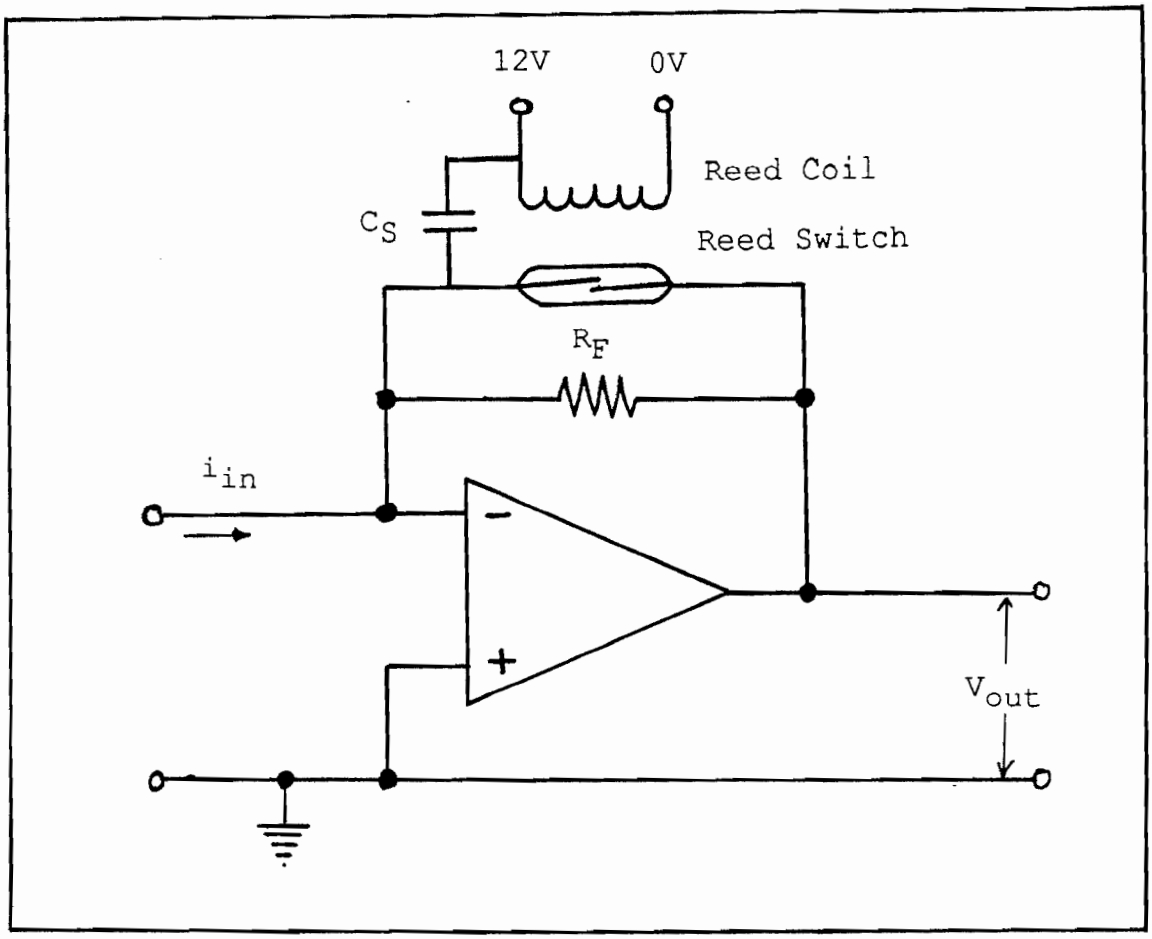

Fig. 3.4.1. Diagram to show the stray capacity between the reed coil and the picoammeter input.

charge $Q = C_S V$ where V is the potential difference between the electrometer input and the coil voltage, 12 volts in this case since the electrometer input is at virtual earth, that is at zero volts.

When the coil operating voltage is turned off the stray capacity C_S can easily discharge as long as the reed remains closed. However the reed opens before the coil operating voltage falls to zero and the remaining bound charge held by C_S can then only flow through R_H producing a current spike at the input. It is a negative going spike since the bound charge is negative.

In order to eliminate this current spike I decided to electrostatically screen the reed operating voltage from the high impedance input. This was done by encasing the coil inside a brass screen and bringing the control voltage to the coil via a screened lead. Since brass is paramagnetic the operation of the reed switch was not impaired in any way. Brass was chosen simply because it is easy to solder.

Having done this the current spike on opening the reed switch was substantially reduced. However there was still a residual positive going spike. This transient was far less serious since it died away much faster, within a second. Thus with the electrostatic screen in place the picoammeter was now suitable for use. I did not have time to investigate the source of the positive going spike, however it could be due to contact potential charging (see Appendix A3.2.).

3.5. Computer measurement and logging of the results

3.5.1. Measurement of picoammeter output voltages

I had decided to use a complete measurement cycle time of one and a half minutes; measuring V_{ZP}, V_{NP} and V_{PP} in turn for twenty five seconds each. The half a second filter limited any high frequency signal content and the signal was sampled about 1500 times over each 25 second period. The average and standard deviation of these measurements was found and recorded. Before each of these measurements there was a five second gap to allow time for the polarization voltage to be changed. Once the electrometer had been shorted, after the previous measurement 25 second measurement had been made, the output voltage was measured briefly before the polarization voltage was altered. Using this measurement I had hoped to see any change in both the input offset voltage and the bias current. This was not entirely successful since the measured voltage depended to some extent on the magnitude of the 25 second measurement made before, however the effect was minimal after the measurement of V_{ZP}. Therefore only one in every three of these measurements was correct.

3.5.2. Logging the results on a computer disc

The conductivity data was stored in disc files by the BBC microcomputer. The format of the data file is shown below

```
XXXX29/07/1990XXXX
15:19:00057B059000004
15:19:30060-014000024
15:20:00056+108000015
15:20:30064B059000004
15:21:00060-018000032
15:21:30057+108000023
15:22:00064B059000004
15:22:30060-022000028
15:23:00057+104000016
15:23:30063B059000005
15:24:00060-023000030
15:24:30056+108000018
```

On the first line was stored the date on which the measurements were begun. The data lines below it have the following structure

15:19:00	057	B	059	000	004
(a)	(b)	(c)	(d)	(e)	(f)

(a) This is the time (GMT) measured in hours, minutes and seconds. The BBC internal clock was used and found to be fairly accurate; it lost just over one minute per day.

(b) This is the output voltage with R_F shorted, in units of 10 mV. Only one in every three of these measurements is correct as explained above. For the data given the correct measurement with the amplifier shorted is 60, or 600 mV.

(c) This letter is used to signify the type of polarization used, that is and

- B for zero polarization (V_{ZP})
- \- for negative polarization (V_{NP})
- \+ for positive polarization (V_{PP})

(d) This is the voltage measured for B, -, or + polarization, in units of 10 mV.

(e) This was not used; I had originally planned to continuously monitor the polarization voltage and store the data here.

(f) This is the standard deviation ie $\pm \sigma$, in units of 1 mV. This is a measure of the high frequency noise in the signal.

The data was stored in this raw state to allow for later processing and calibration. In order to allow data transfer to the main frame computer, the data files had to be in ASCII format. This meant the data had to be stored on disc using the BPUT command. See the apparatus control program in Appendix A4.1. and also Coll(1982) and Bray et. al.(1983) for information on the use of this command.

4. Using and calibrating the instrument.

4.1. Calibrating the Gerdien Condenser.

Accurate calibration of the Gerdien condenser is essential if the results of different observers are to be compared with confidence. However ion concentrations are continually changing in any particular volume of a gas due to recombination and production processes, this means that a gas of stable, standard ion content cannot be made and so the calibration of the Gerdien condenser has to be absolute.

From the simple theory outlined in chapter 2 we have seen that the ohmic conductivity, is given by

$$\lambda = i\varepsilon_o / C_e V_p$$

where C_e is the exposed capacitance, V_p is the polarization voltage and i is the conductivity current. Therefore C_e, V_p and i must be known to be able to determine λ .

4.1.1. Determining the exposed capacity.

(i) Analytical Determination of C_e.

The basic form of the Gerdien condenser electrodes approximates to a standard coaxial capacitor (Fig. 4.1.1.), the capacitance of which can easily be found analytically using Gauss's Law and is,

$$C_e = 2\pi\varepsilon_o L / (\log_e b/a)$$

(For proof see for example, Bleaney and Bleaney(1976), p.21)

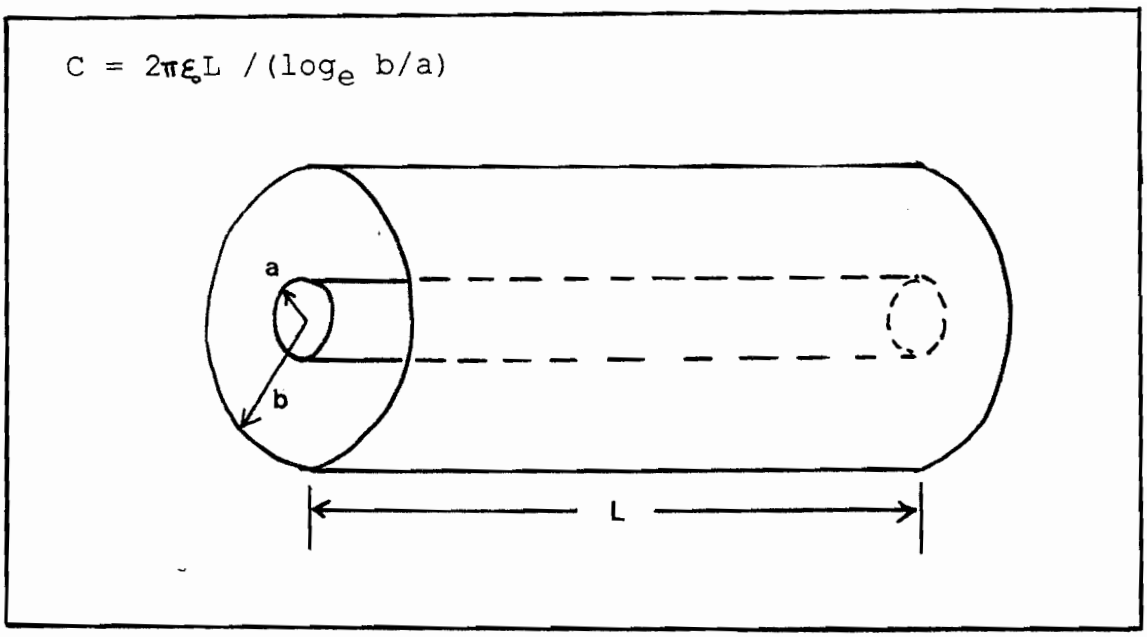

Fig. 4.4.1. The standard coaxial capacitor.

For the apparatus used the values of L, a, and b are approximately:

$$L = 0.80 \text{ metres}$$

$$a = 6 \text{ mm}$$

$$b = 45 \text{ mm}$$

This gives a calculated capacitance of C_e = 22 pF.

However the electrodes in practice will not be of this ideal form and so the exposed capacity will be different to that calculated using the above formula. Usually the central electrode is 'T' shaped (Fig 4.1.2) and so ions are picked up not only by the coaxial bar but also by its support.

Analytically determining this non-ideal capacity is much harder and no one to my knowledge has attempted the calculation.

(ii) Numerical calculation of C_e.

In principle it is possible to calculate C_e numerically and an outline for doing this is given below.

By definition the capacitance of a two conductor system is given by the ratio of the total charge on any one of the plates to the difference in potential between them,

that is $C = Q / V$

However we can restate this since Gauss's Law says that the total flux passing through any gaussian surface is equal to the total charge inclosed within.

Therefore the expression for the capacitance now becomes

$$C = \int \underline{E}.d\underline{A} \; / \; V$$

Using some specified grid it is possible to determine the potential field using the numerical form of Laplace's equation appropriate to the coordinate system chosen. By choosing a suitable gaussian surface surrounding the central electrode it is possible calculate the gradient of the potential field between grid points which lie on either side of it, this gives the magnitude of the electric field perpendicular to the surface. Finally $\int \underline{E}.d\underline{A}$ can be found by multiplying the field by the area of the grid square concerned and then summing across the complete surface.

Although in principle this calculation is possible it would be difficult to ascertain its accuracy in practice. For further information about the use of finite element analysis techniques, see for example Boast(1964).

(iii) Experimental determination of C_e.

The exposed capacity can also be found experimentally, and two similar methods for doing this have been given, one by Gunn(1965) and the other by Smith(1953). The apparatus described by Gunn(1965) had a completely dismountable central electrode system. He measured the total capacity of the electrode system first with and then without the 'T' shaped central electrode in place; the exposed capacity simply being the difference

between the two measurements. This method is much more satisfactory than that outlined by Smith.

However with the apparatus I used it was not possible to measure C_e using Gunn's method because the central electrode was not easily removable. So I decided to determine the exposed capacitance by releasing and measuring the bound charge held on the central electrode. This was possible since the non exposed parts of the central electrode were guarded from the polarization field and thus stored no charge.

In order to make the measurement I replaced the 10^{11} ohm electrometer feedback resistor with a suitable capacitor so that the electrometer circuit was transformed into a high quality current integrator. The feedback capacitor used had a capacity of 45.3 nF, as measured on a digital capacitance meter, accurate to about $\pm$ 1%.

When the polarization voltage was switched off all the bound charge that was previously held on the central electrode was transferred to the feedback capacitor. The voltage rise time was quick enough to obtain a stable output voltage within 2 or 3 seconds.

By finding the voltage increase (10.4 ± 0.2 mV) and multiplying it by the feedback capacitance, the bound charge transferred was calculated to be $(4.71 \pm 0.09) 10^{-10}$ C and as the polarization voltage, V_p, was 19.17 V the exposed capacity C_e, could be found,

$$\text{i.e.} \quad C_e = Q / V_p$$
$$= 23.9 \pm 0.5 \text{ pF}$$

That is about 10% greater than the capacitance calculated above.

4.1.2. Measuring the conductivity current.

In order to accurately measure the conductivity current it is necessary to calibrate the electrometer. The electrometer is made up of basically two circuit blocks, the current to voltage converting input stage and X10 output amplification stage.

The input current is related to the output voltage by the formulae

$$i = (V_{PP} - V_{ZP}) / 10\ R_F$$

$$i = (V_{NP} - V_{ZP}) / 10\ R_F$$

where V_{NP}, V_{PP} and V_{ZP} are defined in section 3.2.2. The factor of 10 is needed because of the x10 gain of the output amplifier and there is no minus sign as the output is in phase with the input. R_F is the feedback resistance and is made up from a parallel combination of the reed switch resistance, R_{reed} and the 10^{11} ohm high value resistor, R_H. I measured the resistance of both these components with a Keithley electrometer (model 602) using the external voltage method; (see instrument manual or Keithley et al, 1984). The voltage I used was roughly 5 volts.

When measuring R_H the external voltage, V_{ex} was found to be 4.99 ± 0.01 V and the measured current was $(5.0 \pm 0.1) 10^{-11}$ A. Since the input resistance of the electrometer was small compared with R_H, its resistance

could be found using ohms law. Thus $R_H = (1.00 \pm 0.02) 10^{11}$ ohms.

In a similar way, although with reduced precision because of its larger value, I found the resistance of the reed switch.

$$R_{reed} = (1.7 \pm 0.3) 10^{12} \text{ ohms}$$

The total parallel feedback resistance R_F is given by

$$R_F = (R_{reed} \cdot R_H) / (R_{reed} + R_H)$$
$$= (9.4 \pm 0.2) 10^{10} \text{ ohms}$$

Both measurements were made after the components had been carefully cleaned using iso-propyl alcohol and before they had been built into the electrometer.

The picoammeter output voltage was measured using the BBC micro A/D converter and the data was stored with a resolution of 10 mV. The gain of the output amplifier was accurately determined by using 0.5% resistors. The 3.9V zener diode placed across the output of the electrometer had low enough a voltage limit to protect the A/D converter, but was large enough so that the gain factor of 10 was accurate to within 1% over the range 0 to 1.2 volts.

Calibrating the amplifier in this way is not practical once the instrument has been constructed, since the resistor and reed switch have to be removed from the circuit, for the measurements to be made. A much better method would be to use a known current source, often called a **current transfer standard.** A design for a portable transfer standard for small dc voltages and currents is given by Landis and Godwin(1982). The

calibration of the finished picoammeter was relative to the Keithley electrometer, which is in effect the calibration current standard for the instrument.

4.1.3. Ion losses in the intake system.

Gunn(1964) made the first investigation of ion losses in the intake systems of different Gerdien condensers. He found that the rather complex intake system used in the conductivity apparatus on the seventh cruise of the research vessel Carnegie (Torreson et al.,1946) reduced the measured conductivity by more than a third as compared with earlier voyages which had used apparatus with much simpler intake systems. He attributed this reduction in conductivity to the removal of small ions by eddy diffusion to the intake walls.

Cobb(1968) experimented further and discovered that the percentage of ions lost depended more on the transit time (velocity / intake length) through the intake system than the amount of turbulence in the air flow. Cobb also suggested that Gerdien condensers with a straight unobstructed intake with a 1:1 ratio of length to diameter should be considered as the measurement standard.

The intake on the Gerdien condenser set up used at Hazelrigg had a right angled bend so that it could be mounted vertically within the field station. The right angle was made of plastic. This would have reduced ion depletion compared to using a metal or foil lined right angled pipe, however it might have led to increased noise

if the plastic was being frictionally charged by the incoming air. No study was made of the effect of different intake designs on the measured conductivity and measurement noise.

4.2. Measurement Drift and noise.

4.2.1. Electrometer Drift and noise.

(a) Drift.

Drift in the output offset level of the amplifier has been compensated for by using sampled measurements as outlined in chapter 3, under the assumption that there was little output voltage noise. However the calibration of the electrometer will drift with time due to changes in the feedback resistance R_F with temperature and aging effects. I had no data on the high value resistance used in the electrometer, however Barker(1979) gives data for temperature coefficients for Victoreen RX1 resistors; the 10^{11} ohm resistor has a temperature coefficient of 0.1 %/^{o}C and thus its would change by 1% for a 10^{o}C change in temperature between night and day. Check on calibration changes due to resistor aging can be made using a current transfer standard, see section 4.1.2.

Ideally the resistance of the reed switch should be at least 100 times larger than R_H, so that the calibration of the instrument is unaffected by any small drifts in resistance it may have.

(b) Noise.

When measuring small currents noise can arise from many sources, both internal and external. Noise pick-up from external sources was initially the most serious problem, however this was reduced to a minimum by improving the screening and making sure the polarization voltage was supplied by a low impedance voltage source.

Screening was improved by filing away paint which had reduced the metal to metal contact between the screening box and its lid and by inserting a wire gauze between the fan and central electrode, to help reduce the pick-up of electrical noise from the fan.

Output voltage noise produced by the Gerdien condenser, during instrument testing at Hazelrigg, is discussed in chapter 5.

4.2.2. Variation in the exposed capacitance.

(a) Capacitance variation due to fan motor vibration.

When a capacitor is vibrated its capacitance will change due to the relative movement of the plates. If there is a voltage across the capacitor a small ac current will be produced. The size of the current is proportional to the applied voltage and the rate of change of capacitance,

$$\text{i.e.} \quad i = V_P \frac{dC}{dT}$$

The currents produced in this way, or indeed piezo-electric currents, since these two current sources in this case can not be separated, were found to be present

but were of a low enough amplitude and high enough frequency to be successfully filtered out. This was done by adding a feedback capacitor to the x10 amplifier to convert it to a one second low pass filter.

If the instrument was being built from scratch I would attempt to reduce the amplitude of the vibration by refining the design of the apparatus. Continuous vibration probably leads to greater measurement drift and reduced component life, as well as increasing instrument noise.

(b) Capacitance drift with time.

Air capacitors open to the free air change in value over time due to:

(a) relative movement of the plates

(b) changes in the permittivity of the air

(c) change with the amount of water adsorbed on the electrode surfaces.

For reasonably rigid constructions these variations appear to be small and measurements only seem to have been made using standard capacitors where the largest changes are not normally greater than 1 part in 1000. (NPL,1969; Ford,1948; Garton,1946). However the air capacitors used in these studies are mostly in the range 1000pF and above and so the results are not necessarily true, in every respect, for capacitances of order 20pF. I have not pursued this matter further and have assumed that changes in the value of the exposed capacitance are

small compared to other sources of error outlined in this chapter.

4.2.3. Currents due to Radioactivity and Cosmic Rays.

During initial testing of the apparatus using the Keithley 602 electrometer connected to a chart recorder, I had observed that when the fan was switched off the output had contained an unexpected a low frequency noise component. The noise consisted of random pulses of current which on average came every two or three seconds. Later I made a more detailed study of this using the computer controlled picoammeter at Hazelrigg Field station.

I made the study at Hazelrigg with the fan switched off and the Gerdien condenser sealed with aluminium foil at both ends. Since my initial measurements I had discovered that these pulses of current could be due to alpha particle decays. In order to test this I made a rough estimate of the amount of charge associated with a single current pulse by finding the area under the one of these pulses on the chart recorder trace shown in Fig. 4.2.1. As shown on the diagram the calculated charge was found to be

$$Q_{pulse} = 9 \times 10^{-15} \text{ C}$$

If it is assumed that a negligible number of the ions recombined, dividing by e, the charge on the electron, will give the number of ion pairs (N) created by the alpha particle. Thus

$$N = 6 \times 10^{4} \text{ ion pairs}$$

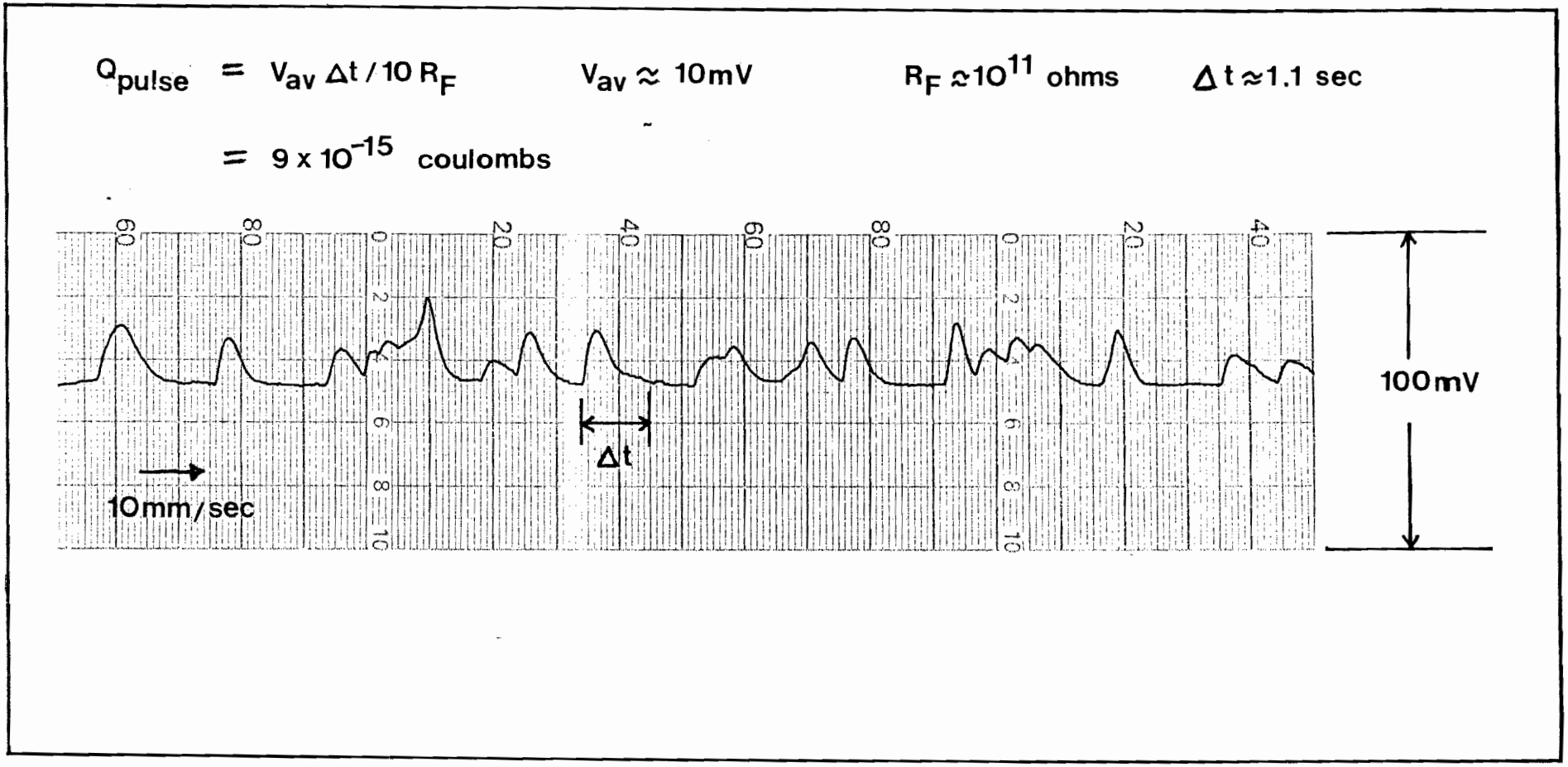

Fig. 4.2.1. Finding the charge associated with a single current pulse from a chart recorder trace giving picoammeter output voltage against time.

The number of ions produced by an alpha particle can be calculated if its initial energy, its path length in air and the ionization energy of the individual gas molecules are known. Israel(1971) gives figures for the ionizing ability of alpha particles from different sources and they are in rough agreement with N given above.*

I tested this idea further by using a weak americium-241 alpha source, placed within the sealed chamber. In Fig. 4.2.2. are traces for both polar conductivities, showing the output from the picoammeter with and without the americium source in the condenser. The source had to be surrounded with aluminium with a small pin hole otherwise the trace went off scale; this was surprising, since when the activity of the source was measured using a Geiger counter it was found to be only 3 counts per sec.

There was also a smaller, more constant, residual current observable which could have been due to a combination of cosmic ray and radioactive B-particle ionization. It was a very small current and was at the limit of resolution of the instrument, so I cannot be completely confident in the correctness of this interpretation. I observed it with the picoammeter connected to a chart recorder.

The current when measured with polarization voltages of both signs was roughly 2×10^{-15} amps. If this current is due to ionization within the condenser, then an associated ionization rate can be determined.

* THE MEASURED VALUE IS ABOUT ½ TO ¼ THE SIZE OF THOSE QUOTED BY ISRAEL(1971)

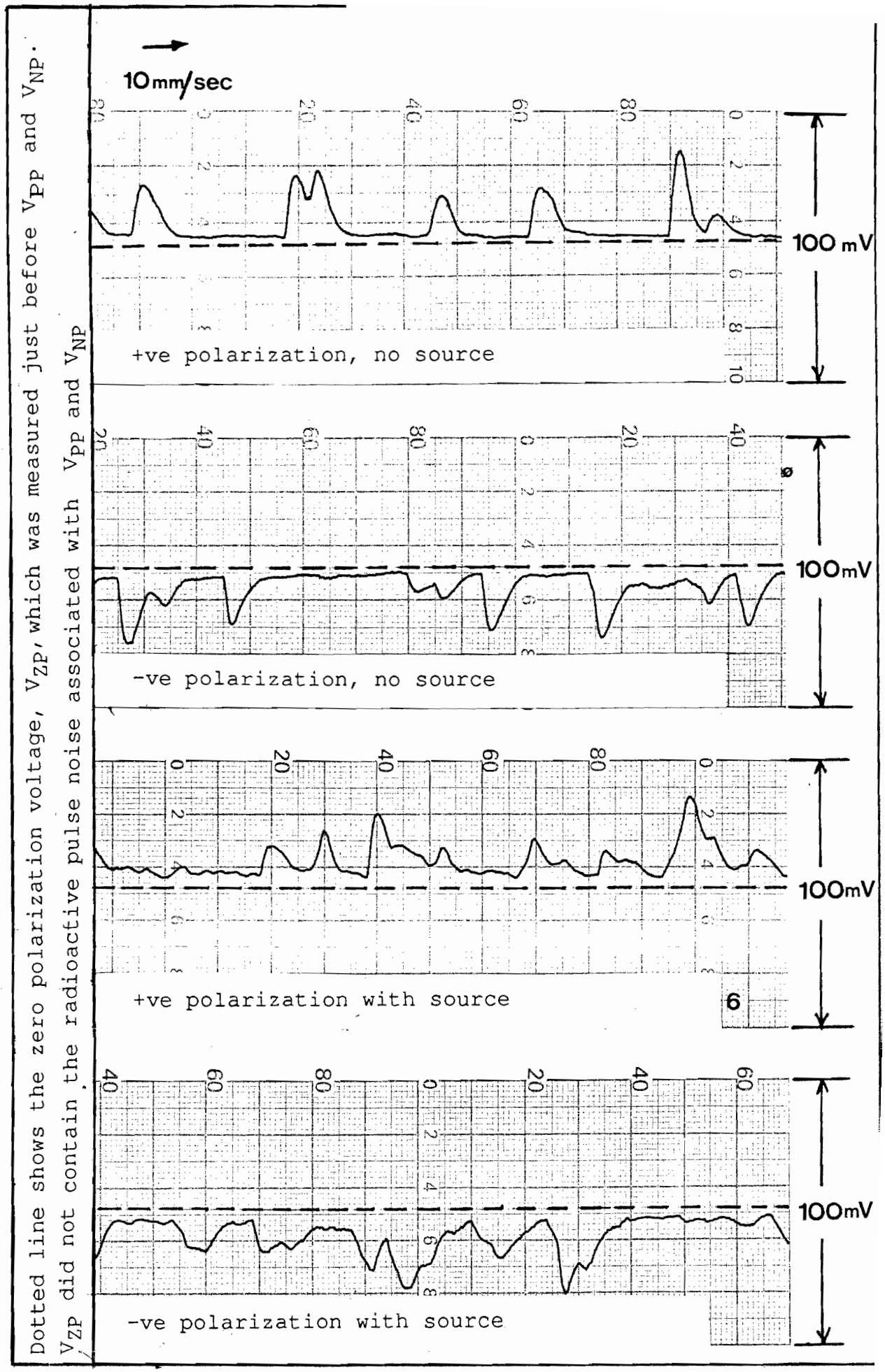
10mm/sec
100 mV
+ve polarization, no source
100mV
-ve polarization, no source
100mV
+ve polarization with source
6
100mV
-ve polarization with source
Dotted line shows the zero polarization voltage, V_{ZP}, which was measured just before V_{PP} and V_{NP}. V_{ZP} did not contain the radioactive pulse noise associated with V_{PP} and V_{NP}

Fig. 4.2.2. Traces showing the output for both polar conductivities with and without the americium source in the condenser.

ionization rate, q = ion pairs formed per cm^3 per second (which do not recombine.)

$$= i\,e\,/\,V$$

where i is the measured current, e is the charge on the electron and V is the volume of air within the sealed Gerdien condenser, which is approximately $\pi b^2 L$.

Therefore the ionization rate, ignoring alpha particle disintegrations is

$$q = 2 \times 10^{-15} / (1.6 \times 10^{-19} \times 5 \times 10^3)$$

$$= 2.6 \text{ ion pairs/cm}^3\text{/sec}$$

This of the same order of magnitude as values of ionization rate given by Israël(1971).

Many observers, such as Gunn(1965), correct for offset error due to these ionization currents every hour or so, without switching off the fan, by using a high voltage capacitor at the entrance to Gerdien capacitor to filter out the in coming ions; thus the instrument just measures the current due to ions generated within the condenser. However I did not regularly measure the ionization currents or make any correction to the conductivity data to allow for them.

4.2.4. Drift in the Polarization voltage.

The drift in polarization voltage appeared to be small over the short time period for which measurements were made at Hazelrigg. The polarization voltage was usually measured at the beginning and end of each

measurement sequence. The computer could be used to monitor it, if there was a possibility that significant drift might occur with large fluctuations in temperature between day and night for example.

4.3. Maintaining adequate insulation

The problem of maintaining adequate insulation is an important and difficult one, especially when measurements are made over long periods of time. For example high humidities* may result in leakage of current across the insulators, thus reducing the measured conductivity current if the central electrode is guarded. To help reduce leakage at high humidities Gunn(1964,1965) used heated insulators, which as a bonus helped deter spiders from building webbs within the central tube. Spiders webbs become good conductors at high humidities and are a serious problem because they can short the polarization voltage to the electrometer input. Although, with protection, the electrometer will not be destroyed all measurements will be lost until the webb is removed. Heavily polluted air flowing through the apparatus may well leave residues on the insulators reducing their surface resistivity.

In order to determine whether or not there are leakage currents flowing across the central electrode insulator, a current source is required (see section 4.1.2.). The electrometer can then be connected to the current source both with and without the central electrode in circuit (Fig. 4.3.1.). Whilst this is done

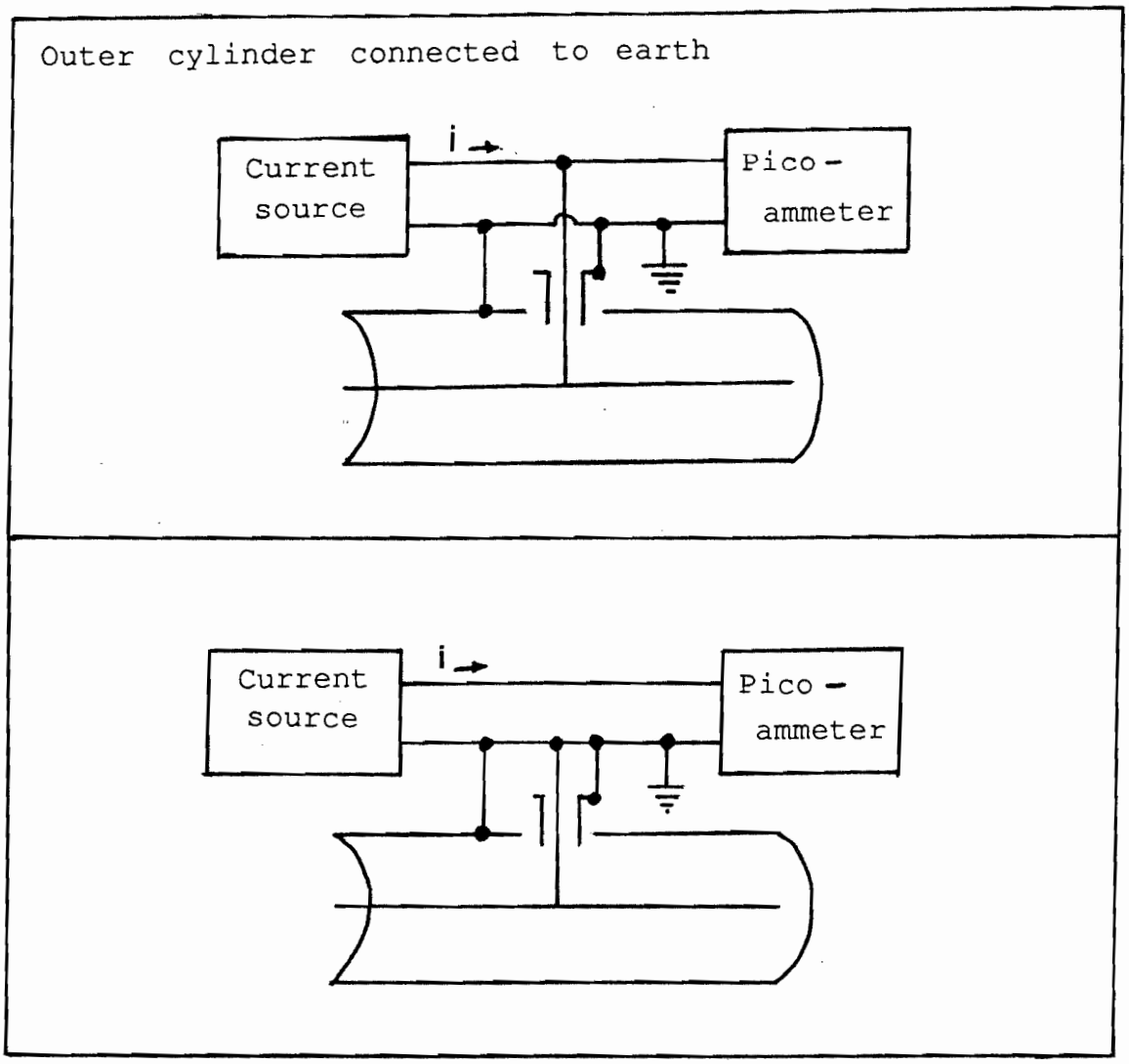

Fig. 4.3.1. Diagram showing a current source connected to the picoammeter with and without the central electrode in circuit.

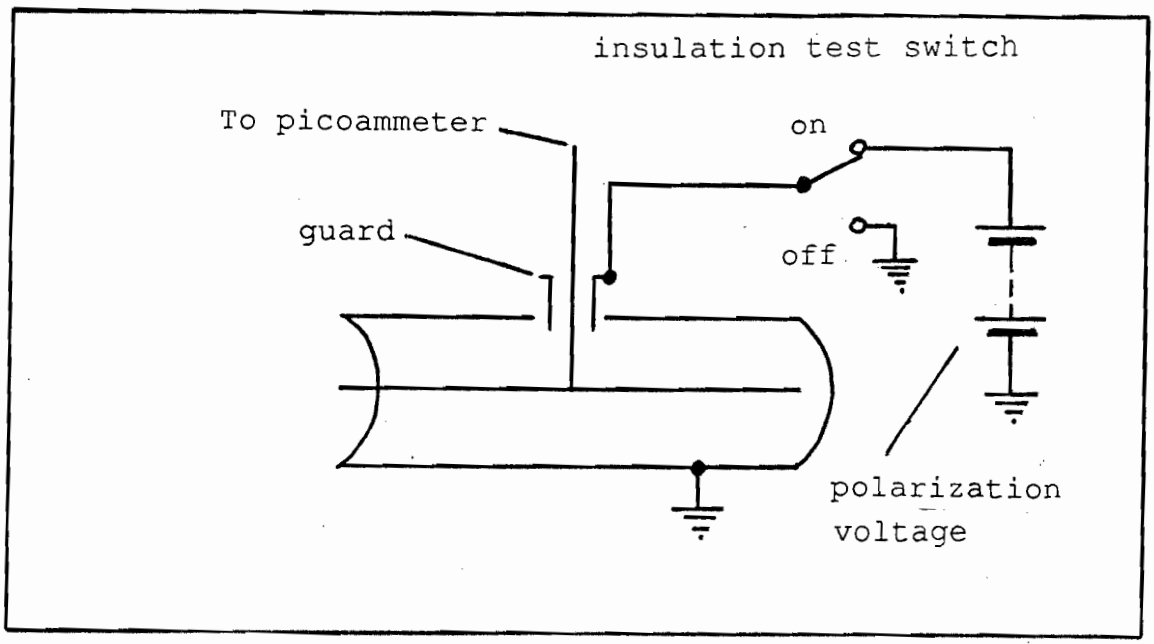

Fig. 4.3.2. Gerdien condenser insulation test using polarized guard.

the polarization voltage and fan should both be switched off and the inlet to the Gerdien condenser can be sealed if excessive wind is gusting through the apparatus. Obviously if the measured current is smaller with the central electrode connected and no spiders webbs have been found, the central electrode insulator probably needs cleaning.

Another much simpler way of doing this is to polarize the guard (Fig.4.3.2.). Leakage currents will then flow across the insulator to the picoammeter. However this cannot be done to often since it will lead to an extra noise source, that of dielectric after-working. (Incidentally the guard is an essential component of the apparatus, if switched polarization measurements are to be made, for this reason alone.)

The PTFE(teflon) insulators used in Gerdien condenser were not designed to be easily and quickly cleaned. Ease of cleaning needs to be taken into account when designing apparatus of this type.

* Recently a mild controversy has arisen over the measurement of atmospheric conductivity in humid air (Moore and Vonnegut, 1988).

ATMOSPHERIC ELECTRICITY INVESTIGATIONS:

THE MEASUREMENT OF ATMOSPHERIC CONDUCTIVITY

JAMES R. ARATHOON

VOLUME 2

This thesis is submitted in partial fulfilment of the requirements for the B.Sc. degree in Geophysical Sciences at the University of Lancaster.

January 1991.

5. Results and data analysis.

5.1. Description of the Results obtained.

The prototype conductivity apparatus was tested at Hazelrigg field station, just to the east of Lancaster University and the M6 motorway. At the field station the apparatus could be left running for long periods of time without being disturbed or tampered with. The condenser was mounted vertically so that by using a plastic 90^{o} bend air could be brought in through a top window, see Fig. 5.1.1.

Measurements were begun on the 21st July 1990. Initially I connected the output of the picoammeter to a chart recorder running at 2mm/min and left the apparatus running for about a day and a half. The polar conductivities and output offset were measured for a minute each, starting at 19.09 GMT. The atmospheric conditions at the time were exceptionally stable with clear skies and little or no convection. The main features of the trace, were a night time peak of conductivity in the early hours of July 22nd and a minimum around 17.00 GMT in the late afternoon of the same day. Samples of the trace are given in Fig. 5.1.3 to Fig. 5.1.5. (Note that the negative polar conductivity voltage, V_{NP}, is more positive than the zero polarization output voltage V_{ZP}, simply because I mistakenly connected the picoammeter to the chart recorder the wrong way round.)

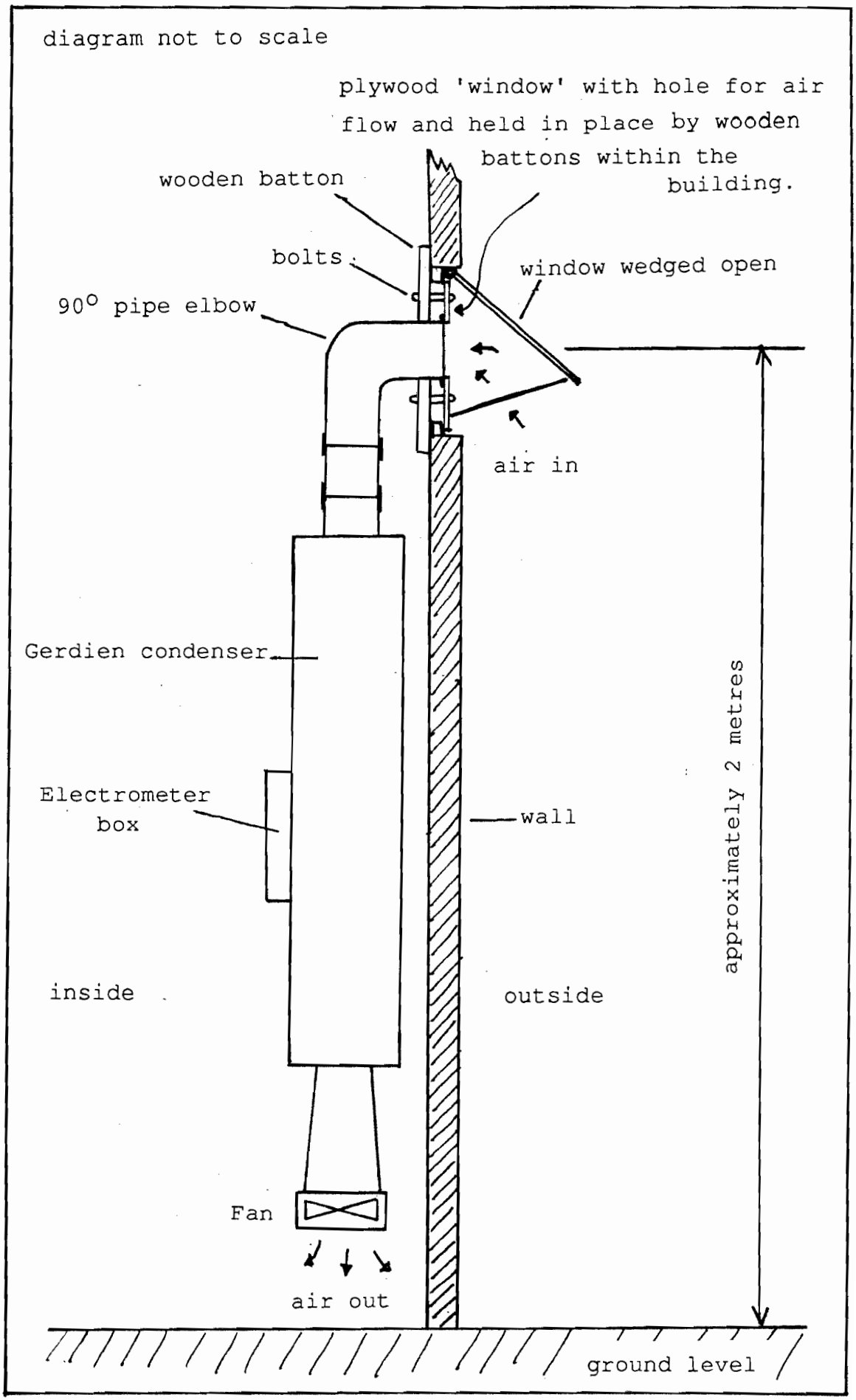

Fig. 5.1.1. Sketch to show the intake arrangement of the vertically mounted Gerdien condenser.

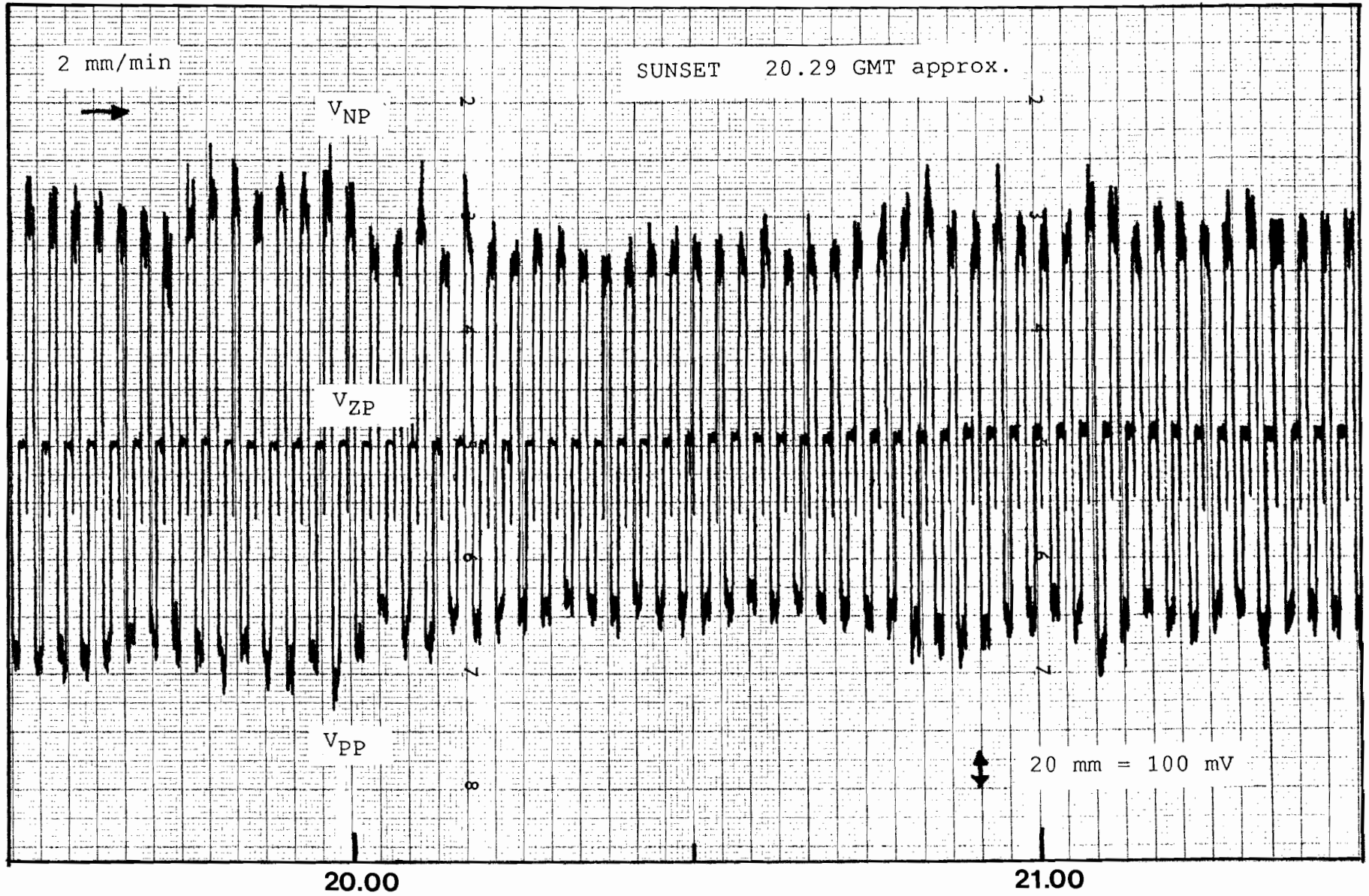

Fig. 5.1.2. Initial uncalibrated trace - readings around sunset between 19.30 and 21.30 (GMT), 21.7.90.

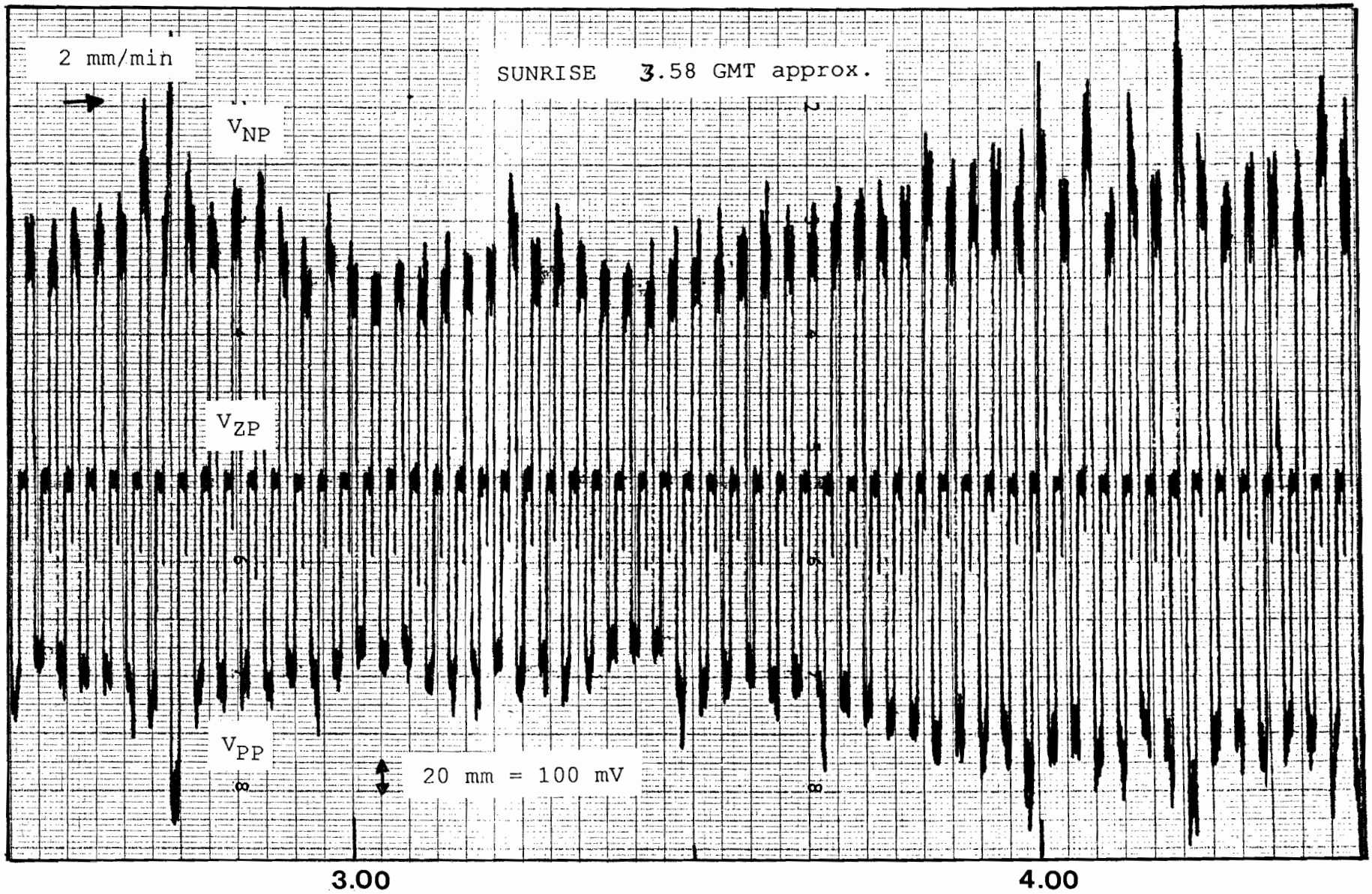

Fig. 5.1.3. Initial uncalibrated trace - readings around sunrise between 2.30 - 4.30 (GMT), 22.7.90.

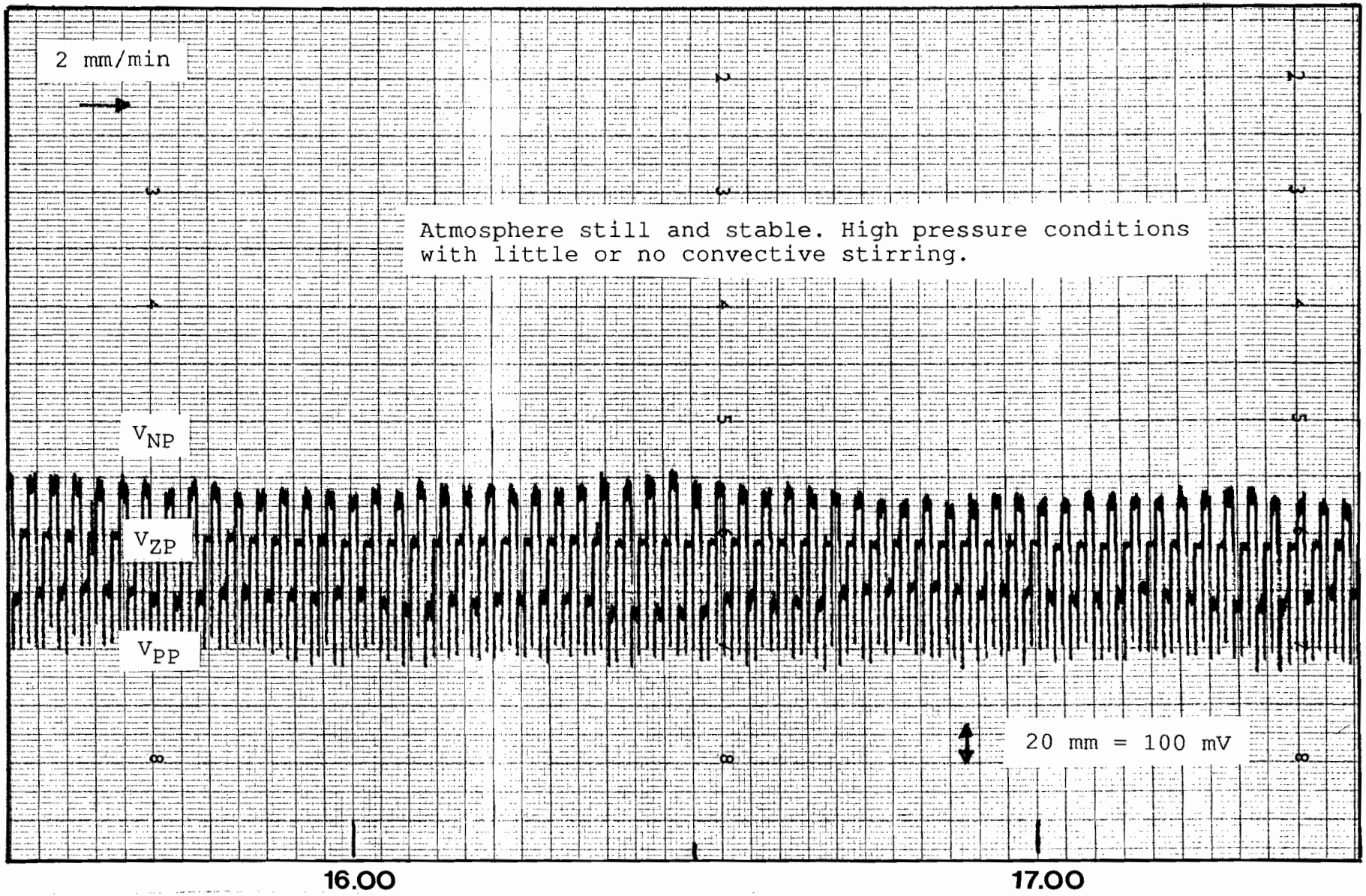

Fig. 5.1.4. Initial uncalibrated trace - readings from late afternoon between 15.30 and 17.30 (GMT), 22.7.90.

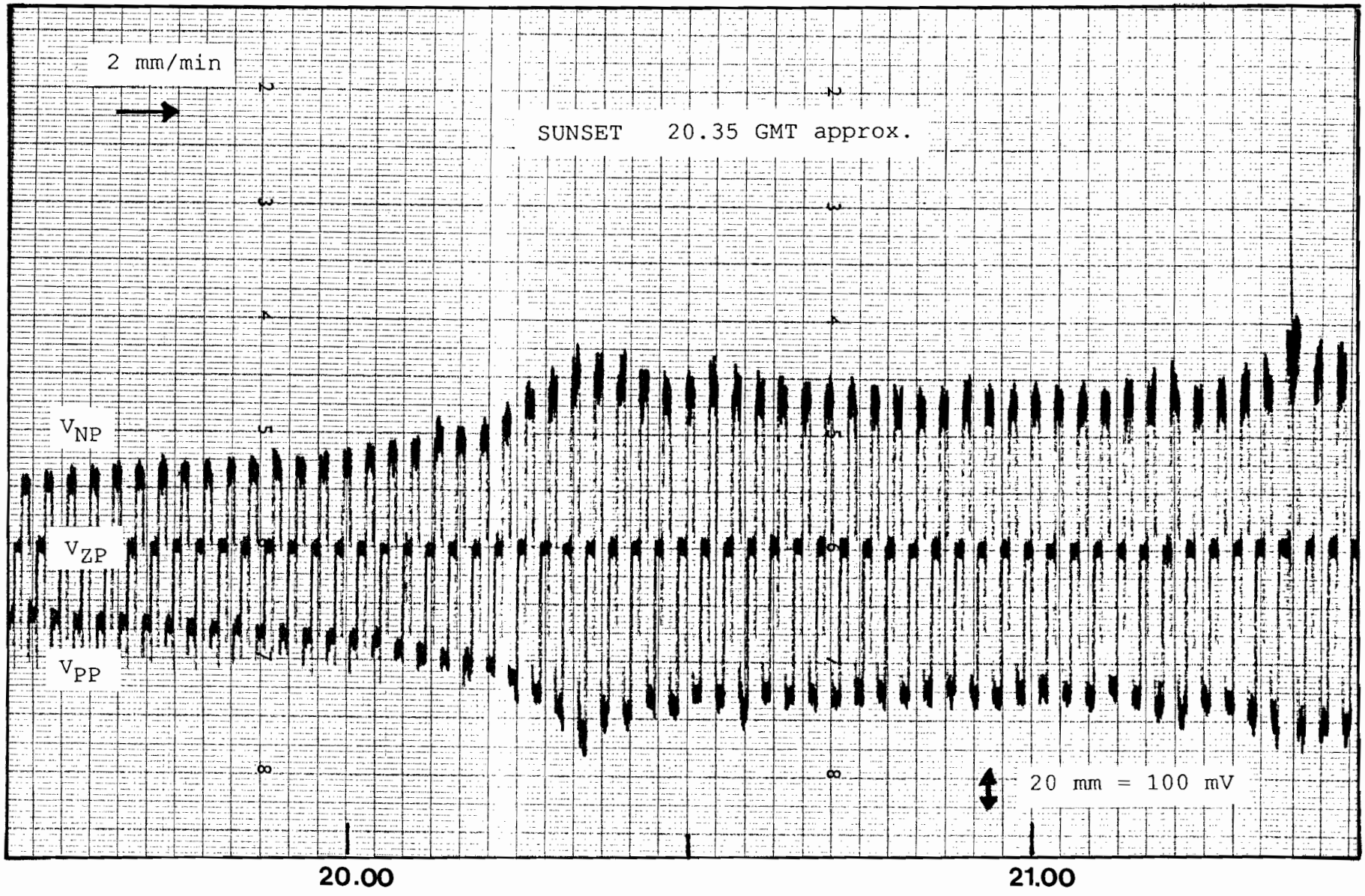

Fig. 5.1.5. Initial uncalibrated trace - readings around sunset between 19.30 and 21.30 (GMT), 22.7.90.

Interesting changes took place around times of sunrise and sunset as shown in Fig. 5.1.2., Fig. 5.1.3. and Fig. 5.1.5. The variation is especially distinctive in Fig. 5.1.3. where in the hour before sunrise the conductivity first drops, then recovers slightly, then drops again and finally recovers to a stable conductivity around about sunrise. A similar variation can just be made out in the sunset conductivities in Fig. 5.1.2. Later computer controlled measurements gave more examples of this effect, shown most spectacularly in Fig. 5.1.8. between 3.00 and 4.30 GMT. I can give no explanation for it. The effect at sunset on Fig. 5.1.5. however did not follow this pattern. Times of sun rise and sunset are shown on each graph (Astronomical Almanac,1989).

The final version of the apparatus control software (Appendix A4.1.) had been completed by the 26th July. Measurements were recommenced soon afterwards and continued to the 1st August. The weather during the whole of this time was dry and calm with no rain, that is fair weather conditions prevailed. However wind speeds were higher and there was some convective activity taking place, as shown by the development of cummuli clouds during the day. The exceptionally stable, hazy, stifling day time conditions found during the initial measurements were not repeated.

A further five long series of measurements were recorded on computer disc, the main details of which are given in Fig. 5.1.6. The data was initially processed and calibrated using the program **datarun.for** given in

FILE NAME	START DATE	TIME INTERVAL (GMT)	POLARIZATION VOLTAGE / volts	NUMBER OF DATA POINTS
AE9011	27.7.90	17.10 - 17.12	9.61	962
AE9014	28.7.90	19.29 - 09.19	19.25	550
AE9015	29.7.90	15.19 - 15.56	19.23	985
AE9016	30.7.90	19.54 - 01.21	19.26	218
AE9018	31.7.90	14.50 - 08.51	19.26	721

Fig. 5.1.6. Table showing the main sequences of coductivity data recorded.

Appendix A4.2. The plotted data is shown in Fig. 5.1.7. through to Fig. 5.1.11. The lower graph shows the variation with time of negative conductivity, positive conductivity and a combined standard deviation for the two measurements. The upper graph shows the variation in the ratio of positive to negative conductivity with time. The data series are all different lengths because more often than not the measurements were stopped prematurely by a BBC micro 'disc full' error. This was not always because the disc was full, but happened because of the way files are stored in spare 'slots' on the disc. If large amounts of data need to be stored it best to use only one file per disc, transfer the data to the mainframe and then re-format the disc before using it again.

Notice that for all the conductivity graphs except the first, the upper limit of measurement is 12 x 10^{-15} ohm^{-1} m^{-1} , just over half way up the graph scale. For the first set of measurements a polarization voltage of 9.61 volts was used, roughly half that used for the other measurements, doubling the upper limit, but giving only half the resolution. Some signal 'clipping' was undoubtedly occurring for example near the end of the conductivity graph in Fig. 5.1.10. and at the very peaks of activity in Fig. 5.1.9.

The most obvious visual characteristic of the data obtained is the difference between the variations during the day and during the night. The day time variations seemed to begin between 6.00 and 8.00 GMT as seen in Fig.

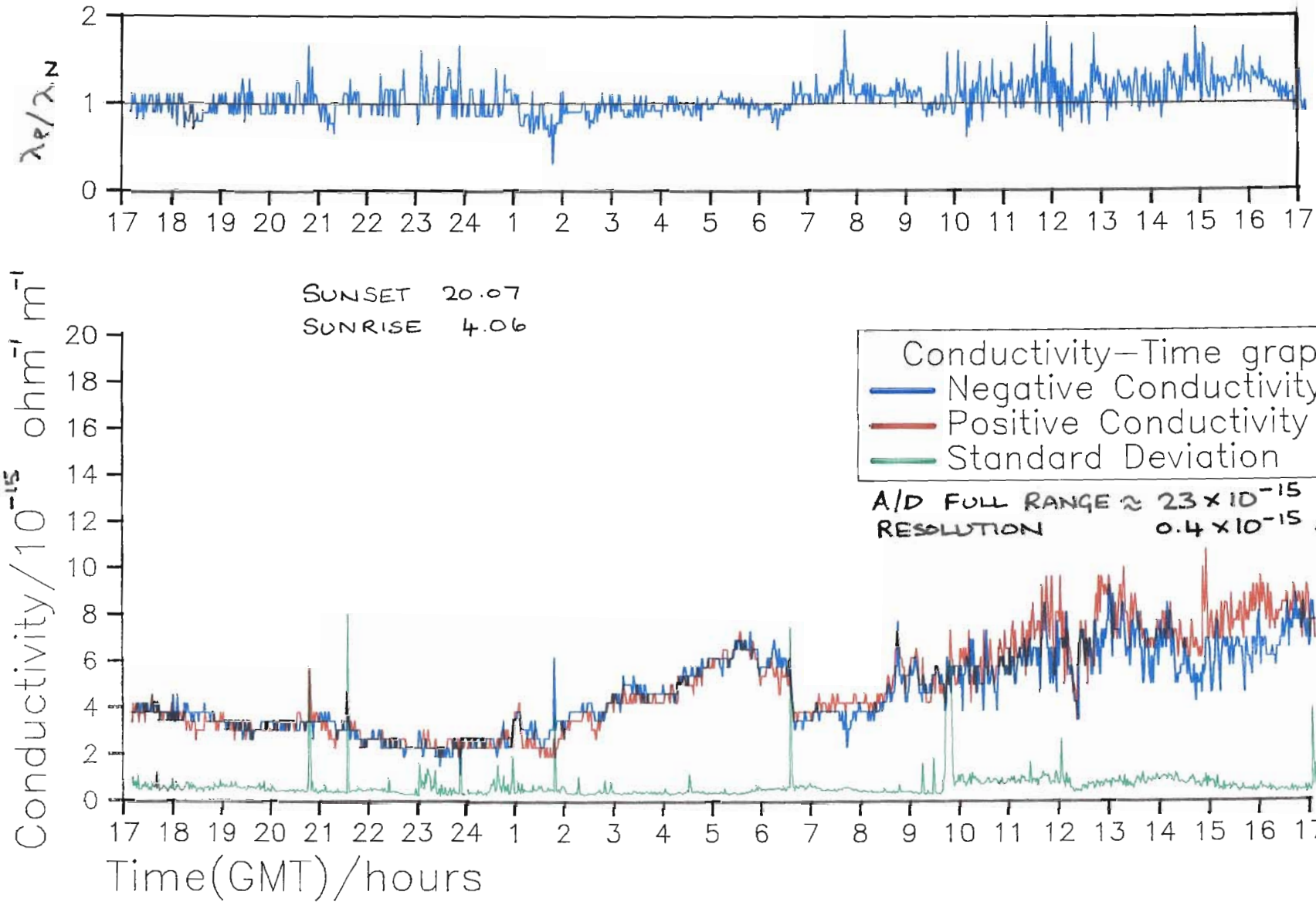

Fig. 5.1.7. Air Conductivity Measurements beginning 27.7.90 : AE9011

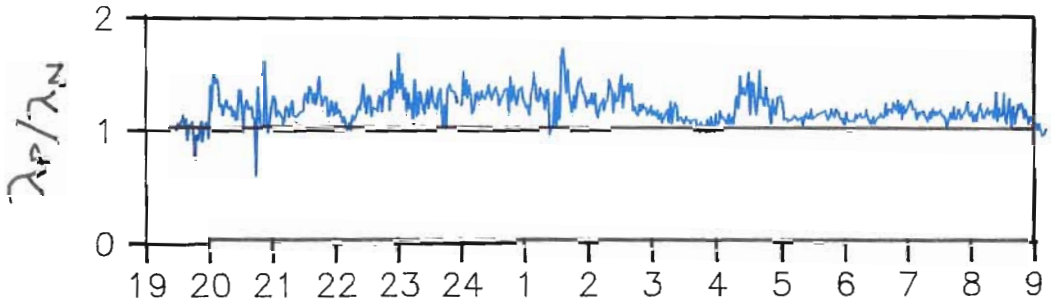

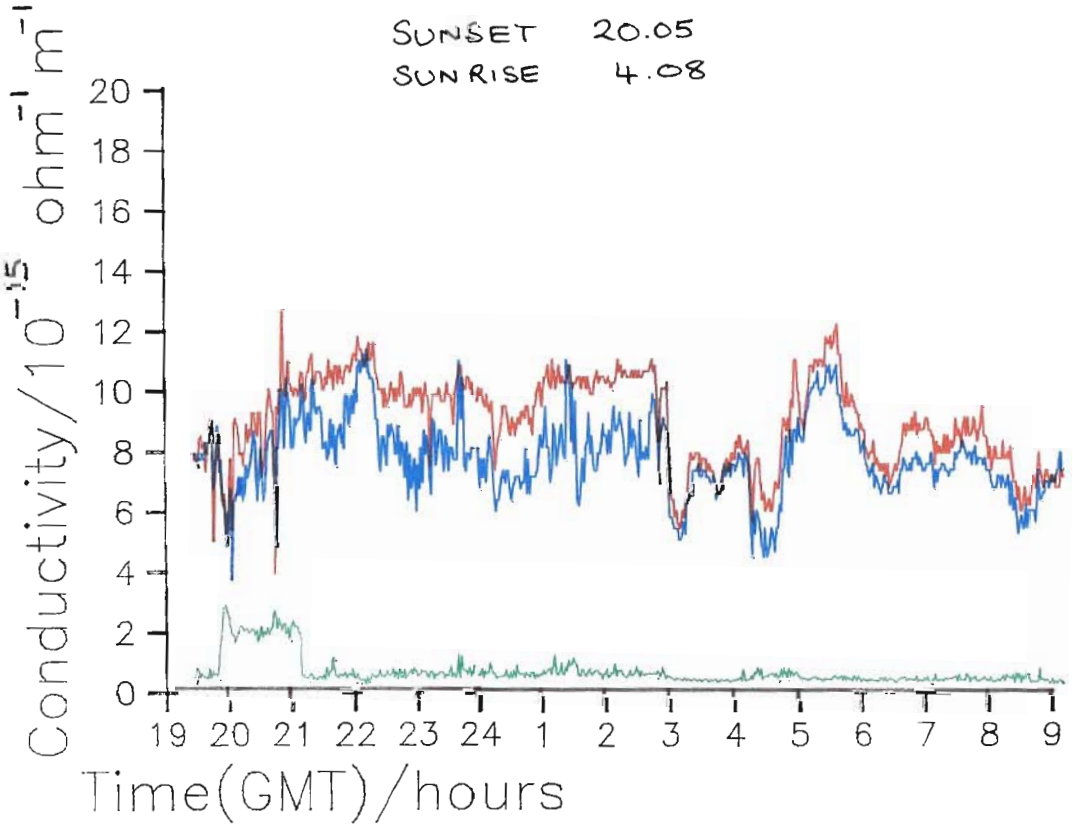

Conductivity–Time graph
Negative Conductivity
Positive Conductivity
Standard Deviation

A/D FULL RANGE ≈ 12 × 10^{-15} ohm^{-1} m^{-1}
RESOLUTION 0.2 × 10^{-15} ohm^{-1} m^{-1}

Fig. 5.1.8. AE9014 Air Conductivity Measurements beginning 28.7.90

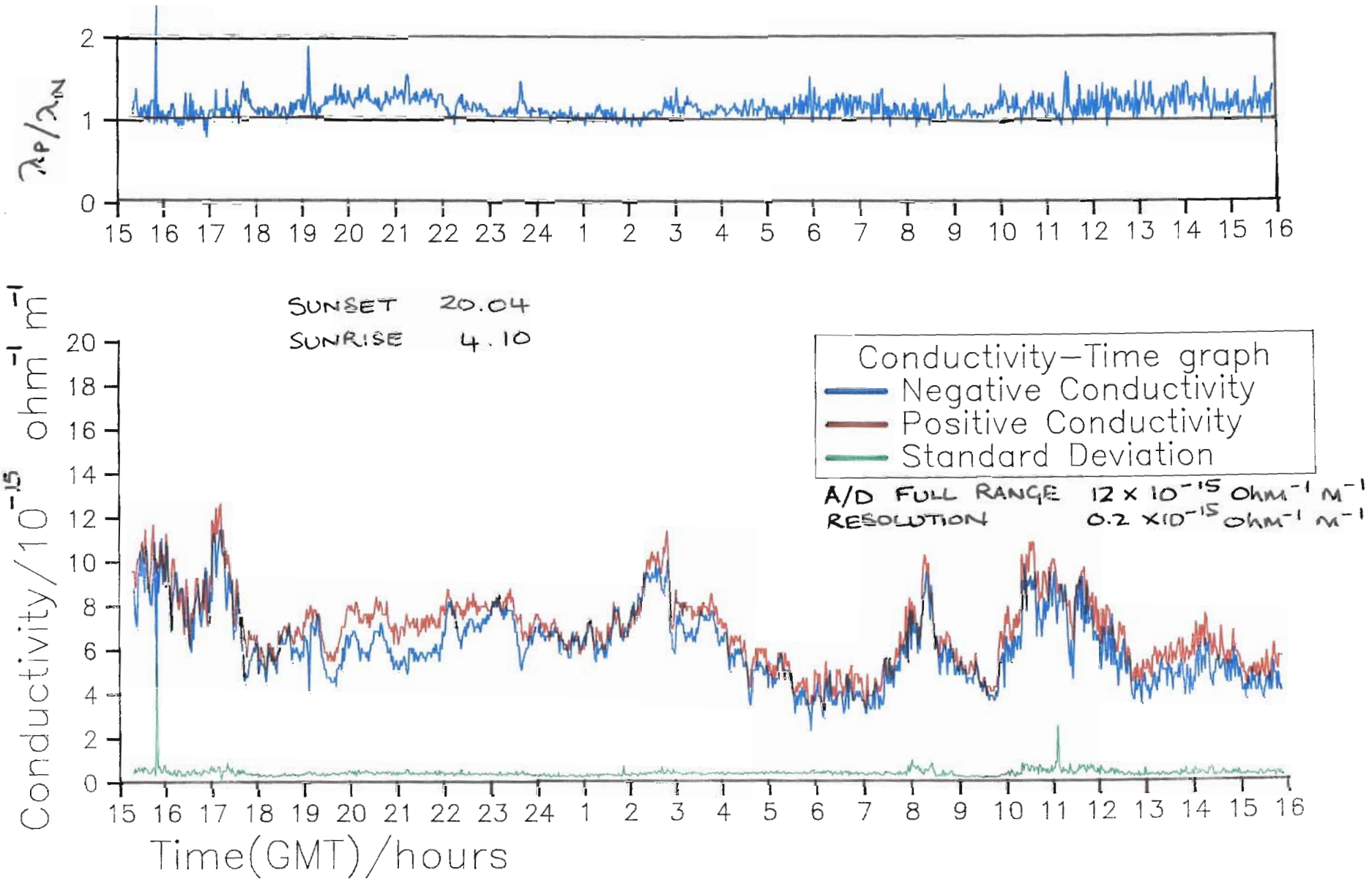

Fig. 5.1.9. AE9015 Air Conductivity Measurements beginning 29.7.90

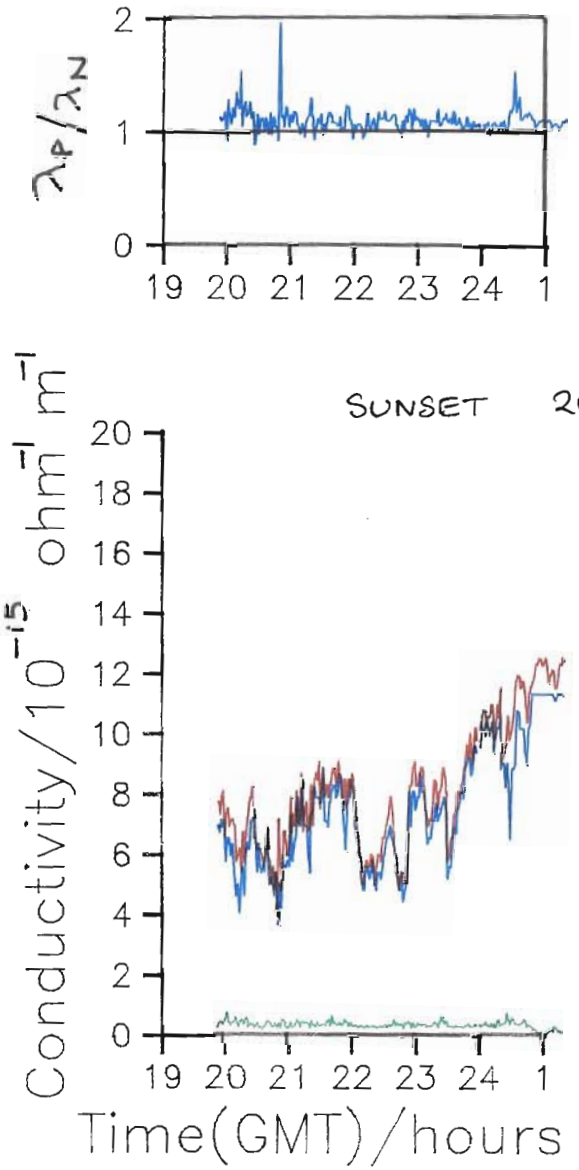

Conductivity–Time graph
Negative Conductivity
Positive Conductivity
Standard Deviation

A/D FULL RANGE ≈ 12×10^{-15} ohm^{-1} m^{-1}
RESOLUTION 0.2×10^{-15} ohm^{-1} m^{-1}

Fig. 5.1.10. AE9016 Air Conductivity Measurements beginning 30.7.90

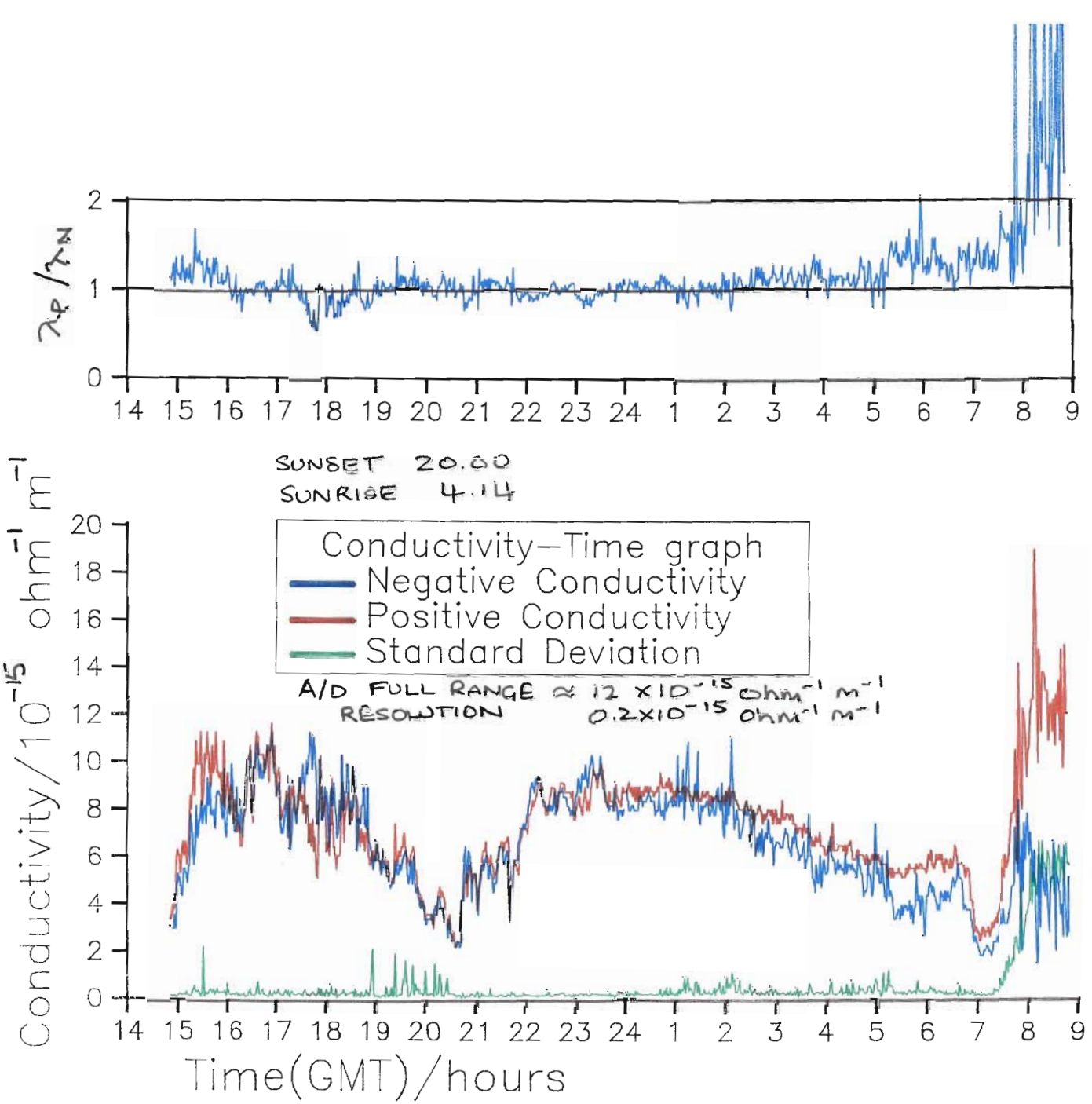

Fig. 5.1.11. AE9018 Air Conductivity Measurements beginning 31.7.90

5.1.7. and Fig. 5.1.9. and seemed to end around 18.00 to 19.00 GMT. Conductivity measurements made during the night were generally less disturbed than those made during the day.

Another thing which is most striking, is that although the variation of positive and negative conductivity are very similar, positive conductivity is generally greater than negative conductivity. This is due to the electrode effect and takes place because positive charge is attracted towards the earth and negative charge repelled, thus altering the near ground ion ratios (Chalmers,1967). This is more easily observable under calm conditions and in trace AE9015 (Fig. 5.1.9.) happens to a much greater degree at night, than during the day.

The average standard deviation for both conductivities, plotted in green, gives a measure of the magnitude of the higher frequency components in the signal, as well as allowing calculation of the uncertainty in the reading. Although the amplitude of this 'noise' relative to that of the main signal is generally small there are some sudden variations which appear rather anomalous. There is also the spectacular and sustained increase in noise found in Fig. 5.1.11. at the end of the trace. In the next section I shall be discussing the various possible origins of this high frequency noise and try to interpret the results obtained.

5.2. Interpretation of the results

5.2.1. Noise and its effect on the measurement record.

In order to study the operation of the electrometer in more detail I have plotted separately the standard deviation of V_{PP}, V_{NP} and V_{ZP}. These plots are contained in Appendix A5. in Figures A5.1., A5.3., A5.5. and A5.7. I have labelled these graphs 'voltage noise' against time. Noise is usually characterized by a root sum of squares value measured for a specified signal bandwidth (Clayton,1979), however I was only interested in relative noise levels and the uncertainties they produce in the measurement. The uncertainty in any particular measurement is given by dividing the measured standard deviation by the square root of the number of measurements. The number of loops the program executed in 25 seconds was about 1500 however this is an over estimate of the number of measurements as the BBC micro stores the A/D data in a buffer which is only updated every 40 milliseconds or so. The software command X= ADVAL(N) will return with the same value if the program reads at intervals smaller than this. Dividing 25 seconds by 40 milliseconds gives the number of measurements as 625, the square root of which is 25. Over reading the A/D buffer does not of course alter the mean of the measurements or substantially change the standard deviation if it is assumed each measurement is repeated just once and this seems reasonable. The uncertainty of a measurement with a standard deviation of say $\pm$20mV is

$$= \pm 20 \; / \; 25 \approx \pm 1\text{mV}$$

which is less than the resolution of the stored data, i.e. $\pm$5mV.

I have also plotted the output offset voltage of the amplifier with and without the contribution from the input bias current. Graphs of these quantities I have labelled 'voltage drift' against time and are given in Figures A5.2., A5.4., A5.6. and A5.8. in Appendix A5. Remember the output voltage offset with R_H shorted (V_{short}) was measured swiftly in the 5 second interval between the main measurements and is slightly dependent on the size of the 25 second measurement made just before. The variation of the two drift parameters, V_{short} and V_{ZP} was relatively generally small, however V_{ZP} drifts more with time and occasionally becomes very disturbed. The difference in V_{short} and V_{ZP}, assuming there are no other current generating mechanisms with zero polarization, can be used to find the input bias current, i_b.

Thus

$$i_b = (V_{ZP} - V_{short}) / 10\ R_F$$

(V_{ZP} - V_{short}) was on average about -10 mV and so i_b could be found and is roughly 10^{-14} amps. (This incidentally is about 10 times lower than the 'typical' bias current given for the AD549J electrometer amplifier in the data sheet in Appendix A3.1.)

These two sets of graphs were a powerful tool to help with the interpretation of the measurements. Some of

the characteristic features of the traces are outlined below.

5.2.2. Some characteristic features of the traces.

On time series AE9011 (Figures A5.1. and A5.2. there is a minimum background noise of about 15 mV or so across the whole graph for all traces, Fig. A5.1. In addition to this noise there are some rather sharp peaks of disturbance of various magnitudes. Although these appear on all three traces they are of much greater magnitude when the polarization voltage is on. An exception to this rule is the massive disturbance, just before 10.00 GMT. Here V_{ZP} as well as V_{PP} and V_{NP} are highly disturbed. It leads to a period of about 5 hours or so where i_b drifts excessively (Fig. A5.2.) after which it seems to return to a stable level again, just before the data series ends. The AE9011 conductivity graph in Fig. 5.1.2. there does not appear any sharp changes across the disturbance, suggesting that drift compensation was working. Obviously the uncertainty in the readings will have increased and this is reflected by the curve of average standard deviation on that graph.

On the time series AE9011 there is what appeared to me to be a discontinuity in the reading at about 6.45 (GMT) associated with a large noise spike. It was thought at first that this could be due to an instrument defect, however there is no evidence of this on the drift graph, and so strange effect appears to be real. The sharp disturbances sometimes only last long enough to effect

the noise on one conductivity reading, but at other times they may effect two readings. As can be seen they are sometimes associated with an increase in conductivity and sometimes with a decrease.

Looking at the other time series in more detail shows up other interesting effects such as the strange decrease in the noise of the negative conductivity readings in the hour before sunrise for the AE9014 time series shown in Fig. A5.3. and the rise in V_{ZP} noise during the coldest part of the night as shown in Fig. A5.5. There is also a 'top hat' like increase in noise on the AE9014 conductivity graph, this looks just as if it was due to amplifier instability. However on studying the detailed noise graphs in Fig. A5.3., this increase in noise is found to be present only when the cylinder is polarized and is due I believe to real ion changes. The air that night was very clear and I could see Blackpool Tower. There was no wind and the sun was setting. The noise reduced as the sun reached the horizon. This strange effect seemed to be linked with sunset since nothing else appeared to be happening. During the next few hours the negative conductivity was found to be much lower and the high frequency variations much greater, than the positive conductivity.

My interpretation of many of the phenomenon was hampered by the fact that no simultaneous meteorological measurements were made, such as wind speed etc., with the speed of response and time accuracy required for purposes of correlation. Also there were no simultaneous

measurements of electric field to see if any changes in conductivity were mirrored by changes in potential gradient.

5.2.3. The massive disturbance on data series AE9018 beginning just after 7.00 GMT. (see Fig. 5.1.11.)

This was the greatest disturbance found during the period in which measurements where made and was completely unlike those previously found since drift compensation appeared not to be working.

The noise levels were huge as shown in Fig. A5.7. On Fig. A5.8. it can be seen that the voltage offset with the electrometer shorted did not change significantly, yet V_{ZP} was enormously disturbed, with similar noise levels to V_{NP} and V_{PP}.

During the late afternoon, the day before this took place, one of the researchers in the ES department laid out some coal tar contaminated soil, in order to dry it in the sun over the next few days. The soil was water logged, but also contained a lot of organic chemical contamination, including volatiles. On the morning of the conductivity disturbance, I had arrived at the field station at 8.30 GMT (9.30 BST) and the volatiles could be smelt in the air well away from the drying site, which was about 40m or so from the conductivity apparatus mounted within the building.

The clue to what I believe was happening came from looking the ratio of the polar conductivities against time graph, shown in Fig. 5.1.11. From about midnight

that night the ratio of positive ions to negative ions had slowly but continually increased, with quite large decreases in the overall magnitude of the conductivity. Although this could have been due to the electrode effect (Chalmers,1967), it would also arise if the volatiles evaporating from the soil were positively charged. An increase in the rate of volatile evaporation due to solar heating in the morning would then account for the dramatic increase in positive conductivity and the decrease in negative conductivity just after 7.00 GMT (Fig.5.1.11.). (Incidentally the positive conductivity remains unclipped because V_{ZP} is much lower than normal at this time, due to an increase in bias current.) However this hypothesis seemed to fail to account for the level of the noise that occurred.

Although the bias current had almost certainly increased during this period, variations of i_b of magnitude needed to account completely for the huge noise on V_{ZP} would I am sure be associated with overall amplifier instability, jet V_{short} remained stable, as if nothing was happening, Fig. A5.8. Interestingly enough the noise levels on V_{ZP}, V_{NP} and V_{PP} are all of a similar magnitude. If the current was due to some changing property of the air, how was it generated?

The idea that these currents might be displacement currents, that is ac currents flowing to and from the central electrode due to time varying potential gradients within the apparatus, caused by variations in space charge, was suggested by Dr. B. K. Jones as a possible

mechanism. I searched the literature (Chalmers(1967), Israel(1971) and various other sources to hand) and found no mention of it. So I set about investigating this problem myself, to see if variations in space charge could account for the effects encountered experimentally. I initially thought that changes in free unbalanced charge might directly lead to the generation of a displacement current; thus the rate of change of charge on the central electrode would directly equal the rate of change of space charge, i.e.

$$\frac{dq}{dt} = - \frac{d\rho}{dt} \qquad (5.2.1)$$

However this theory ignores any effect due associated changes in the amount of bound charge on the outer cylinder and so is undoubtedly wrong.

I derived what I believe is the correct theoretical relationship between displacement current in the Gerdien condenser and changes in space charge a few days later, and this is given in Appendix A6. The condenser is assumed to be an ideal coaxial capacitor. Using Poisson's equation in cylindrical polar coordinates, together with a boundary condition for the electric field at the surface of the central electrode, an expression for the variation of potential gradient within the condenser with radial distance, r can be derived. This expression is integrated with respect to r and a time derivative taken under the assumption that the changes are slow enough to

justify the use of the DC approximation i.e. that the effects due to magnetic fields are negligible.

The following equation results

$$\frac{dq}{dt} = k_q \frac{d\rho}{dt}$$

where kq = $\left[\pi a^2 L - \frac{\pi L(b^2 - a^2)}{2 \ln(b/a)}\right]$

As k_q = - 0.0012 the calculated displacement currents are about a thousand times smaller that those that would be calculated using equation 5.2.1.

5.2.4. Making an estimate of the magnitude of the displacement currents produced by varying space charge.

Now let us assume a wave of space charge passes through the apparatus, thus

$$\rho(z,t) = \rho_o \sin w(t - z/c)$$

if w is the angular frequency of the wave and z the distance along the axis of the coaxial.

Differentiating this with respect to time gives

$$\frac{\partial \rho}{\partial t} = \rho_o w \cos w(t - z/c)$$

Thus magnitude of the current $\frac{dq}{dt}$ is given by

$$\left|\frac{dq}{dt}\right| = \rho_o \omega k_q$$

and so it depends not only on the amplitude but also the angular frequency of the incoming waves; the higher the frequency the larger the amplitude of the current.

The period of the disturbances was certainly lower than 25 seconds, so assuming a 5 period, T for the incoming disturbance w could be found from $w = 2\pi / T$. If the maximum current generated is full scale i.e.

$$i = 0.6 / 10^{12} = 6 \times 10^{-13} \text{ amps}$$

The the space charge variation required would be

$$\rho_o = i / k_q \omega = 6 \times 10^{-13} / (0.0012 \times 1.25)$$
$$= 4 \times 10^{-10} \text{ C} / \text{m}^3$$

which is of the rough order of magnitude (probably 5 to 10 times greater) than the space charges normally found to occur in the atmosphere (Chalmers,1967).

The length scale over which these changes occurred, D is given by $w = 2\pi c/D$ where c is the velocity of the wave through the apparatus and D is the wavelength. The velocity of the wave through the apparatus can be found from the volume flow rate, ($\dot{V}$) thus

$$c = \dot{V} / (b^2 - a^2)\pi$$
$$= 0.32 \text{ m/s}$$

Now although I did not measure the air volume flow rate I have estimated it to be 2 litres/sec. This equals

$$\dot{V} = 2 \times 10^{-3} \text{ m}^3/\text{sec}.$$

Thus the length scale can be calculated and is approximately 1.6 metres. Such small scales of variation do not normally occur in the free atmosphere, because it is usually well mixed, but with a large local source of space charge this seems perfectly possible. It seemed that the displacement current at this time of disturbance completely overwhelmed the conduction current. This theory is consistent with the fact that the noise

amplitudes, found on V_{ZP}, V_{NP} and V_{PP} at this time, were very similar because the magnitude of the displacement current is independent of the voltage across the plates, see Appendix A6.

To sum up ,it is believed that currents measured in the Gerdien condenser are made up of two components, that is dc conduction currents and ac displacement currents due to varying space charge within the apparatus. (the term displacement current is used in the same sense as Chalmers(1967). They must not be thought of as in any way imaginary.). Displacement currents are of generally small magnitude compared to the conduction currents as shown by the negligible drift of V_{ZP} under normal circumstances. However if the length scale of the space charge change is small they will dominate as found on trace AE9018. This is a completely new result, although once seen it seems obvious that this should happen. Notice that the theory is derived under the assumption that the fields with in the condenser do not vary with z. This will not be the case when space charge changes occur on a length scale of the order of the length of the apparatus and below, so the theory needs to be generalized further.

Although I have not had the chance to develop the theory very far, it does give something to test and hopefully improve on. However the basic principles appear to be clear that space charge variation can lead to displacement currents with the apparatus. It is information on the quantitative scale of this effect that now needs improvement.

I do not know why evaporating volatiles produce positive space charge as I have assumed in the above argument, Chalmers(1967) discusses space charges originating from pollution.

5.2.4. Some tentative interpretations of the general variations.

It is well known that the largest contributor to changes in atmospheric conductivity is the amount of aerosol in the air (Israel,1971). Aerosols 'mop' up the small ions in the air decreasing the average ion mobility and therefore decreasing the atmospheric conductivity. It is thus possible to look on the trace for times when the local traffic may have increased such as in the morning before work or at lunch time. An example of this could be at 12.15 GMT on trace AE9011 in Fig. 5.1.7. However because most of the local aerosol presumably comes from the M6 motorway, the aerosol levels will probably depend greatly on wind direction. This was not studied.

The strongest effect though, observable best on Fig. 5.1.7. and Fig. 5.1.9. is the difference between night and day. It appears that the still night time air was stirred into motion by the morning sun, with warm air in contact with the ground rising and colder, denser and presumably cleaner air coming down to replace it. This naively explains both the increase in both conductivity and its variability.

5.3. Aliasing and spectral analysis.

If a time varying signal is sampled instantaneously at intervals T_S, that is with a sample frequency

$$f_S = 1 / T_S$$

the highest frequency that can possibly be recorded is equal to twice the sample frequency $2f_S$ which is normally referred to as the Nyquist frequency. Frequencies higher than this can not be accurately reproduced and appear spuriously as lower frequency signals in the measurement record. This is referred to as aliasing (Bath,1974).

The computer controlled Gerdien condenser sampled at a rate of 1/90 Hz and so the Nyquist frequency is 1/180 Hz. The samples were not made instantaneously, but over a measurement time, T_m of 25 seconds. How can we determine the extent to which aliasing is occurring in any given signal? This is a difficult question since aliasing by its very nature can not be undone once it has occurred. One simple approach is to ascertain the sensitivity of a signal to the sampling frequency by for example resampling the data. Fig. 5.3.1. shows the conductivity time series AE9015 resampled at every second data point. It is visually very similar the original time series shown in Fig. 5.1.9. suggesting that the frequency spectrum will not have altered substantially. However the variation of the ratio of polar conductivities has been significantly changed. The variation of this ratio appears very sensitive to the sampling interval and so the original variation may have been simply an artifact of the sampling method.

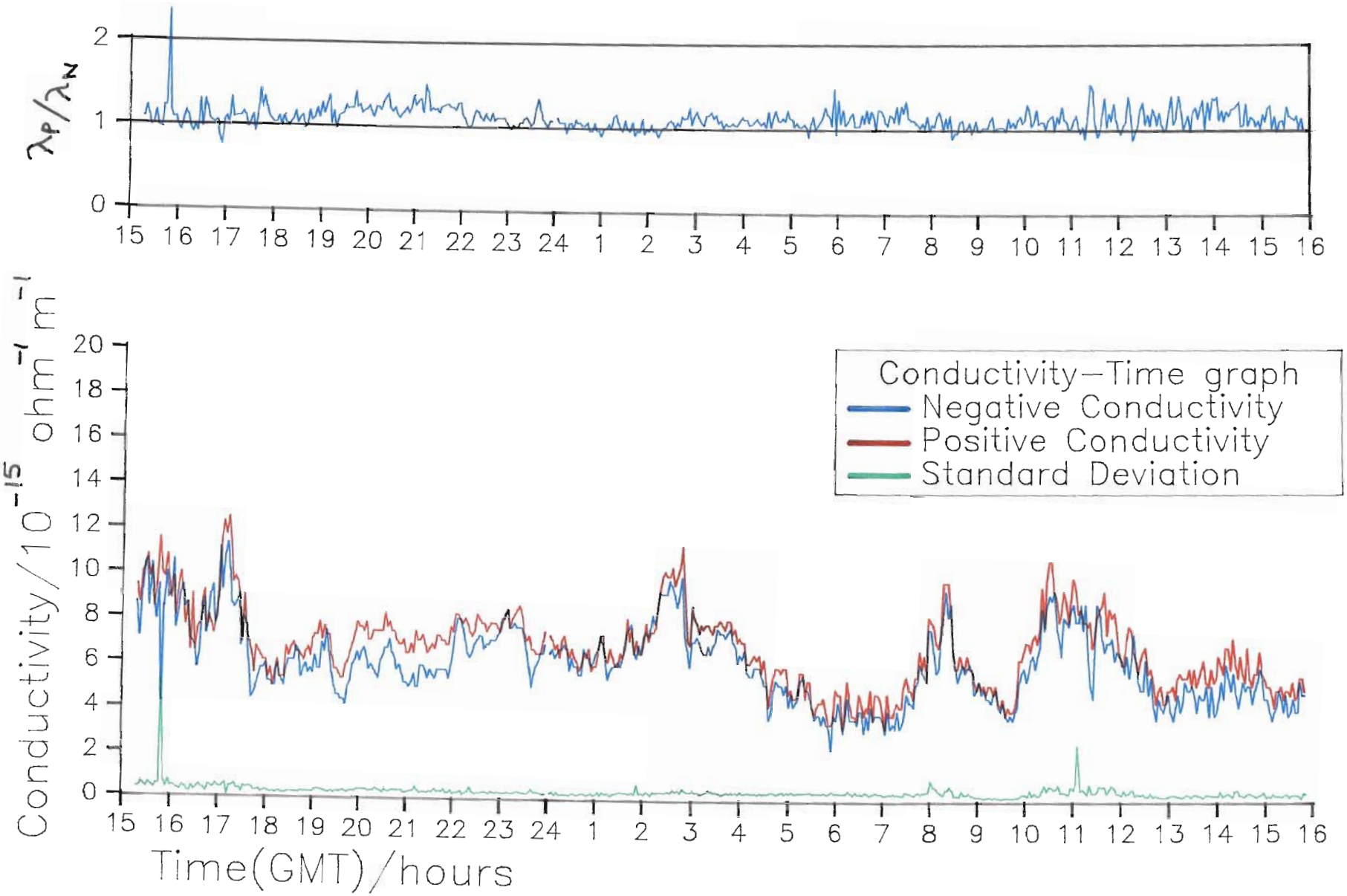

Fig. 5.3.1. Time-series AE9015 resampled at every second data point.

Fig. 5.3.2. shows a normalized amplitude frequency spectrum for both the positive and negative conductivities in the time series AE9015. The Nyquist frequency is at the far right hand end of the graph. Wave components with periods between 10 hours and 0.5 hours have very similar amplitudes even though they were measured at slightly different times. Higher frequency or shorter period waves are less well correlated. The main point to note is that the higher the frequency of the wave component, the smaller is its amplitude. This can more readily be seen when the spectrums for several time series have been averaged, after being normalized by dividing by the number of points in the series (see Fig. 5.3.3. At the Nyquist frequency, the amplitude of the wave components is approximately 1/40 that of the 2.5 hour period waves.

FIG. 5.3.2 NORMALIZED AMPLITUDE FREQUENCY SPECTRUM FOR BOTH POSITIVE AND NEGATIVE CONDUCTIVITIES FOR TIME SERIES AEGOIS.

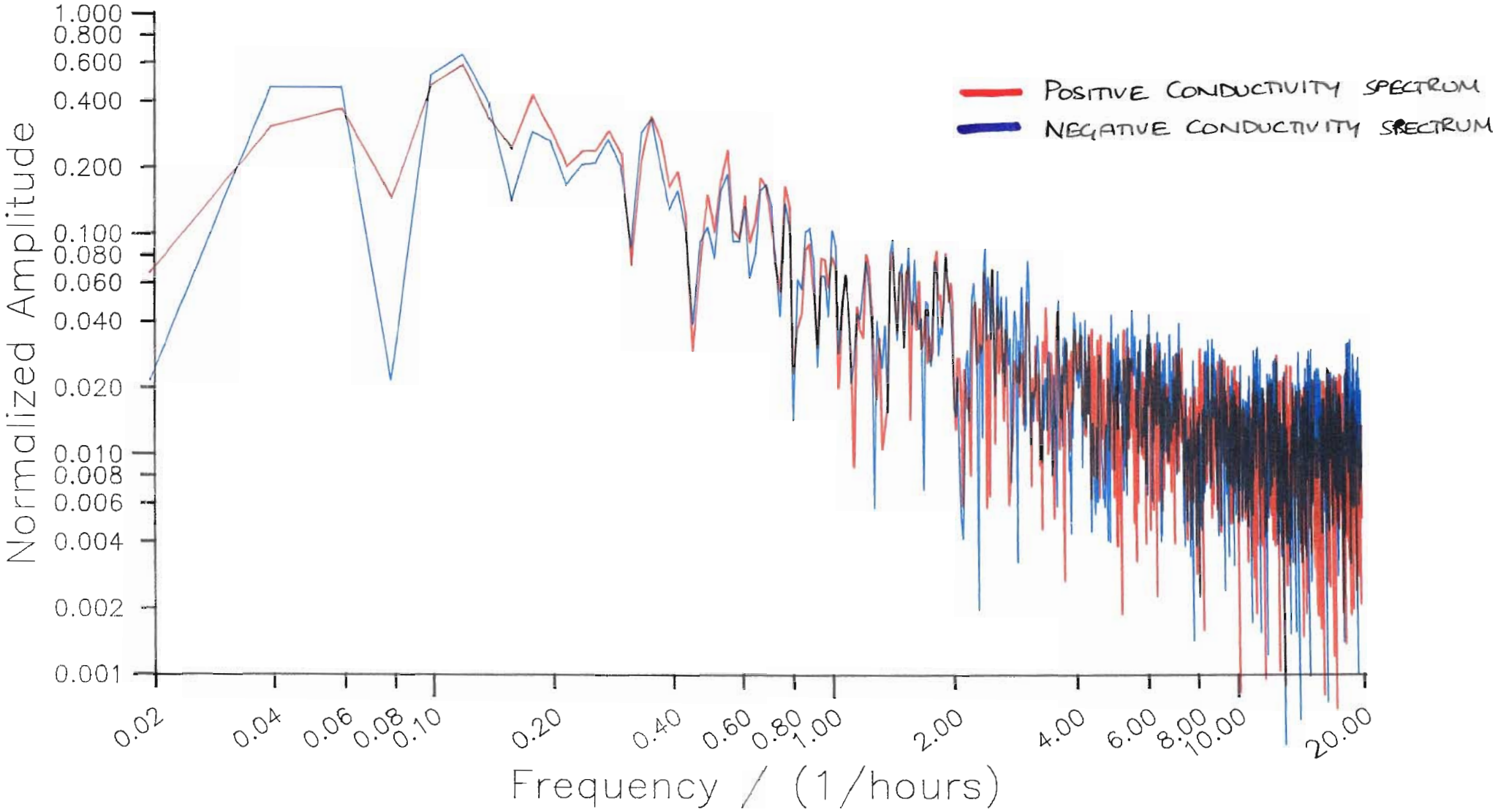

FIG. 5.3.3. NORMALIZED AMPLITUDE FREQUENCY SPECTRUM — AVERAGE OF A NUMBER OF TIME SERIES. — TO SHOW THE AMPLITUDE FALL OFF WITH FREQUENCY

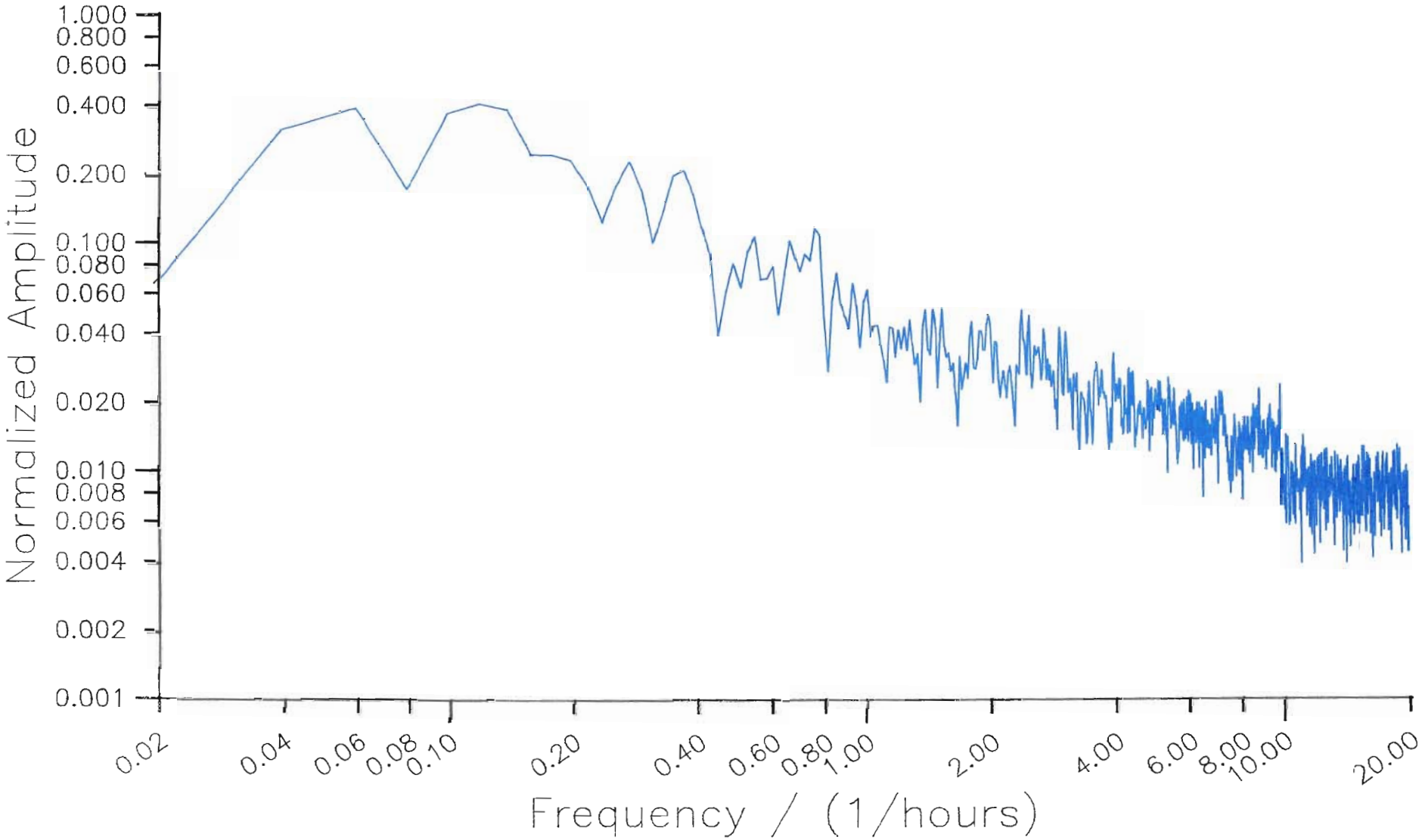

6. Summary and Conclusions.

6.1. Summary of the dissertation

1. In the first chapter I briefly introduce the subject of atmospheric electricity and try to put it into context, within the broard framework of global electricity and magnetism, a subject termed Geoelectricity by Webb(1980).

2. In chapter 2 I introduce the theory of the Gerdien condenser, make comparison of various electrometers old and new, and then look in detail at the DC amplifier electrometer.

3. In chapter 3 I briefly describe the design of the original Gerdien condenser and then discuss the design, construction and testing of the new instrument. The techniques of computer controlled conductivity measurements are outlined.

4. Chapter 4 deals with the calibration of the apparatus. Amongst other things, currents due to radioactivity and cosmic rays and also the problems of maintaining adequate insulation are discussed.

5. In chapter 5 I descibe and try to interpret the results obtained. I develop a relationship (Appendix A6.), linking changes in the space charge density of air flowing through the apparatus with displacement currents

flowing to and from the central electrode. Finally the effects of aliasing are briefly delt with.

6.2. Conclusions.

As far as I know this is the first time that a DC amplifier electrometer has been used to give a continuous record of atmospheric conductivity over time. Sampled measurements were used to avoid problems of drift and this was generally successful. Periods where drift compensation did not work, due to high noise levels, could be easily identified on the measurement record and this proved very useful.

Improvements could obviously made to the apparatus, such as reductions in motor vibration. If a Gerdien condenser is to be designed from scratch special attention should be given to the design, to allow easy insulator cleaning.

Incorporating the guard into the Gerdien condenser has been the central linch pin to the success of this work; it reduces leakage currents, it eliminates noise due to dielectric after-working (allowing the polarization voltage to be continually reversed), it allows the exposed capacity to be easily measured and can even be occasionally polarized, to test for leakage across the central electrode insulator.

I believe that with a little more development, and the use of an improved specification A/D converter plus datalogger, the apparatus described could be used to reliably record the variations of atmospheric

conductivity over extended periods. Although the sampling technique leads to aliasing of the higher frequency components, lower frequency components generally are little affected and so can be used to build up a picture of the daily and yearly variations fairly accurately. The measurement technique used also highlights periods of disturbance very well, without the need to store huge amounts of high frequency data.

Importantly the cost of the instrument is very small; the electrometer, including control circuitary cost in the region of £50 to build, a vibrating reed electrometer will cost at least twenty times as much and you would require two of them to measure both polar conductivities continuously.

The sampling technique outlined in this work may have uses in other fields of measurement, although I do not know of any at the present time.

7. Suggestions for further work.

Although there is a need to further develop the conductivity apparatus, so that it can be reliably used for extended periods, my main thoughts are towards how controlled experiments can be used to increase our understanding of the measurement properties of this disceptively simple instrument. For example, experiments using various ion sources, ion filters and aerosols, which I did not have the time to carry out.

The available ion sources appear to be radioactive materials, high voltage points like those used in negative ion generators, and splashing water, which produces a negative space charge. Also direct tests can be carried out to see if evaporated volatiles really do produce space charge, perhaps under more controlled conditions, for example with and without a potential gradient present.

Controlled experiments could be carried out with aerosol to see its effect on the conductivity under different conditions.

An ion filter, consisting of a high voltage air capacitor placed at the inlet of the Gerdien condenser, could be used to see if low mobility ions can give rise to significant currents if created in large numbers.

The apparatus could also be sealed with the fan switched off, to investigate the magnitude of any sudden enhancements in ionization due to cosmic ray showers.

References

References are in alphabetical order. Citation page numbers are given in square brackets after each reference.

Barker,R.W.J. (1979). Modern electrometer techniques, *Proc. IEE.* **126**, 1053-68. [2.3,4.2.1]

Bath,M. (1974). Spectral analysis in Geophysics, Elsevier Scientific Pub. Co., Amsterdam. [5.3]

Bleaney,B.I. and Bleaney,B. (1976). Electricity and Magnetism, Oxford University Press. [4.1.1]

Boast, W.B. (1964). Vector Fields, Harper and Row, New York. [4.1.1]

Bray,A.C., Dickens,A.C. and Holmes,M.A. (1983). The Advanced User Guide for the BBC Micro, The Cambridge Microcomputer Centre, Cambridge. [3.2.2,3.5.2]

Chalmers,J.A. (1967). Atmospheric Electricity, Pergamon Press, Oxford, 2nd ed. [1.1,1.2,1.6,1.7,2.1.3,5.1,5.2.2]

Chater,W.T. (1971). A Digitizing Electrometer system using an Integrating Circuit Preamplifier, *Rev. Sci. Instrum.* **42**, 129-34. [A3.2]

Clayton,G.B. (1979). Operational Amplifiers, Newnes-Butterworths, London, 2nd ed. [2.4,5.2.1,A2.1]

Cobb,W.E. (1968). The Atmospheric Electric Climate at Mauna Loa Observatory, Hawaii, *J. Atmos. Sci.* **25**, 470-80. [4.1.3]

Cobb,W.E. (1973). Oceanic Aerosol Levels Deduced from Measurements of the Electrical Conductivity of the Atmosphere, *J. Atmos. Sci.* **30**, 101-6.

Cobb,W.E. and Wells,H.J. (1970). The Electrical Conductivity of Oceanic Air and Its Correlation to Global Atmospheric pollution, *J. Atmos. Sci.* **27**, 814-9.

Coll, J. (1982). BBC Microcomputer User Guide, British Broadcasting Corporation, London. [3.2.2,3.5.2]

Coulomb,C.A. (1785). Mem. Acad. Sci., Paris, p. 616. [1.3]

Elster,J and Geitel,H. (1899). Über die Existenz elekrischer Ionen in der Atmosphäre (On the Existence of Electric Ions in the Atmosphere), *Terr. Magn. Atmos. Elect.* **4**, 213-34. [1.3]

Elster,J. and Geital,H. (1900). Über die Elekrizitätszerstreuung in der Luft (On the Dissipation of Electricity in Air), *Annln. Phys.* **2**, 425-46. [1.3]

Fleming,J.A.(ed.) (1939). Terrestrial Magnetism and Electricity, McGraw-Hill, New York.

Ford,L.H. (1948). The effect of humidity on the calibration of precision air capacitors, *J. Instn. elect. Engrs.* **95**, 709-12. [4.2.2]

Garton,C.G. (1946). The characteristics and errors of capacitors used for measurement purposes, *J. Instn. elect. Engrs.* **93**, 398-408. [4.2.2]

Gerdien,H. (1905). Demonstration eines Apparates zur absoluten Messung der elektrischen Leitfähigkeit der Luft (Demonstration of a Device for the Absolute Measurement of the Electrical Conductivity of Air), *Phys. Z.*, **6**, 800-1. [2.1.3]

Grant,I.S. and Philips,W.R. (1975). Electromagnetism (The Manchester physics series), John Wiley and Sons. [A1.1]

Gunn,R. (1964). The Secular Increase of the World-Wide Fine Particle Pollution, *J. Atmos. Sci.* **21**, 168-81. [2.3,4.1.3,4.3]

Gunn,R. (1965). Improved Apparatus for the Measurement of Atmospheric Electrical Conductivity, *Rev. Sci. Instrum.* **36**, 594-598. [2.1.3,2.3,4.1.1,4.2.3,4.3]

Hess,V.F. (1928). The electrical conductivity of the atmosphere and its causes, Constable and Co., Ltd., London. (Translated from the German original by Codd,L.W.) [2.1.3]

Israël,H. (1971). Atmospheric Electricity, Volume I: Fundamentals, Conductivity, Ions, Israel Program for Scientific Translations, Jerusalem. [1.1,1.5,1.6,2.1.3,4.2.3,5.2.2,5.2.3]

Israël,H. (1973). Atmospheric Electricity, Volume II: Fields, Charges, Currents, Israel Program for Scientific Translations, Jerusalem. [1.1]

Keithley,J.F., Yeager,J.R. and Erdman,R.J. (1984). Low Level Measurements, Keithley Instruments Inc., Cleveland, Ohio. (Formerly entitled "Electrometer Measurements") [2.3,2.4,3.2.1]

Knowles Middleton,W.E. (1965). A History of the Theories of Rain (and Other Forms of Precipitation), Oldbourne, London. [1.1]

Landis,G. and Godwin,M. (1982). Portable precision dc voltage-current transfer standard for electrometer calibration, *Rev. Sci. Instrum.* **53**, 1290-1. [4.1.2]

Moore,C.B. and Vonnegut,B. (1988). Measurements of Electrical Conductivities of Air over Hot Water, *J. Atmos. Sci.* **45**, 885-90. [3.2.1,4.3]

NPL (1969). Standard capacitors and their accuracy in practice, National Physical Laboratory, Teddington, Middlesex. [4.2.2]

Palevsky,H., Swank,R.K. and Grenchik,R. (1947). Design of Dynamic Condenser Electrometers, *Rev. Sci. Instrum.* **18**, 298-314. [2.3,A3.2]

Rowland,H,J. (1878). On the magnetic effect of Electric convection, *Am. J. Sci.* **15**, 30-38. [A1.2]

Saunders,C.P.R. (1988). Thunderstorm electrification, *Weather* **43**, 318-24. [1.1,A3.2]

Schonland,B.F.J. (1953). Atmospheric Electricity, Methuen, London, 2nd Ed. [1.1]

Sharpless,G.T., Aspinall,W.P. and Hutchinson,W.C.A. (1971). Atmospheric Electricity observations at a Land Station in Fair Weather, *J. Geomag. and Geoelec.* **23**, 335-46. [2.3]

Smith,L.G. (1953). On the calibration of conductivity meters, *Rev. Sci. Instrum.* **24**, 998. [4.1.1]

Swann,W.F.G. (1914). The theory of electrical dispersion in the free atmosphere, with a discussion of the theory of the Gerdien conductivity apparatus, and a theory of the collection of radioactive deposit by a charged conductor, *Terr. Magn. Atmos. Elect.* **19**, 81-92. [2.1.3]

Thomson,J.J. (1898). Discharge of Electricity through Gases, Westminster. [1.3,1.4]

Torreson,O., Parkinson,W.C., Gish,O.H. and Wait,G.R. (1946). Scientific results of cruise VII of the "Carnegie" during 1928-1929, ocean atmospheric results. Carnegie Institute of Washington, Publ. No. 568, 1-176. [4.1.3]

Twomey,S. (1977). Atmospheric Aerosols, Elsevier Scientific Publishing Company, Amsterdam. [1.5,1.6]

Vonnegut,B. (1960). Electrical theory of tornadoes, *J. Geophys. Res.* **65**, 203-12. [1.1]

Vonnegut,B. (1980). Atmospheric Electricity, McGraw-Hill Encyclopedia of Environmental Science, Parker,S.P. (ed.), McGraw-Hill, 2nd Ed. [1.1]

Wilson,C.T.R. (1897). *Phil. Trans. A* **189**, 265. [1.4]

Wilson,C.T.R. (1899). *Phil. Trans. A* **192**, 403. [1.4]

Webb,W.L. (1980). Geoelectricity, University of Texas at El Paso. [1.1,6.1]

APPENDICIES

Appendix A1

A1.1. Outward pressure on a uniformly charged sphere.

A1.2. Is the magnetic dipole created by a spinning charged earth large enough to account for the earths magnetic field?

Appendix A2

A2.1. DC Amplifier Terminology

A2.1. Response of a picoammeter to a step current input

Appendix A3

A3.1. Data sheet for the AD549 DC amplifier electrometer.

A3.2. Contact potential charging

Appendix A4

A4.1. Apparatus control program

A4.2. Data Extraction Program

Appendix A5

Graphs of noise and drift for V_{ZP}, V_{NP} and V_{PP} over time.

Appendix A6

Displacement currents in the Gerdien condenser due to changes in space charge density with time.

Appendix A1

A1.1. Outward pressure on a uniformly charged sphere.

Assume the sphere, Fig. A1.1. has a charge Q uniformly distributed over its surface with charge density,

$$\sigma = Q / 4\pi R^2$$

The charge dQ_1 on a small elemental area dA_1 is

$$dQ_1 = \sigma\, dA_1$$

and the charge dQ_2 on a thin elemental ring of area dA_2 is

$$dQ_2 = \sigma\, dA_2$$
$$= 2\pi a l\, d\theta$$

and as $a = l.\mathrm{Sin}\theta$

$$dQ_2 = 2\pi l^2.\mathrm{Sin}\theta\, d\theta$$

The force between these two elemental charges is given by coulombs law

$$d\underline{F} = \frac{1}{4\pi\varepsilon_o} \frac{dQ_1.dQ_2}{\underline{r}^2} \qquad (A1)$$

However all the components of force, except those perpendicular to the surface cancel out. Therefore the force on dA_1 due to dQ_2

$$dF_Z = \frac{1}{4\pi\varepsilon_o} \frac{(\sigma\, dA_1)(\, 2\pi l^2.\mathrm{Sin}\theta\, d\theta\,)\, \mathrm{Cos}\theta}{l^2}$$

Dividing both sides by dA_1 and simplifying gives

$$\frac{dF_Z}{dA_1} = \frac{\sigma^2}{4\varepsilon_o} \mathrm{Sin}\, 2\theta\, d\theta$$

and the total outward pressure, P is found by integrating this expression between 0 and $\pi/2$.

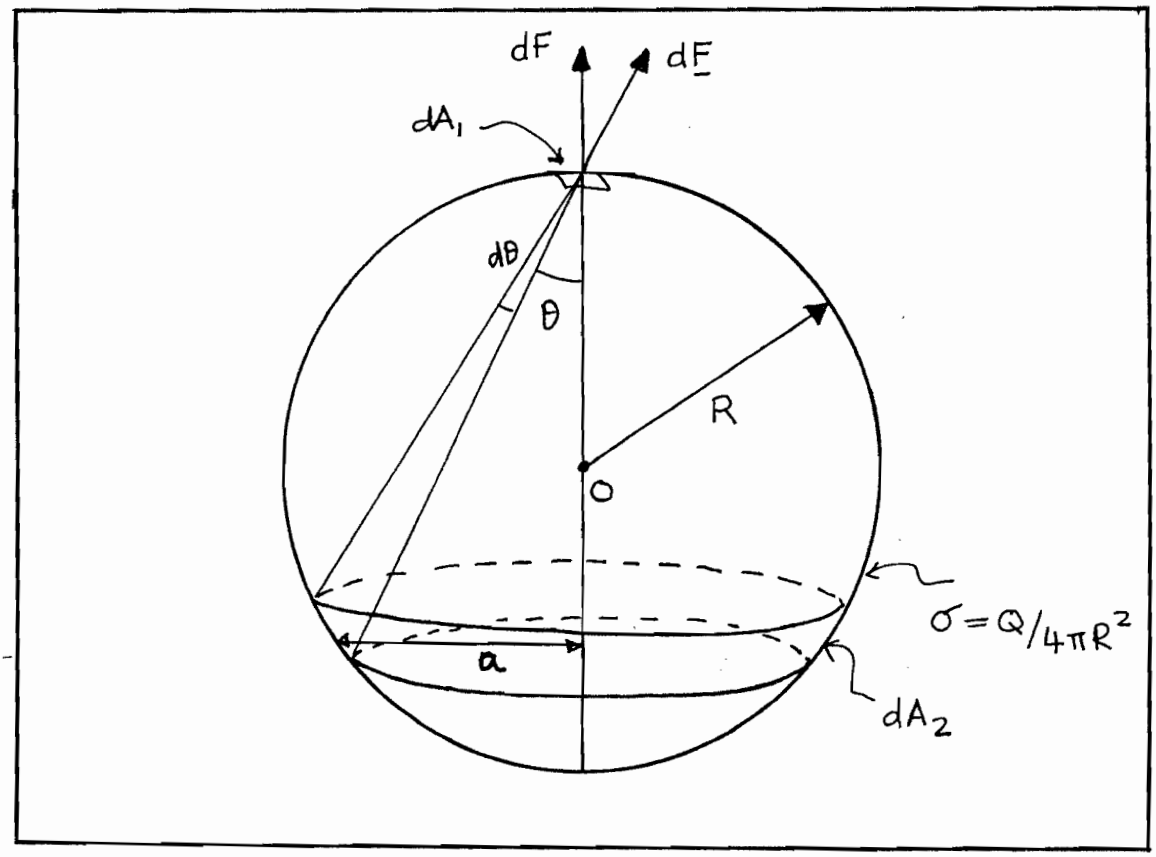

Fig. A1.1. Spherical Earth with uniformly distributed surface charge Q.

This gives $P = \sigma^2 / 4\varepsilon_o$ and if we assume there is a fair weather field of 100 V/m across the entire globe then the outward pressure due to the surface charge is

$$P = 2.2 \times 10^{-8} \text{ N/m}^2$$

This is a very small pressure indeed and to give some feeling for the figure, it is approximately 100 times smaller than the maximum solar radiation pressure at the earths surface.

The solar radiation pressure is equal to the radiation momentum flux, if all the radiation is absorbed. We can calculate the momentum flux from the energy flux if we use the following relation which holds true for photons, i.e.

$$\text{momentum flux} = \text{energy flux} / c$$

where c is the velocity of light (Grant and Philips,1975).

As the maximum solar enery flux at the earths surface is approximately 1300 W/m^2, the maximum solar radiation pressure P_R is

$$P_R = 1300 / 3.0 \times 10^8$$
$$= 4 \times 10^{-6} \text{ N/m}^2$$

A1.2. Is the magnetic dipole created by the spinning charged earth large enough to account for the earths magnetic field ?

Rowland(1878) first showed that a magnetic field could be set up by the rapid rotation of an electrified disc or sphere and it occured to him that the magnetic field of the earth might be produced in the same way.

In order to test this theory it is necessary to calculate the magnetic dipole moment of a spinning charged sphere, Fig. A1.2. Consider a sphere of radius R and with a surface charge density $\sigma = Q / 4\pi R^2$ spinning with an angular velocity ω. The dipole moment of a current loop is defined by the equation, $\underline{m} = i\underline{A}$ where $\underline{m}$ is the dipole moment and $\underline{A}$ is the area of the current loop.

The current flowing di along a spinning elemental ring is

$$di = \frac{\text{charge on the ring}}{\text{period of revolution}}$$

$$= \frac{(Q / 4\pi R^2)(2\pi R.\text{Cos}\theta\, dl)}{(2\pi / \omega)}$$

substituting $R\, d\theta$ for dl and simlifying gives,

$$di = \frac{Q\omega}{4\pi} \text{Cos}\theta\, d\theta$$

and so the magnetic dipole moment due to the elemental current ring is

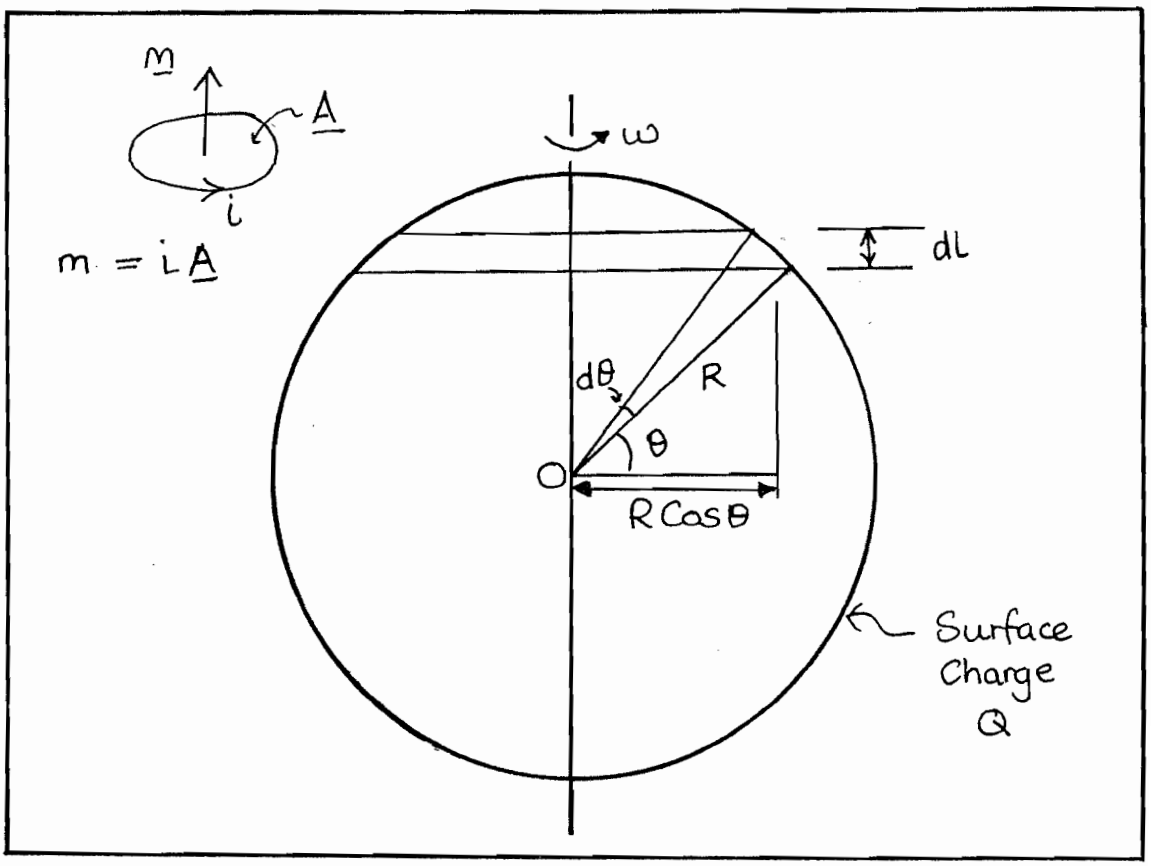

Fig. A1.2. Diagram showing a uniformly charged spherical earth spinning with angular velocity ω .

$$dm = A\, di$$

$$= \frac{Q\omega R^2}{4} \cos^3\theta \, d\theta$$

Now integrating this expression to obtain the total magnetic moment, M due to the rotating sphere

$$M = 2 \int_0^{\pi/2} \frac{Q\omega R^2}{4} \cos^3\theta \, d\theta$$

$$= \frac{1}{3} Q\omega R^2$$

taking $R = 6.4 \times 10^6$ m, $\omega = (2\pi)/(24 \times 3600)$ and $Q = -4.6 \times 10^5$ coulombs we find that

$$M = -4.5 \times 10^{14} \text{ A m}^2$$

However the observed geomagnetic dipole moment is approximately -8×10^{22} A m^2 which is 8 orders of magnitude larger than the magnetic moment calculated above. This means that although the negatively charged spinning earth would produce a magnetic field in the right direction it is of negligible size compared to the observed field and could not possibly account for it.

Positive charge in the atmosphere above, spinning with the earth would act to nullify the calculated dipole moment to a large degree, making it smaller still. Also it would seem very unlikely that changes in atmospheric circulation, and thus changes in the movement of space charge around the earth, could lead to measurable changes in the magnetic field of the earth.

Appendix A2

A2.1 DC Amplifier Terminology

The main step towards choosing the best Operational Amplifier (Op Amp) for a particular application is to be able to read and understand the manufacturers data sheets. Instead of wading comprehensively through op amp theory, which is delt with in books such as Clayton(1979), I have compiled a ready reference guide to op amps.

Op Amp parameters.

Supply Voltage

Op amps are normally powered by a three rail supply, for example -15 V, 0 V and +15 V. A wide range of votages can normally be used, say from $\pm$5 V to $\pm$18 V, however the measured quantities in the data sheet will be correct only for the supply voltage used in the tests, in the case of the AD549 this is $\pm$15 V.

Supply Current

The current specified usually is the quiescent or no load current. The current requirement of the device will of course rise when the amplifier is loaded.

Open Loop Gain (OGL)

The larger the open loop gain the more like an ideal op amp the amplifier can become. It is defined as the ratio of the change in output voltage to the change in input voltage which produced it. For example under the measurement conditions stated in the data sheet, the AD549 is specified to have a minimum open loop gain of 300,000, which is in fact expressed in units of V/mV as 300 V/mV. Sometimes the gain is expressed in decibels defined as OLG = 20 $\log_{10}(V_{out}/V_{in})$ decibels. Thus an open loop gain of 300,000 is equal to 110 db.
(see Clayton(1979,p.108) for greater detail on the measurement of open loop gain.)

Unity Gain Bandwith

Most operational amplifiers have a frequency response similar to Fig. A2.1., and this can be defined in several ways although it is usual to quote the frequency at which the gain falls to unity. This is shown by point X on Fig. A2.1. and is called the **unity gain bandwidth**.

Slew rate

If a step input is applied to an amplifier input, and the step is sufficient to drive the output to saturation, the output will change in a ramp form as in Fig. A2.2. The slope of the ramp is determined by the amplifier circuit, and is called the **slew rate**. It is usually specified in volts/μs and the greater it is the better will be the amplifiers high frequency response.

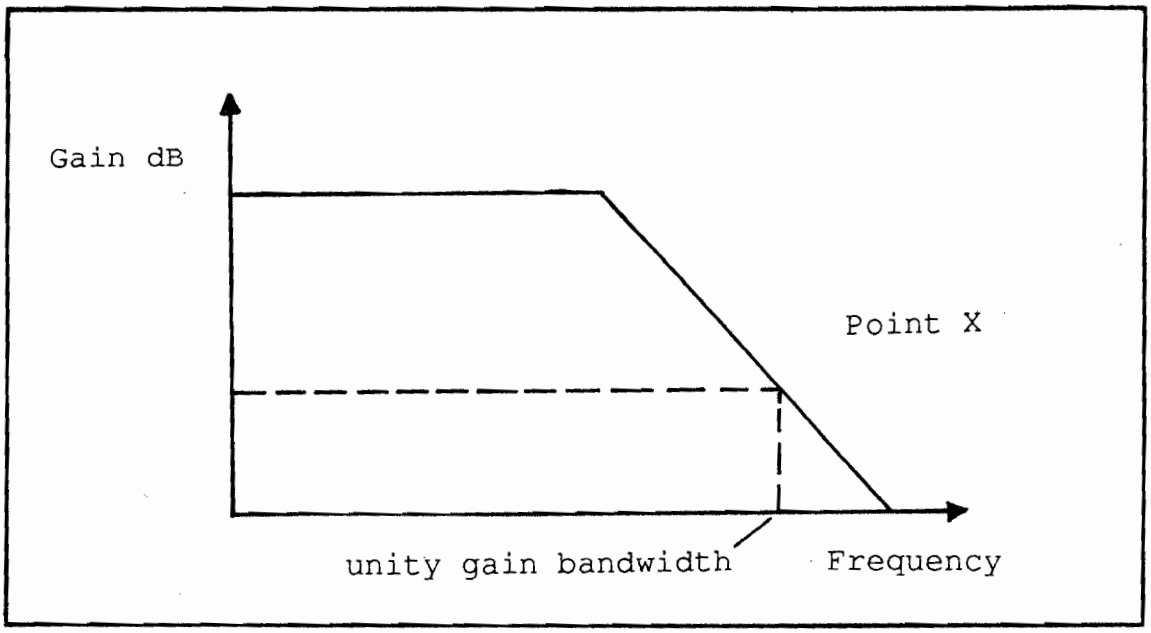

Fig. A2.1. Typical frequency response of a DC amplifier.

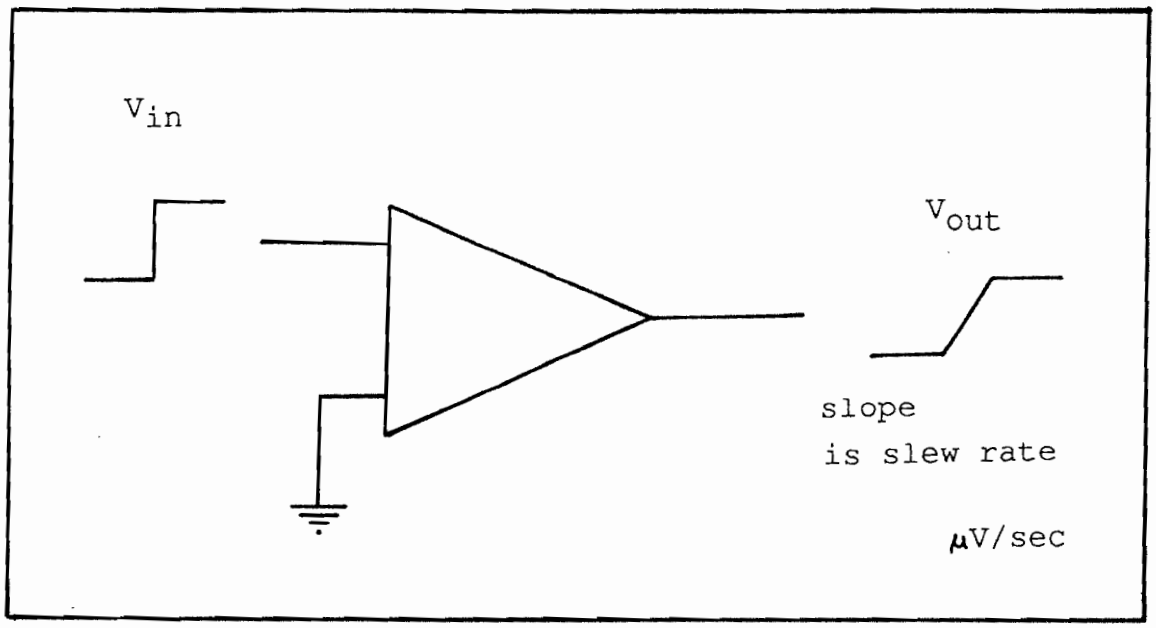

Fig A2.2. Slew rate.

The slew rate of the AD549 is typically 3 V/μs. The slew rate is not so important in electrometer design since the frequency response of an electrometer is usually limited by the passive components used.

Input Impedance

The input impedance of an op amp is made up of a resistive element and a capacitive element, which are effectively in parallel. In the data sheets two different input impedances are quoted, the **differential input impedance** and the **common mode input impedance.** The differential input impedance is the impedance measured directly between the inverting and non-inverting input terminals of the amplifier. The common mode input impedance is the impedance which exists between each input terminal and earth (or the power supply common). Operational amplifier input impedance is of critical importance in electrometer design. See Clayton(1979,p.106) for information on the measurement of input impedance.

Input Offset Voltage (V_{io})

A practical DC amplifier, with its inputs shorted together, is found to have a non zero output voltage or offset. It is usual to specify amplifier offsets by refering them to the input of the amplifier since for most high gain op amps even a small offset at the input can lead to voltage saturation at the output. Therefore the **input offset voltage** is defined as the input voltage

which would have to be applied across the + and - terminals inorder to make the amplifier output voltage zero.

The input offset voltage is temperature dependent and so is always measured at a specified temperature. It also varies with the supply voltage and as the amplifier ages.

Input Bias Current (I_b) and Input Offset Current (I_{io})

All operational amplifiers require a small current to flow, either to or from each input terminal in order to operate correctly. These are called **input bias currents**. By convention the bias current to the inverting input is labled I_{b1} and the bias current to the non inverting input is labled I_{b2}. Ideally both bias currents should be the same, however in practice there is always a difference between them. This difference is called the **input offset current**. In the data sheets only one average value of input bias current is given. Input bias currents also vary with temperature.

A2.2. Response of a picoammeter to a step current input.

If a step current input is applied to the input of a shunt picoammeter (Fig. A2.3.) by opening switch SW1, then the voltage across C_S and R_S will gradually rise as if there was just a capacitor across the electrometer inputs, which was being being charged by a voltage source in series with R_S; the voltage being given by $V = i_c R_S$ where i_c is the contant current flowing after SW1 is opened.

Therefore

$$V_2 = i_c R_S \ (1 - \exp(-t/R_S C_S))$$

which can easily be derived from the theories of Thevenin and Norton, which are described in most introductory texts on circuit theory.

Thus the speed at which the input voltage V_2 will rise to $V_2 = i_c R_S$ depends on the time constant $C_S R_S$. It will take 3 time constants for the output voltage to be within 5% of its final value.

An analogous result can be derived for a feedback picoammeter exept that the time constant becomes $C_F R_F$. The rise time t_r of a circuit is sometimes quoted. This is defined as the time required for the output to rise from 10% to 90% of its final value. It is easily shown by substitution into the above formula that $t_r = 2.2\ RC$ (Keithley et al.,1984).

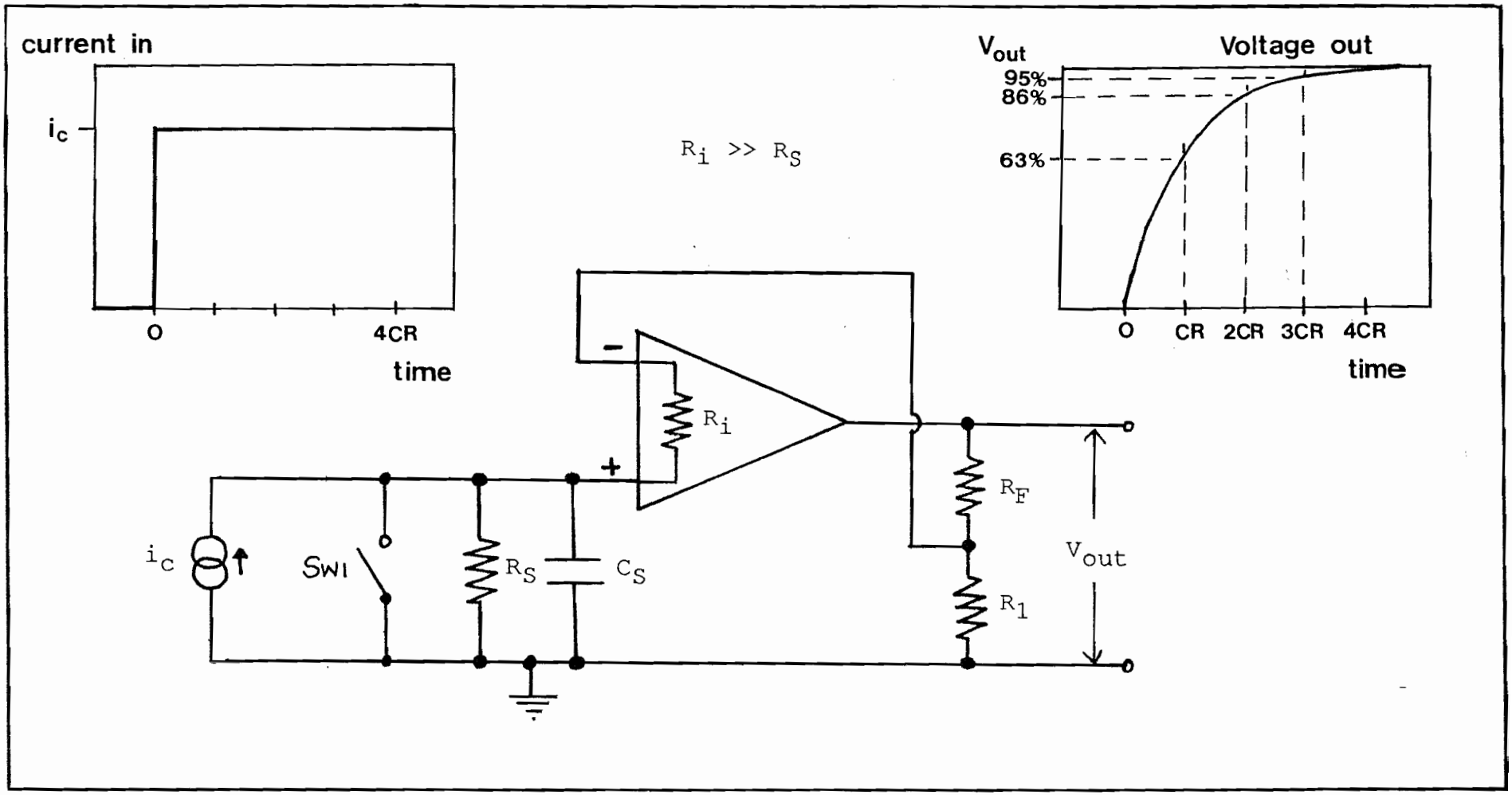

Fig. A2.3. Step current applied to the input of a shunt picoammeter

APPENDIX A3

A3.1. Data sheet for the AD549 DC amplifier electrometer.

A3.2. Contact potential Charging

Chater(1971) found that all reeds display a residual potential across the contacts at the moment of contact break of up to several millivolts. He found that the small potential could be reversed by reversing the reed switch in the circuit but not by reversing the magnetic field used to operate it. This effect is due to a contact potential developing between the reeds when they touch.

If a condenser with plates of different surface composition is shorted a charge will flow between the plates . Volta proved that the charge appearing across a shorted condenser varies directly as the capacitance, that is it is a potential effect. Lord Kelvin showed that the contact potential is dependent only apon the nature of materials at the dielectric interface and not on the metal to metal junction. Milikan(1921) later showed that the contact potential difference between the two surfaces is equal to the difference in the work functions of the two surfaces (Palevsky et al.,1947).

The theory of contact potential charging has only been clearly formulated for metals. The effect is also observable for non-metals. The phenomena has often been resorted to, to help explain the origin of thunderstorm electrification, however contact charging in clouds is not understood (Saunders,1988).

APPENDIX 4

A4.1. Apparatus control program.

This program has been written in BASIC on a BBC microcomputer model B and was used to make computer controlled conductivity measurement. The computer controlled the apparatus by switching relays via the user port.

```
   10 REM CONDUCTIVITY APPARATUS CONTROL
   20 REM ******************************
   30 REM WRITTEN BY
   40 REM JAMES ARATHOON
   50 REM FOR DISSERTATION WORK CARRIED OUT IN THE SUMMER
OF 1990.
   60 PRINT" USING THIS PROGRAM THE COMPUTER"
   70 PRINT" AUTOMATICALLY MEASURES "
   80 PRINT
   90 PRINT"a) The Bias current of the amplifier."
  100 PRINT"b) The negative conductivity"
  110 PRINT"c) The positive conductivity"
  120 CLS
  130 PRINT:PRINT
  140 PRINT"PLEASE INPUT THE CORRECT TIME (GMT)"
  150 PRINT:PRINT
  160 PRINT"        IN HOURS AND MINUTES"
  170 PRINT:PRINT
  180 PRINT" ACCORDING TO THE 24 HOUR CLOCK"
  190 PRINT
  200 PRINT"(GMT = BST - 1)"
  210 FOR H=1 TO 1000 :NEXT H
  220 *FX15,1
  230 PRINT
  240 INPUT "HOURS (24 HOUR CLOCK)",H
  250 PRINT
  260 INPUT "MINUTES ",M
  270 TIME = H* 360000 + M* 6000
  280 PRINT
  290 PRINT
  300 PRINT
  310 PRINT "IS THIS THE CORRECT TIME (Y/N)?"
  320 SEC=(TIME DIV 100) MOD 60
  330 MIN=(TIME DIV 6000) MOD 60
  340 HR =(TIME DIV 360000) MOD 24
  350 PRINT
  360 PRINT TAB(7,20) HR;":";MIN;":";SEC;"    "
  370 IF INKEY(-69) =-1 THEN GOTO 400
  380 IF INKEY(-86) =-1 THEN GOTO 120
```

```
  390 GOTO 320
  400 CLS
  410 PRINT:PRINT
  420 PRINT"WHAT IS TODAYS DATE ?"
  430 FOR H=1 TO 1000 :NEXT H
  440 PRINT:PRINT
  450 *FX15,1
  460 INPUT"DAY (1-31) ",D
  470 DAY$=STR$(D)
  480 IF LEN(DAY$) =1 THEN DAY$="0"+DAY$
  490 PRINT
  500 INPUT"MONTH (1-12) ",M
  510 MONTH$=STR$(M)
  520 IF LEN(MONTH$) =1 THEN MONTH$="0"+MONTH$
  530 PRINT
  540 INPUT"YEAR eg 1990 ",Y
  550 YEAR$=STR$(Y)
  560 PRINT:PRINT:PRINT
  570 PRINT"IS TODAYS DATE  ";D;" / ";M;" / ";Y;"
(Y/N)?"
  580 IF INKEY(-69) =-1 THEN GOTO 610
  590 IF INKEY(-86) =-1 THEN GOTO 400
  600 GOTO 580
  610 REM
  620 FOR H=1 TO 1000 :NEXT H
  630 *FX15,1
  640 CLS
  650 PRINT:PRINT
  660 PRINT"DO YOU WISH TO CREATE A NEW FILE (Y/N)?"
  670 IF INKEY(-69) =-1 THEN GOTO 700
  680 IF INKEY(-86) =-1 THEN GOTO 830
  690 GOTO 670
  700 REM CREATING A FILE
  710 CLS
  720 PRINT:PRINT
  730 PRINT"CREATING A FILE"
  740 FOR H=1 TO 1000 :NEXT H
  750 *FX15,1
  760 PRINT:PRINT
  770 INPUT"WHAT IS THE FILE NAME (6 LETTERS) ",NAME$
  780 IF LEN(NAME$) > 6 THEN GOTO 770
  790 X=OPENOUT(NAME$)
  800 CLOSE#X
  810 CLS
  820 GOTO 920
  830 REM CHOOSING AN OLD FILE IN WHICH TO STORE THE DATA
  840 CLS
  850 PRINT:PRINT
  860 PRINT"CHOOSING AN OLD FILE"
  870 PRINT
  880 *CAT
  890 PRINT:PRINT
  900 INPUT"WHAT IS THE FILE NAME (6 LETTERS) ",NAME$
  910 IF LEN(NAME$) > 6 THEN GOTO 900
  920 REM DATA BEGIN ROUTINE
  930 X=OPENUP(NAME$)
  940 PTR#X = EXT#X
  945 BPUT#X,13
```

```
 950 FOR H=1 TO 4
 960 N=ASC("X")
 970 BPUT#X,N
 980 NEXT H
 990 E$=MID$(DAY$,1,1)
1000 N=ASC(E$)
1010 BPUT#X,N
1020 E$=MID$(DAY$,2,1)
1030 N=ASC(E$)
1040 BPUT#X,N
1050 BPUT#X,47
1060 E$=MID$(MONTH$,1,1)
1070 N=ASC(E$)
1080 BPUT#X,N
1090 E$=MID$(MONTH$,2,1)
1100 N=ASC(E$)
1110 BPUT#X,N
1120 BPUT#X,47
1130 FOR H=1 TO 4
1140 E$=MID$(YEAR$,H,1)
1150 N=ASC(E$)
1160 BPUT#X,N
1170 NEXT H
1180 FOR H=1 TO 4
1190 BPUT#X,88
1200 NEXT H
1205 BPUT#X,13
1210 REM CONDUCTIVITY ROUTINE
1220 STAN =0
1225 CSEC=0
1226 MIN=(TIME DIV 6000) MOD 60
1230 REM SWITCH ON USER PORT LINES (1-4)
1240 *FX151,98,15
1250 *FX151,96,12
1260 GOSUB 1540
1270 *FX151,96,0
1280 N$="B"
1290 REPEAT
1300 SEC=(TIME DIV 100) MOD 60
1310 UNTIL SEC= CSEC
1320 GOSUB 1640
1330 *FX151,96,12
1340 *FX151,96,13
1350 GOSUB 1540
1360 *FX151,96,1
1370 N$="-"
1380 REPEAT
1390 SEC=(TIME DIV 100) MOD 60
1400 UNTIL SEC= CSEC
1410 GOSUB 1640
1420 *FX151,96,13
1430 *FX151,96,15
1440 GOSUB 1540
1450 *FX151,96,3
1460 N$="+"
1470 REPEAT
1480 SEC=(TIME DIV 100) MOD 60
1490 UNTIL SEC= CSEC
```

```
1500 GOSUB 1640
1510 GOTO 1250
1520 STOP
1530 REM
1540 REM SHORT DELAY TIME
1550 TT =0
1555 NN=0
1560 FOR H=1 TO 1000 :NEXT H
1565 FIN=TIME+150
1570 REPEAT
1590 ZERO =ADVAL(1)
1600 TT = TT + ZERO
1605 NN=NN+1
1610 UNTIL TIME>=FIN
1620 MEAN= TT/NN
1630 RETURN
1640 REM LONG DELAY AND MEASUREMENTS
1650 SEC =(TIME DIV 100) MOD 60
1660 MIN =(TIME DIV 6000) MOD 60
1670 HR  =(TIME DIV 360000) MOD 24
1680 NUM=0
1690 TCON=0
1700 TBAT=0
1705 SCON=0
1710 REPEAT
1720 NUM=NUM+1
1730 CON=ADVAL(1)
1740 TCON=TCON+CON
1745 SCON=SCON+(CON*CON)
1750 BAT=ADVAL(2)
1760 TBAT=TBAT+BAT
1770 TSEC =(TIME DIV 100) MOD 60
1780 UNTIL TSEC-SEC>=25
1790 MCON=TCON/NUM
1792 SIG=(SCON - (TCON*TCON)/NUM)/(NUM-1)
1794 STAN=SQR(SIG)
1800 MBAT=TBAT/NUM
1810 MCON=MCON/655.36*1.237
1820 MCON=INT(MCON+0.5)
1830 MBAT=MBAT/655.36*1.237
1840 MBAT=INT(MBAT+0.5)
1850 MEAN=MEAN/655.36*1.237
1860 MEAN=INT(MEAN+0.5)
1862 STAN=STAN/65.536*1.237
1864 STAN=INT(STAN+0.5)
1870 PRINT HR;":";MIN;":";SEC;"   ";MEAN;"   ";N$;"
";MCON;"   ";STAN;"   ";NUM
1880 REM DISK STORE ROUTINE
1890 A$=STR$(HR)
1900 GOSUB 2080
1910 BPUT#X,58
1920 A$=STR$(MIN)
1930 GOSUB 2080
1940 BPUT#X,58
1950 A$=STR$(SEC)
1960 GOSUB 2080
1970 C$=STR$(MEAN)
1980 GOSUB 2170
```

```
1990 N=ASC(N$)
2000 BPUT#X,N
2010 C$=STR$(MCON)
2020 GOSUB 2170
2030 C$=STR$(MBAT)
2040 GOSUB 2170
2050 C$=STR$(STAN)
2060 GOSUB 2170
2061 BPUT#X,13
2065 CSEC=(CSEC+30) MOD 60
2070 RETURN
2080 REM TIME STORE ROUTINE
2090 IF LEN(A$)=1 THEN A$="0"+A$
2100 B$=LEFT$(A$,1)
2110 N=ASC(B$)
2120 BPUT#X,N
2130 B$=RIGHT$(A$,1)
2140 N=ASC(B$)
2150 BPUT#X,N
2160 RETURN
2170 REM MEASUREMENT STORE ROUTINE
2180 IF LEN(C$)=1 THEN C$="00"+C$
2190 IF LEN(C$)=2 THEN C$="0"+C$
2200 FOR C= 1 TO 3
2210 D$=MID$(C$,C,1)
2220 N=ASC(D$)
2230 BPUT#X,N
2240 NEXT C
2250 RETURN
```

A4.2 Data Extraction Program

```
C
C     THIS PROGRAM IS USED TO ANALYSE THE DATA OBTAINED
C     USING THE CONDUCTIVITY APPARATUS DESIGNED, BUILT
C     AND USED IN THE SUMMER OF 1990
C
C     WRITTED BY JAMES ARATHOON
C
C     PROGRAM  :  datarun.for
C
      CHARACTER*10 DATE
      CHARACTER*1 ITYPE
      PRINT *,'Program datarun.for'
      PRINT *,'BBC data file'
      CALL OPENFI(1,'OLD')
      READ(1,100) DATE
      N=1
      PRINT *,'Input Polarization voltage'
      READ *, VOLTAGE
      PRINT *,'INPUT NAME OF FILE DATA TO BE STORED'
      CALL OPENFI(9,'NEW')
  1   TTIME = 0.0
      DO 20 J= 1, 3
      READ(1,101,END=999)
IHOUR,IMIN,ISEC,IDC1,ITYPE,IDC2,IDC3,IDC4
      K=0
      IF(ITYPE.EQ.'B') K=1
      IF(ITYPE.EQ.'-') K=2
      IF(ITYPE.EQ.'+') K=3
      IF (K.EQ.1) THEN
            IBIAS=IDC2
            BSTAND = IDC4 / 10.0
      END IF
      IF (K.EQ.2) THEN
            INCURR= -(IDC2 - IBIAS)
            YNSTAND= IDC4 / 10.0
            TNSTAND  = SQRT (YNSTAND*YNSTAND +
BSTAND*BSTAND)
      END IF
      IF (K.EQ.3) THEN
            IPCURR=   IDC2 - IBIAS
            YPSTAND= IDC4 / 10.0
            TPSTAND = SQRT (YPSTAND*YPSTAND +
BSTAND*BSTAND)
      END IF
      TIME = IHOUR + (IMIN /60.0) + (ISEC /3600)
      TTIME = TTIME + TIME
  20  CONTINUE
      ATIME = TTIME / 3
C
C     DATA CALIBRATION
C
      YNCURR = ((INCURR /0.94)* 8.85)/(2.39*VOLTAGE)
      YPCURR = ((IPCURR /0.94)* 8.85)/(2.39*VOLTAGE)
      TNSTAND = ((TNSTAND /0.94)* 8.85)/(2.39*VOLTAGE)
      TPSTAND = ((TPSTAND /0.94)* 8.85)/(2.39*VOLTAGE)
```

```
      YRATIO = YPCURR / YNCURR
      PRINT
250,ATIME,YNCURR,YPCURR,YRATIO,TNSTAND,TPSTAND
      WRITE (9,250)
ATIME,YNCURR,YPCURR,YRATIO,TNSTAND,TPSTAND
      GOTO 1
  999 PRINT *,'Finished'
C
      STOP
  100 FORMAT(4X,A10,4X)
  101 FORMAT(I2,1X,I2,1X,I2,I3,A1,I3,I3,I3)
  250 FORMAT (6F9.3)
      END

      SUBROUTINE OPENFI(IFILE,INOUT)
      CHARACTER*3 INOUT
      CHARACTER*40 FILENA
      PRINT *,'Enter file name (in full)'
      READ(*,100) FILENA
      OPEN(IFILE,FILE=FILENA,STATUS=INOUT)
      RETURN
  100 FORMAT(A40)
      END
```

(If lines appear to start on the first row or comment row then they are merely a continuation of the last line.)

Some additional computing details

File transfer between the BBC and the Symmetry mainframe at Lancaster was done using the 'Kermit' software. Plotted graphics were produced using 'Bizpak' which is called from within Fortran programs.

APPENIX A5.

Graphs of noise and drift for V_{ZP}, V_{NP} and V_{PP} over time.

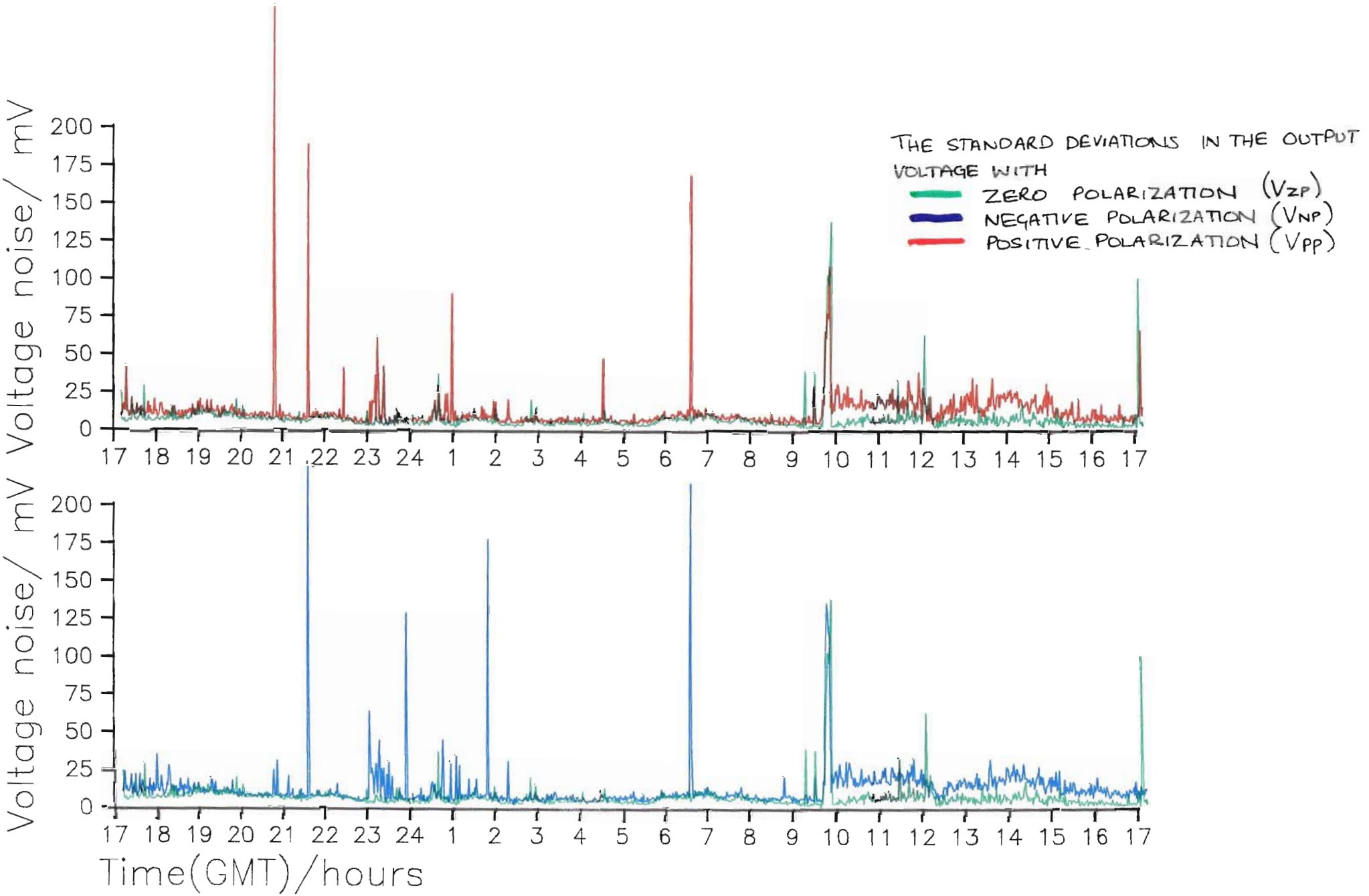

Fig. A5.1. AE9011 Noise in V_{ZP}, V_{NP} and V_{PP}

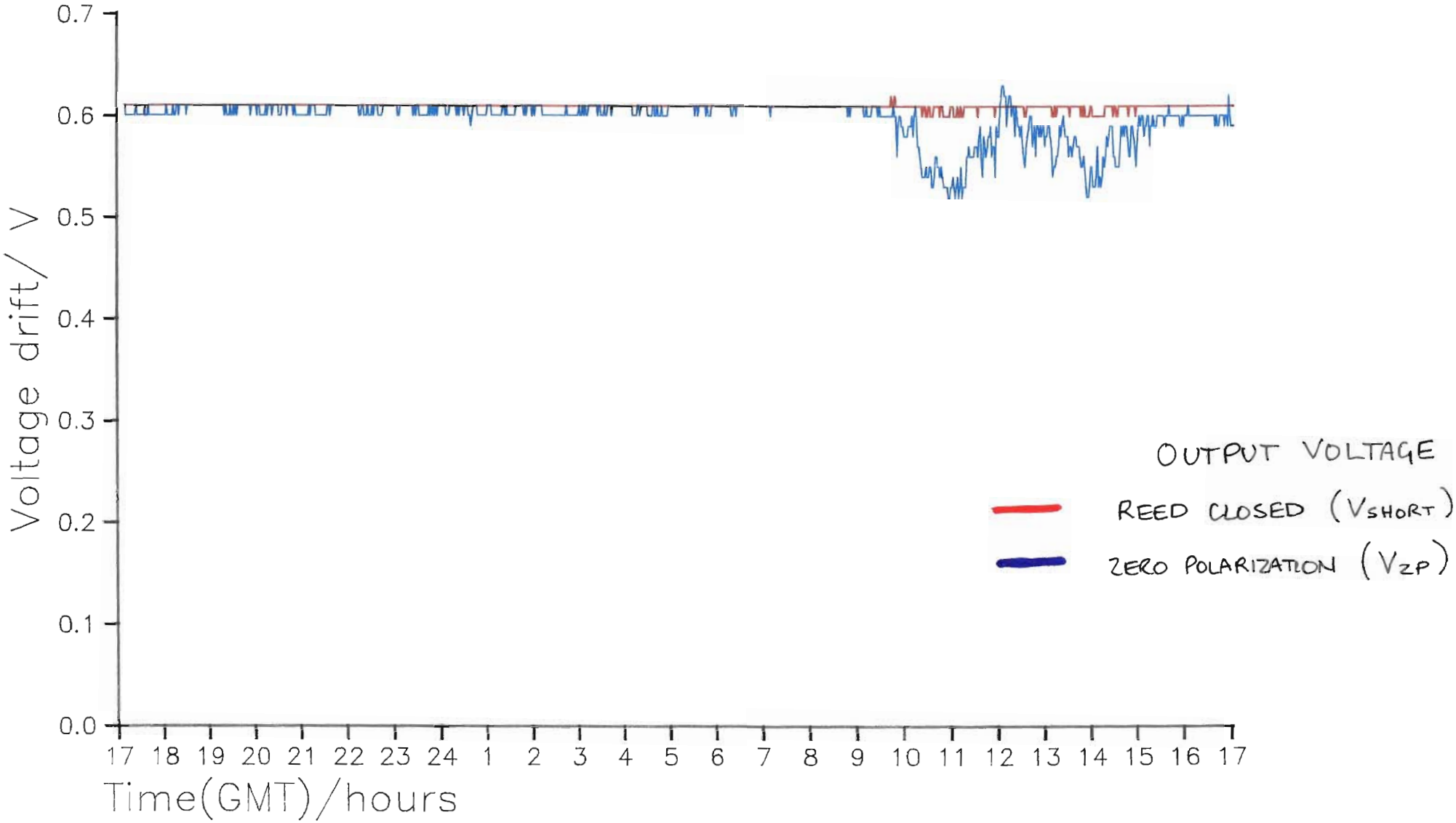

FIG. A5.2. AE9011 PICOAMMETER DRIFT SHOWN BY CHANGES IN V_{SHORT} and V_{ZP}

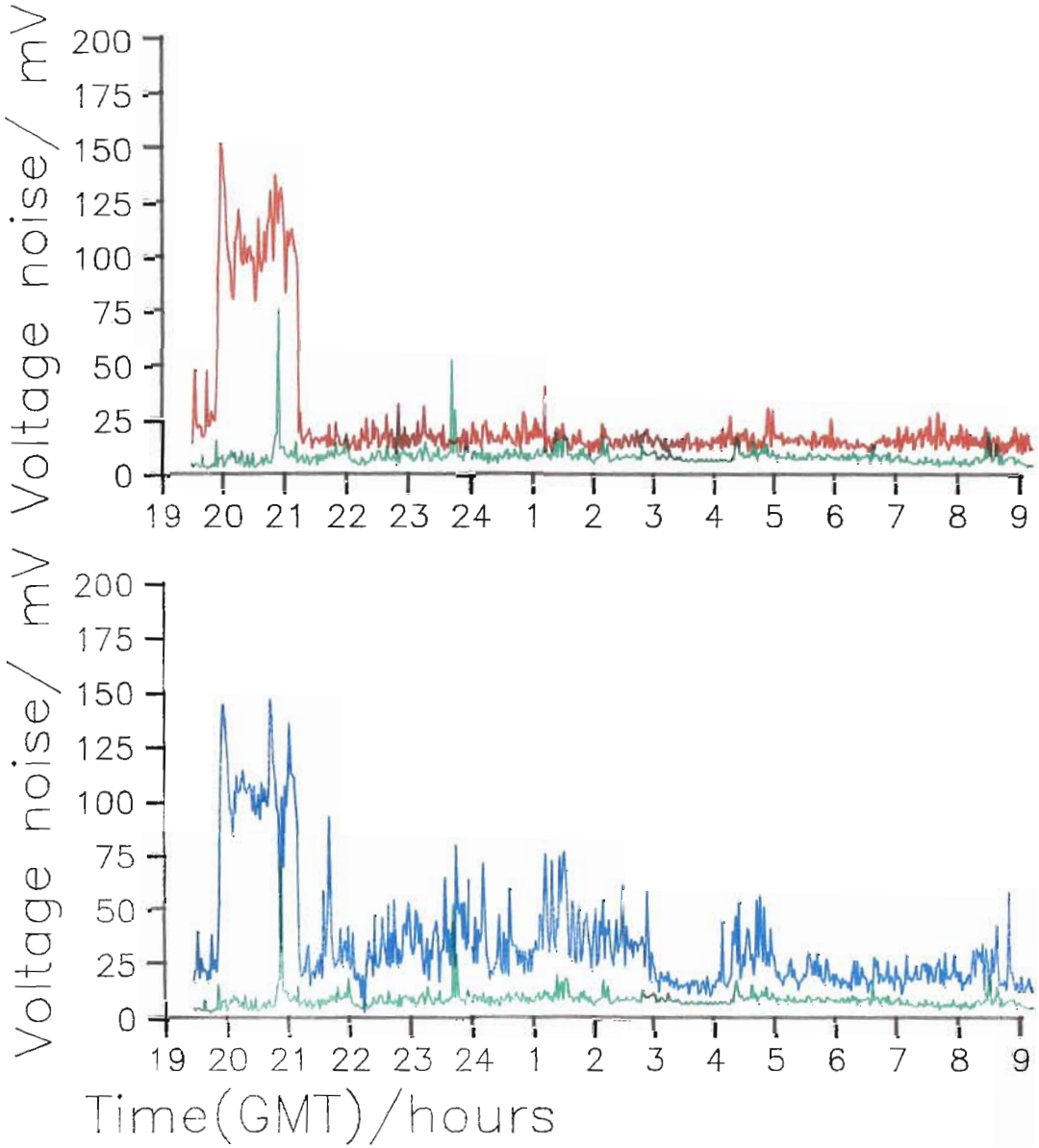

THE STANDARD DEVIATIONS IN THE OUTPUT VOLTAGE WITH

- ZERO POLARIZATION (V_{ZP})
- NEGATIVE POLARIZATION (V_{NP})
- POSITIVE POLARIZATION (V_{PP})

FIG A5.3. AE9014. NOISE IN V_{ZP}, V_{NP} and V_{PP}.

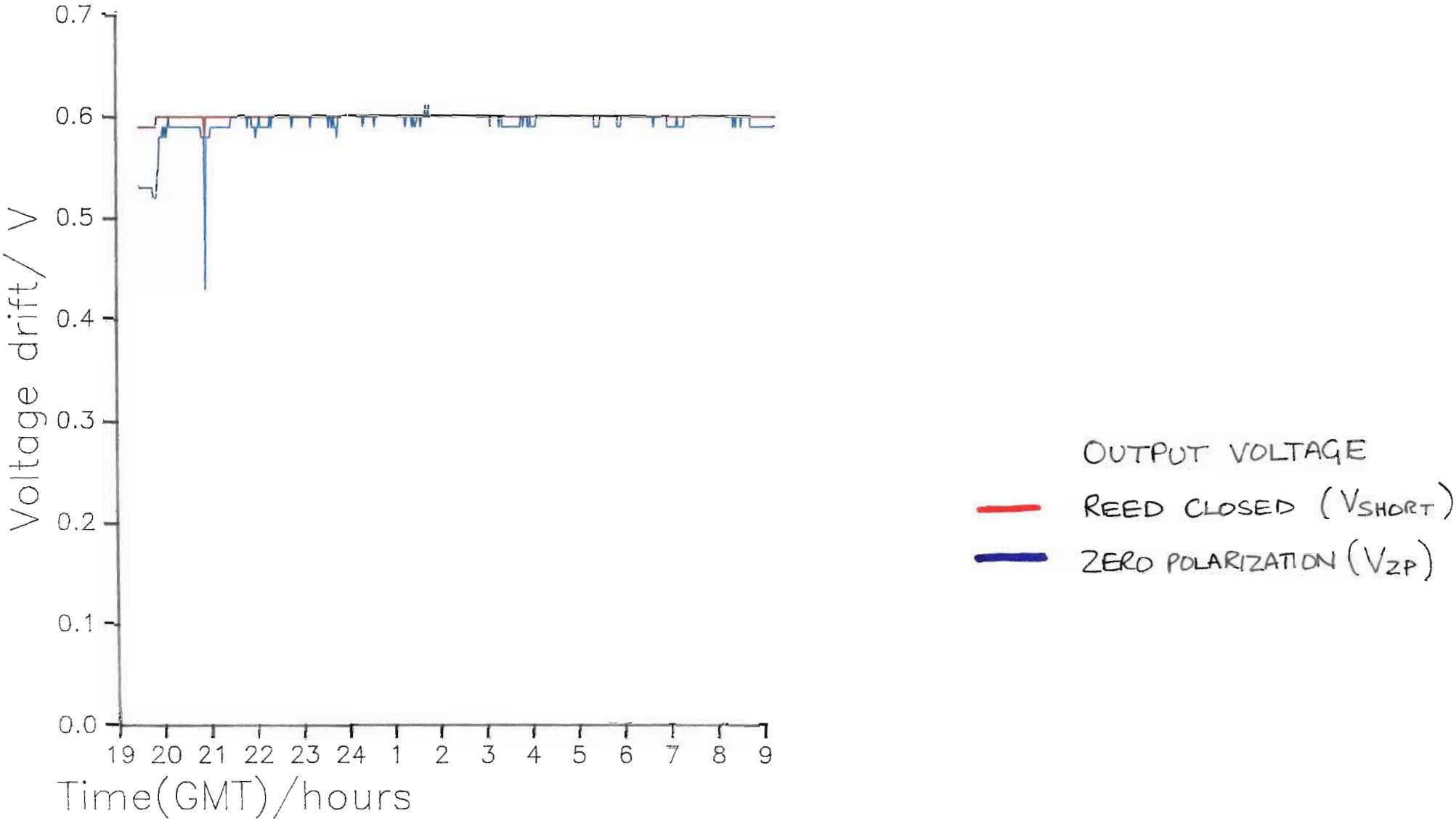

FIG. A5.4. AE9014 PICOAMMETER DRIFT SHOWN BY CHANGES IN V_{SHORT} and V_{ZP}

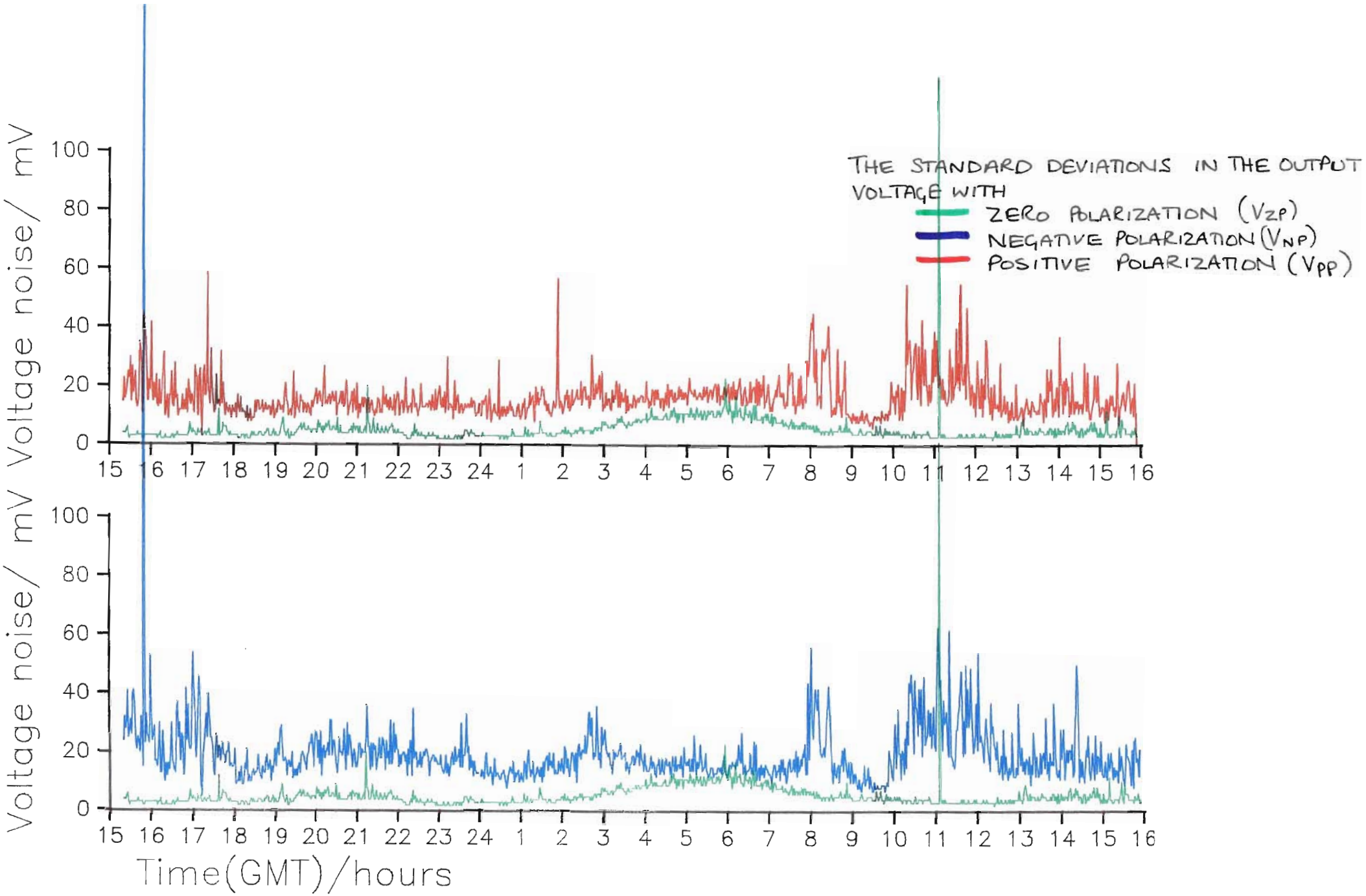
THE STANDARD DEVIATIONS IN THE OUTPUT VOLTAGE WITH
ZERO POLARIZATION (V_{ZP})
NEGATIVE POLARIZATION (V_{NP})
POSITIVE POLARIZATION (V_{PP})
Voltage noise/ mV
Time(GMT)/hours
0
20
40
60
80
100
15 16 17 18 19 20 21 22 23 24 1 2 3 4 5 6 7 8 9 10 11 12 13 14 15 16

FIG. A5.5. AE9015 NOISE IN V_{ZP}, V_{NP} and V_{PP}

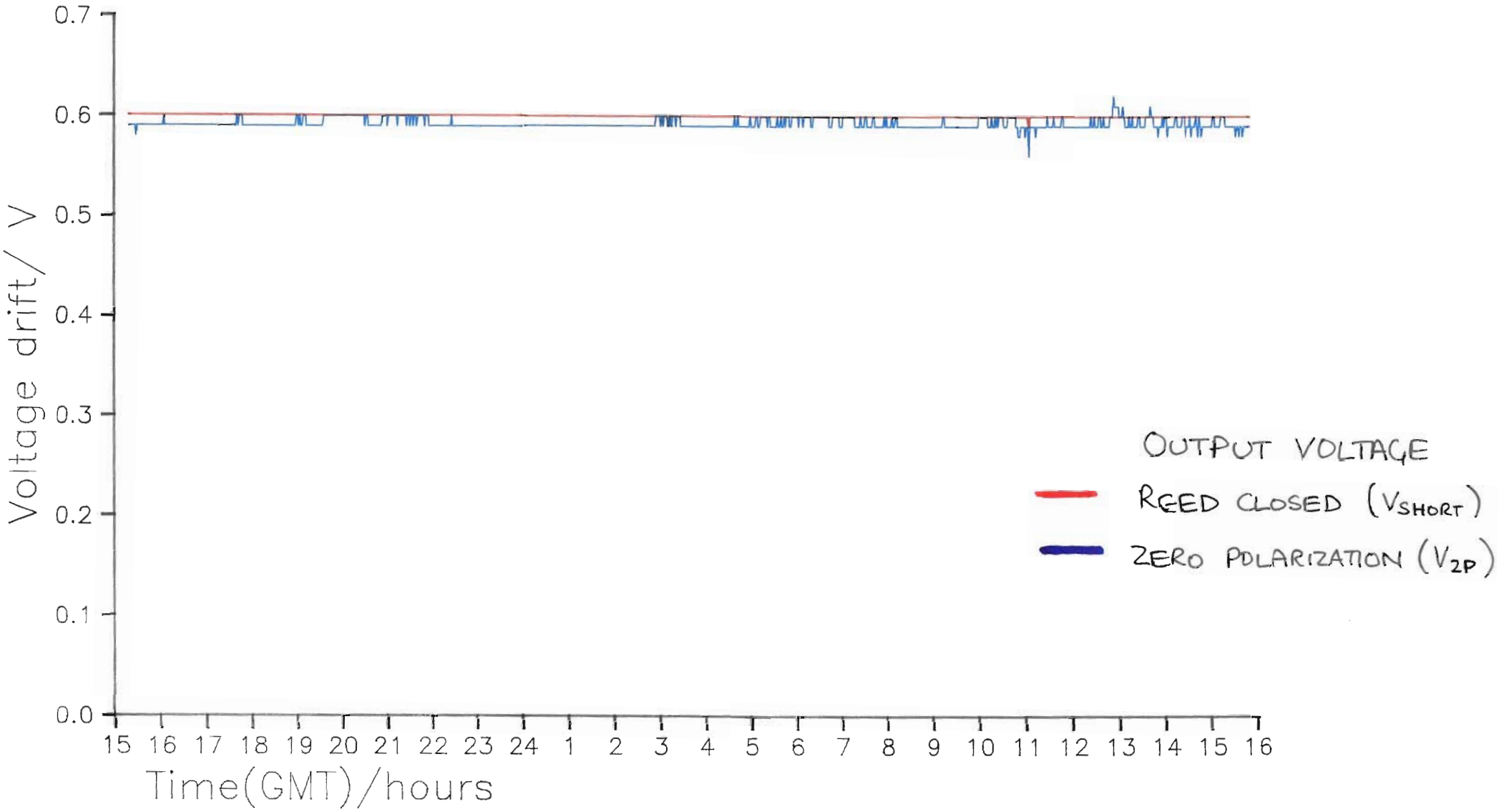

Fig. A5.6. AE9015 PICOAMMETER DRIFT SHOWN BY CHANGES IN V_{SHORT} and V_{ZP}

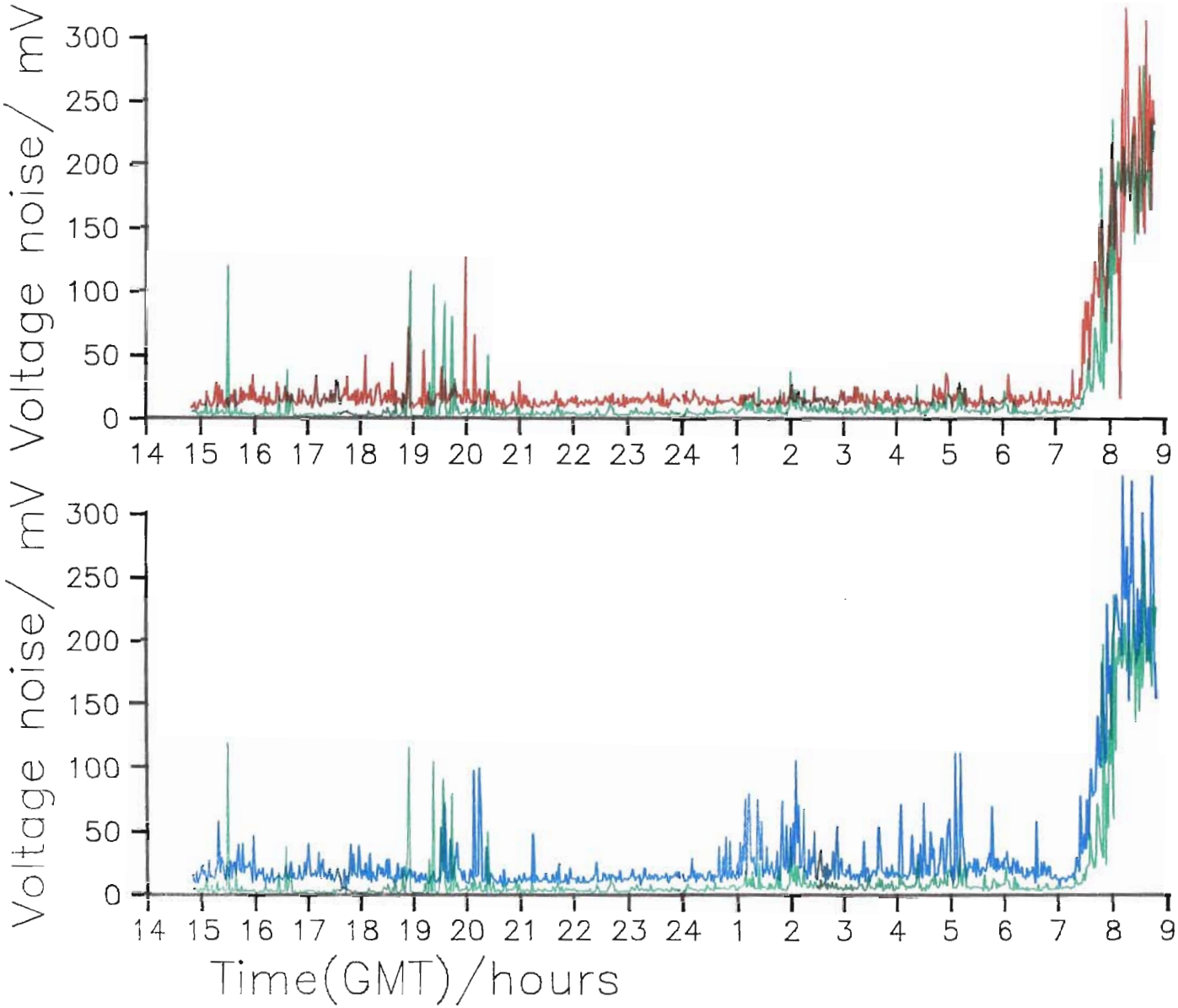

THE STANDARD DEVIATIONS IN THE OUTPUT VOLTAGE WITH
- ZERO POLARIZATION (V_{ZP})
- NEGATIVE POLARIZATION (V_{NP})
- POSITIVE POLARIZATION (V_{PP})

FIG. A5.7. AE9018 NOISE IN V_{ZP}, V_{NP} and V_{PP}.

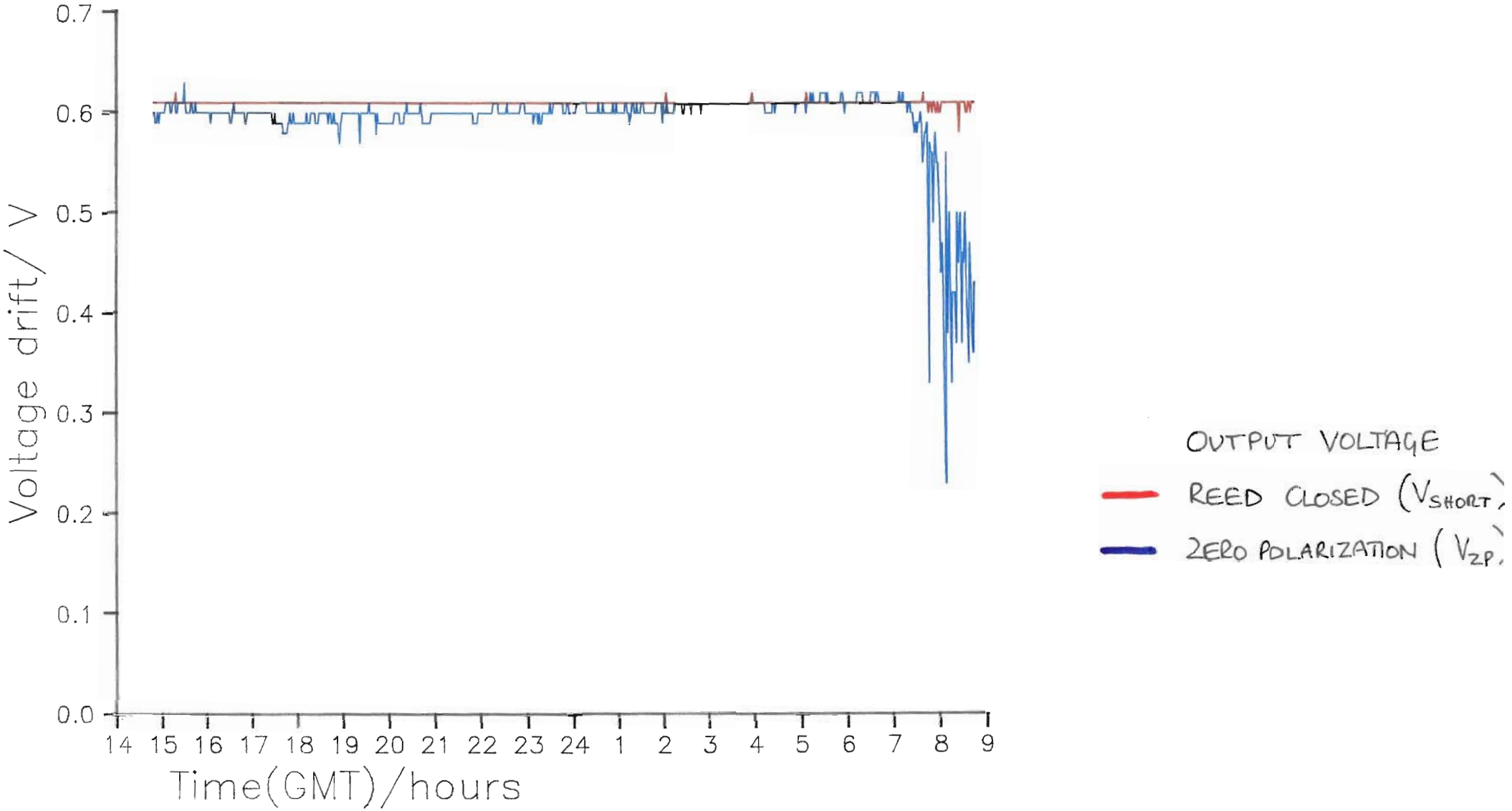

Fig. A5.8. AE9018 PICOAMMETER DRIFT SHOWN BY CHANGES IN V_{SHORT} and V_{ZP}

A6. Displacement currents in the Gerdien condenser due to changes in space charge density with time.

Consider a coaxial cylinderical condenser as was shown in Fig. 4.1.1. with the air flowing through it having a uniform space charge density, ρ . The space charge density is the free unbalanced charge per unit volume and is related to the positive ion density, ρ_P and the negative ion density, ρ_N by the formula below

$$\rho = (\rho_P - \rho_N) \qquad \text{(A6.1.)}$$

In order to find the fields within the condenser under these conditions it necessary to use Poisson's equation

$$\nabla^2 V(r) = -\rho/\varepsilon_o$$

where V(r) is the potential, dependent on the radial distance r.

In cylinderical polar coordinates the Laplacian operator, has the form

$$\nabla^2 = \frac{1}{r}\frac{\partial}{\partial r}\left(r\frac{\partial}{\partial r}\right) + \frac{1}{r^2}\frac{\partial^2}{\partial \theta^2} + \frac{\partial^2}{\partial z^2}$$

Since the coaxial cylinder has cylinderical symmetry there is no θ dependence and neglecting the end effects, no z dependence either.

Therefore this reduces to

$$\nabla^2 = \frac{1}{r}\frac{\partial}{\partial r}\left(r\frac{\partial}{\partial r}\right)$$

Thus

$$\nabla^2 V(r) = \frac{1}{r}\frac{\partial}{\partial r}\left(r\frac{\partial V}{\partial r}\right) = -\rho/\varepsilon_o$$

Integrating this expression with respect to r gives

$$\frac{\partial V(r)}{\partial r} = -\frac{\rho r}{2\varepsilon_o} + \frac{A}{r} \qquad \text{(A6.2.)}$$

At the surface of the central electrode, at r = a the field is $\frac{\partial V(a)}{\partial r} = -\sigma/\varepsilon_o$

where σ is the surface charge density. Therefore the integration constant A can be found and is

$$A = -\frac{\sigma a}{\varepsilon_o} + \frac{\rho a^2}{2\varepsilon_o}$$

Thus substituting for A in equation A6.2. gives

$$\frac{\partial V(r)}{\partial r} = -\frac{\rho r}{2\varepsilon_o} + \frac{1}{r}\left(-\frac{\sigma a}{\varepsilon_o} + \frac{\rho a^2}{2\varepsilon_o}\right)$$

Now integrating this expression with respect to r, between the limits a and b gives the potential difference between the two plates

$$\Delta V = \int_a^b \frac{\partial V(r)}{\partial r}\, dr$$

$$= \int_a^b -\frac{\rho r}{2\varepsilon_o} + \frac{1}{r}\left(-\frac{\sigma a}{\varepsilon_o} + \frac{\rho a^2}{2\varepsilon_o}\right)$$

$$= \left[-\frac{\rho r^2}{4\varepsilon_o} + \left(-\frac{\sigma a}{\varepsilon_o} + \frac{\rho a^2}{2\varepsilon_o}\right)\ln r\right]_a^b$$

which on simplifying becomes

$$\Delta V = -\frac{\rho(b^2-a^2)}{4\varepsilon_o} - \frac{\sigma a}{\varepsilon_o}\ln(b/a) + \frac{\rho a^2}{2\varepsilon_o}\ln(b/a)$$

Now differenciating this expression with respect to time gives $\frac{\partial(\Delta V)}{\partial t} = \frac{\partial \rho}{\partial t}\left[\frac{a^2}{2\varepsilon_o}\ln(b/a) - \frac{(b^2-a^2)}{4\varepsilon_o}\right] - \frac{\partial \sigma}{\partial t}\left[\frac{a}{\varepsilon_o}\ln(b/a)\right]$

but $\frac{\partial(\Delta V)}{\partial t} = 0$ since V is the constant polarization voltage, or zero volts, if there is zero polarization

Therefore

$$0 = \frac{\partial \rho}{\partial t}\left[\frac{a^2}{2\varepsilon_0}\ln(b/a) - \frac{(b^2-a^2)}{4\varepsilon_0}\right] - \frac{\partial \sigma}{\partial t}\left[\frac{a}{\varepsilon_0}\ln(b/a)\right]$$

and upon rearrangement this becomes

$$\frac{\partial \sigma}{\partial t} = \left[\frac{a}{2} - \frac{(b^2-a^2)}{4a\ln(b/a)}\right]\frac{\partial \rho}{\partial t}$$

which can be written as

$$\frac{\partial \sigma}{\partial t} = k\frac{\partial \rho}{\partial t}$$

where $k = \left[\frac{a}{2} - \frac{(b^2-a^2)}{4a\ln(b/a)}\right]$

However since

$$\frac{\partial \sigma}{\partial t} = \frac{1}{(2\pi aL)}\frac{\partial q}{\partial t}$$

where $\frac{\partial q}{\partial t}$ is the rate of change of charge on the central electrode.

It follows that

$$\frac{\partial q}{\partial t} = k_q\frac{\partial \rho}{\partial t} \qquad \text{(A6.3.)}$$

where $k_q = \left[\pi a^2 L - \frac{\pi L(b^2-a^2)}{2\ln(b/a)}\right]$

The values of a and b for the condenser used in this dissertation were, a = 0.006m and b = 0.045m.

therefore $k_q = -0.0012 = 1.2\times10^{-3}\ m^3$

Acknowledgements

I wish to record my thanks to Dr. J.F.R. McIlveen (ES Division) and Dr. B.K. Jones (Physics department), my supervisors, for their patient support and advice during the many weeks that I worked on the project. Also I wish to thank Brian Robinson (ES Division) and John Pritchard (Computing centre) for helping with my computing queries.

I am also indebted to a great many technicians in both the Physics and Environmental Science Departments for their help with the building of the apparatus.